FINAL REPORT

STUDY OF PRECISE
POSITIONING AT L-BAND USING
COMMUNICATIONS SATELLITES

Prepared for

National Aeronautics and Space Administration
Wallops Station
Wallops Island, Virginia 23337

Under NASA Contract No. NAS6-1962

Applied Information Industries
345 New Albany Road
Moorestown, New Jersey 08057

FINAL REPORT

STUDY OF PRECISE POSITIONING AT L-BAND USING COMMUNICATIONS SATELLITES

Prepared for

National Aeronautics and Space Administration
Wallops Station
Wallops Island, Virginia 23337

Under NASA Contract No. NAS6-1962

j

TABLE OF CONTENTS

TABLE OF CONTENTS (Continued)

LIST OF ILLUSTRATIONS

LIST OF ILLUSTRATIONS (Continued)

LIST OF TABLES

SECTION 1

INTRODUCTION

A study at Williamstown, Massachusetts, in August 1969, jointly
sponsored by the National Aeronautics and Space Administration
and by the Massachusetts Institute of Technology* recommended:

> Develop navigation systems capable of economically
> determining ship velocities to +5 cm/sec over several-
> minute time averages and ship positions to +100 m at
> the same time, plus free instrument float locations with
> +2-km accuracy at intervals of about 5 days: to obtain
> better knowledge of current patterns and diffusion rates.

In response to this recommendation and requests from other
Governmental agencies for precision position fixing equipment,
NASA Wallops Station by direction of the NASA Office of Space
Sciences and Applications defined a program for the study and
experiment described in this final report. This work was per-
formed under NASA Contract No. NAS6-1962 by Applied Information
Industries, using unique proprietary equipment. During the
course of this contract effort the applications of precision
position fixing became increasingly apparent to the individuals
involved in the program. Requirements for position fixing with
accuracies of less than 50 feet have been expressed by all three
Armed Services, the Coast Guard, the Maritime Administration,
the Federal Aviation Administration, the National Oceanic and
Atmospheric Agency, and the Department of the Interior. Many
areas of private industry are also most concerned; these include
geophysical exploration teams, ship owners and operators and air
lines.

The test results described here verify the ability of a satellite-
based system to satisfy the requirements of precision position
fixing. The potential for serving the user needs by using
communications satellites in synchronous orbit and low-cost
ground terminal receiving equipment is most attractive.

---

*The Terrestrial Environment, Solid-Earth and Ocean Physics,
Application of Space and Astronomic Techniques, August 1969,
NASA ERC, Cambridge, Massachusetts

SECTION 2

SUMMARY

2.1 PROGRAM SYNOPSIS

The L-Band Precision Positioning Experiment, sponsored by the
National Aeronautics and Space Administration, Wallops Station,
encompassed seven months of experiment design, experimentation,
and data reduction and analysis. In the experiment the ATS-5
synchronous satellite L-band transponder was used in conjunction
with the modified AII ALPHA II navigation receivers to demonstrate
the technical capability of precision position fixing for oceano-
graphic purposes. The test program proved ·the feasibility of
using relative ranging techniques implemented by two identical
receiving systems, properly calibrated, to determine a line of
position accurately on the surface of the Earth. As this final
report shows, the program achieved the objectives established in
the work statement; i.e., to demonstrate

- Level of resolution
- Repeatability
- Precision, and
- Accuracy

of existing modest-cost effective navigation equipment.

Figure 2-1 summarizes the major tasks and events that comprised the
program. The experiment configuration and data reduction techniques
were developed in parallel with the hardware modification tasks.
In the hardware modification phase, two existing AII L-band receiving
systems were specifically revised for the test and then calibrated
by operating with the AII system modulator; also, a tape control
unit was developed for interfacing the receivers with a magnetic
tape drive for data recording.

A PN code modulator was installed at the NASA STADAN Station at
Rosman, North Carolina, to provide the ranging signal for trans-
ponding by the ATS-5 satellite.

After the installation of the receiving systems at the NASA Wallops
facilities, three weeks of testing were conducted to evaluate the
equipment precision and determine the accuracy of relative position
fixing. The initial data reduction was accomplished in near-real-
time using the NASA computer facilities at Wallops Station.

The location of the average LOP for each test period was offset
from the remote site, the location of which was to be determined

	CY 1971							
	M	A	M	J	J	A	S	O
● Test Plan Design	▓							
● Definition of Data Reduction Method		▓	▓					
● Receiver Modification and Alignment		▓	▓	▓				
● Development of Tape Control Unit		▓	▓					
● Modulator Installation				◆				
● Receiver Installation					◆			
● Field Test					▓			
● Data Reduction						▓	▓	
● Draft Final Report							▓	▓
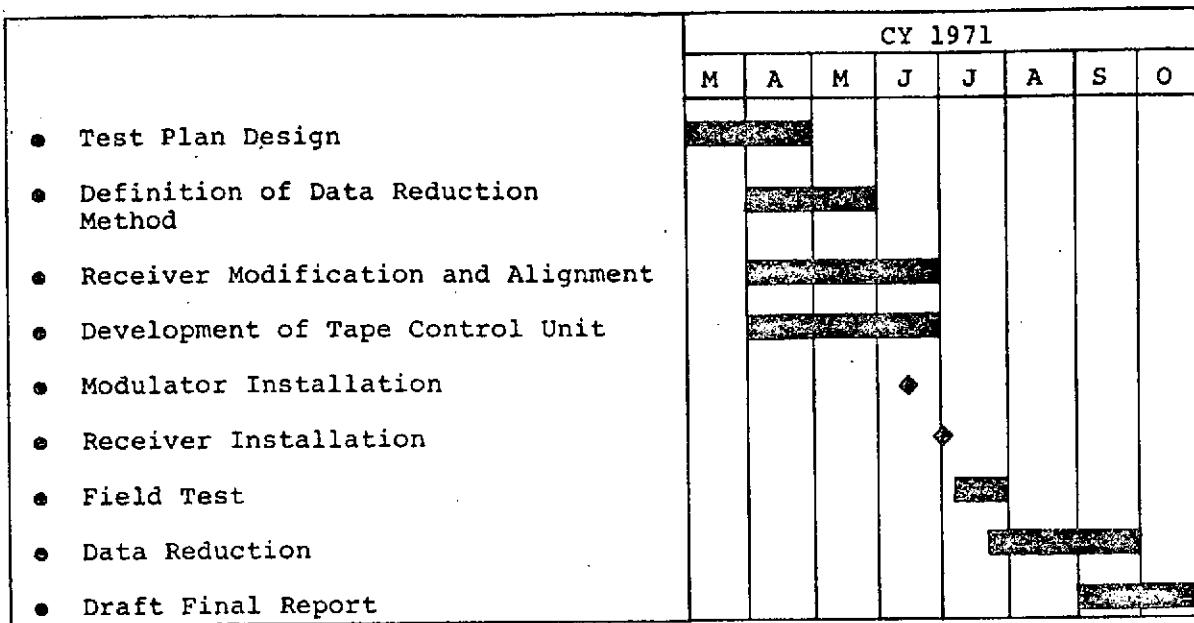
Figure 2-1. Program Plan and Schedule

relative to the position of the fixed site, by not more than 8.5
feet. This offset is believed due to the inaccuracies in the
satellite ephemerides. The rms noise was on the order of 30 feet.
Lines of position (LOP's) resulting from individual pairs of
range measurements, one measurement resulting from each receiver,
indicate that for oceanographic and geophysical purposes 20
successive bursts from the ATS-5 satellite will yield an LOP which
is offset from the true location by not more than 50 feet. These
data were collected in 16 seconds. Since the duty cycle of the
ATS-5 satellite is such that data can be collected for 50 milli-
seconds every 780 milliseconds, an improvement in duty cycle, as
would result from a nonspinning satellite, will permit the same
accuracy to be realized in approximately one second of ranging on
the satellite or an equivalent improvement in accuracy if data
were smoothed over 16 seconds.

2.2 INSTRUMENTATION CONFIGURATION

The synchronous ATS-5 satellite is the only satellite of the ATS
series with L-band transmission capability and thus was selected
as the platform for the relative ranging test. Because the ATS-
5 satellite is rotating, its directional antennas scan the Earth
approximately once every 780 milliseconds. This results in
common illumination of the transmitting and receiving terminals

for approximately 50 milliseconds every revolution. During the experiment period, the ATS-5 L-band receiver was temporarily inoperative, thus necessitating C-band transmission from the Rosman site. Operating the satellite transponder in the C-band to L-band cross-strap mode, permitted L-band transmission from the satellite to the receiving systems located at the NASA Wallops site. However, the transponder bandwidth was limited to approximately 6 MHz when operating in this mode, thus degrading the 10-megabit code-modulated signal by approximately 6 dB.

The AII ALPHA II receiving system employed during the experiment was an L-band ranging system operating with a 10-megabit PN code. The PN code is transmitted as coherent phase-shift-key (CPSK) modulation from the NASA Rosman STADAN station, using an ALPHA II modulator. The 10-megabit code provides the capability for determining the coarse range granularity to within 100 nanoseconds. Additional circuitry within the ALPHA II code correlator provides quantization to 1-nsec intervals. The ALPHA II correlation receiver employs a demodulation technique which does not require carrier acquisition prior to code lock-on. This accelerates the lock-on time and enables operation in the presence of the intermittent signal from the ATS-5 satellite. A digital memory exists in the range tracking loop of the code correlator to provide continuity between the satellite bursts.

Figure 2-2 shows a simplified version of the test configuration for the relative ranging experiment. An AII ALPHA II modulator was used to drive the NASA C-band transmitter, while the ATS-5 transponder transmits at L-band to the two independent ALPHA II receiving systems, located at the NASA Wallops Station. A common magnetic-tape data recording subsystem provided a permanent record of the range measurement data.

The data recording subsystem consisted of a tape control unit developed by AII to interface the ALPHA II code correlator with a 7-track incremental tape recorder. The receiver at the fixed site was connected directly to the tape control unit, while the receiver located at the remote site interfaced with the tape control unit via a data modem and a conventional telephone line. Range readings were taken for each satellite burst and if the two receivers measured the range reading within 50 milliseconds of each other, the tape control unit would accept the readings as being valid and record them, with time information. The resulting data tapes were then reduced using the computer facility at the NASA Wallops Station.

2.3 TEST CONFIGURATION

The test configuration illustrated in Figure 2-2 was implemented at the Wallops facility as shown on the simplified site map of Figure 2-3. The fixed receiving site was located according to a

ATS-5

C-Band

L-Band

L-Band

| NASA C-Band Transmitter | ALPHA II Receiving System "A" | ALPHA II Receiving System "B" |

| ALPHA II Modulator | Data Recording Subsystem | Phone Lines |

Rosman, N.C.

Wallops Main Station

Wallops Island
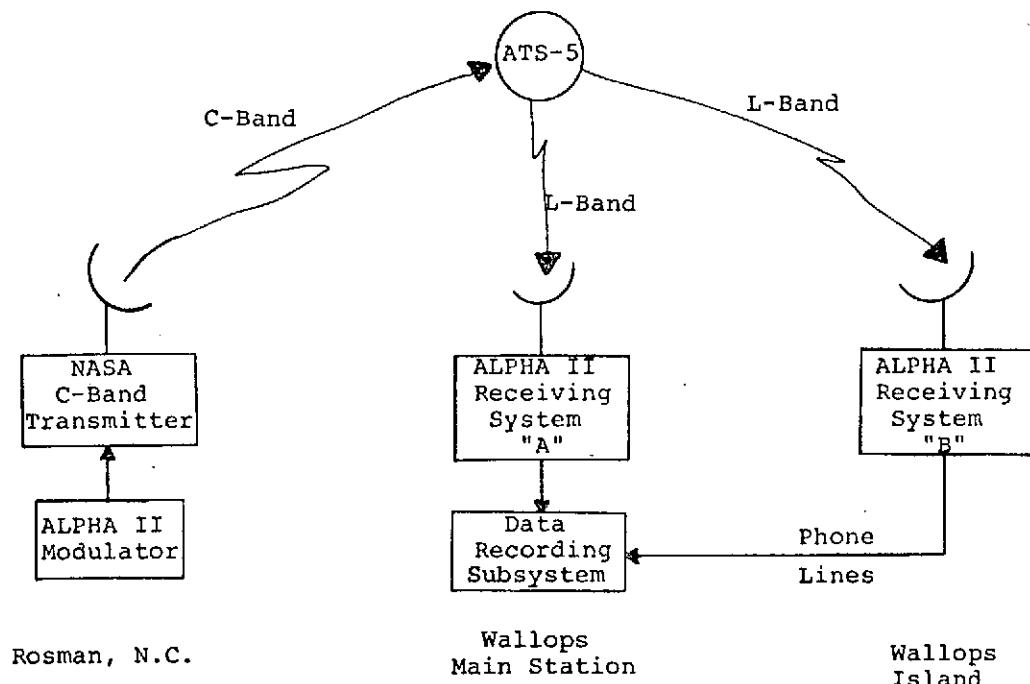
Figure 2-2. Test Configuration for the Relative Ranging Experiment

first order survey and the range to the satellite measured by the fixed receiver and the remote receiver. The geometry is such that by knowing the location of the fixed receiver and the pre-dicted satellite position as a function of time and by measuring the ranges R_A and R_B from the satellite with the two receivers as shown in Figure 2-4, the line of position (LOP) containing the remote receiver can be calculated. This line of position can then be compared to the surveyed position of the remote receiver to determine the precision and repeatability of the system.

The range measurements include several biases and error sources which were evaluated prior to computing the line of position. A fixed bias representing the delay difference between the antenna feeds and the correlation point within the code correlators was calibrated. Rubidium standards were used to drive the PN code generators in each code correlator and these contributed what appeared to be the most significant noise and bias errors en-countered in the experiment. Calibration of the slowly varying bias term was accomplished by comparing the phase difference between the two rubidium standards before and after each satellite ranging test period and fitting the resultant points to a straight line. The magnitude of the frequency standard noise errors was determined by performing a series of special tests designed to measure the stability characteristics between the two rubidium standards.

WALLOPS
MAIN BASE

FIXED
RECEIVER

WALLOPS
ISLAND

REMOTE
RECEIVER

0   1   2
SCALE-MILES
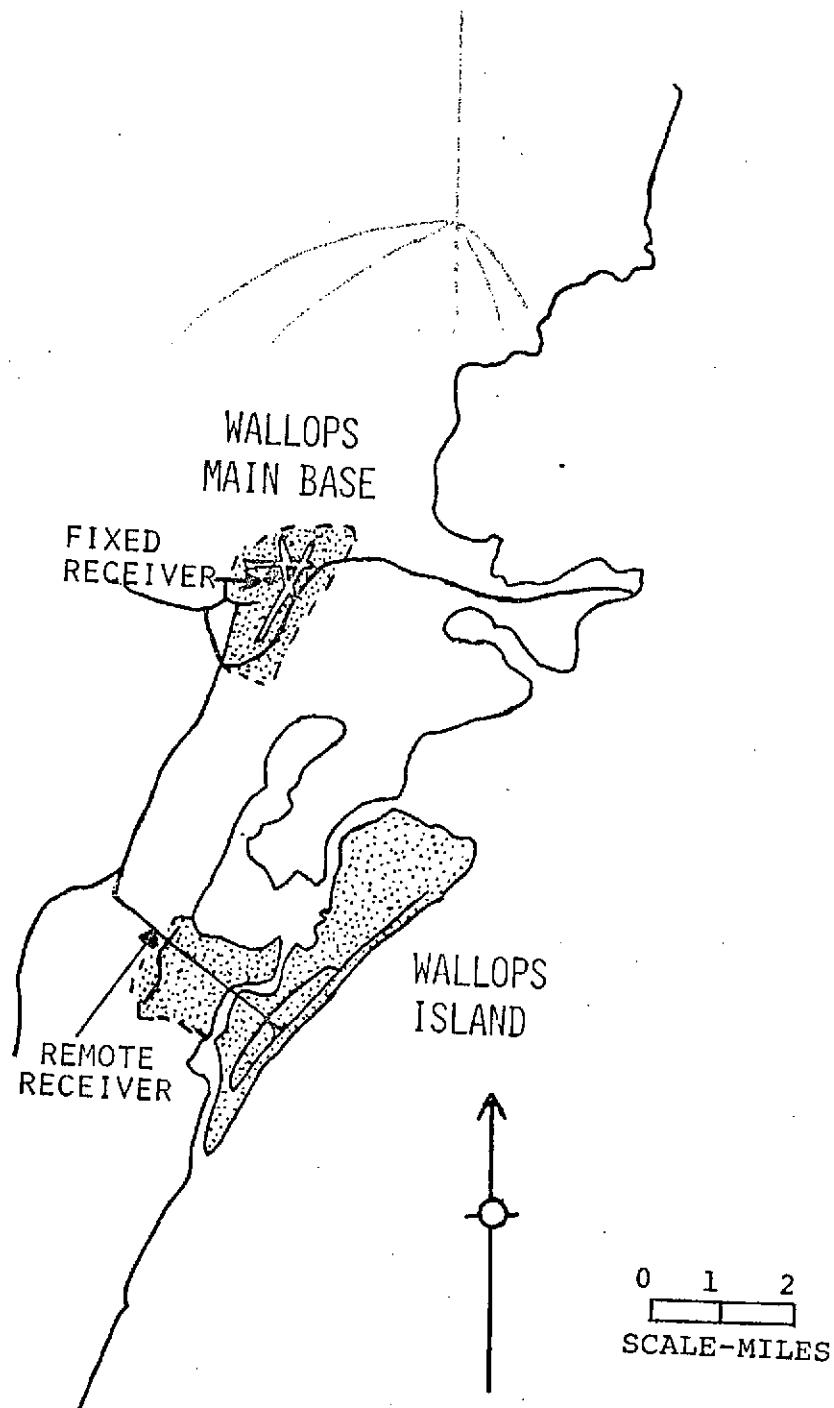
Figure 2-3.   Site Map Showing Relative Locations
of Fixed and Remote Receivers
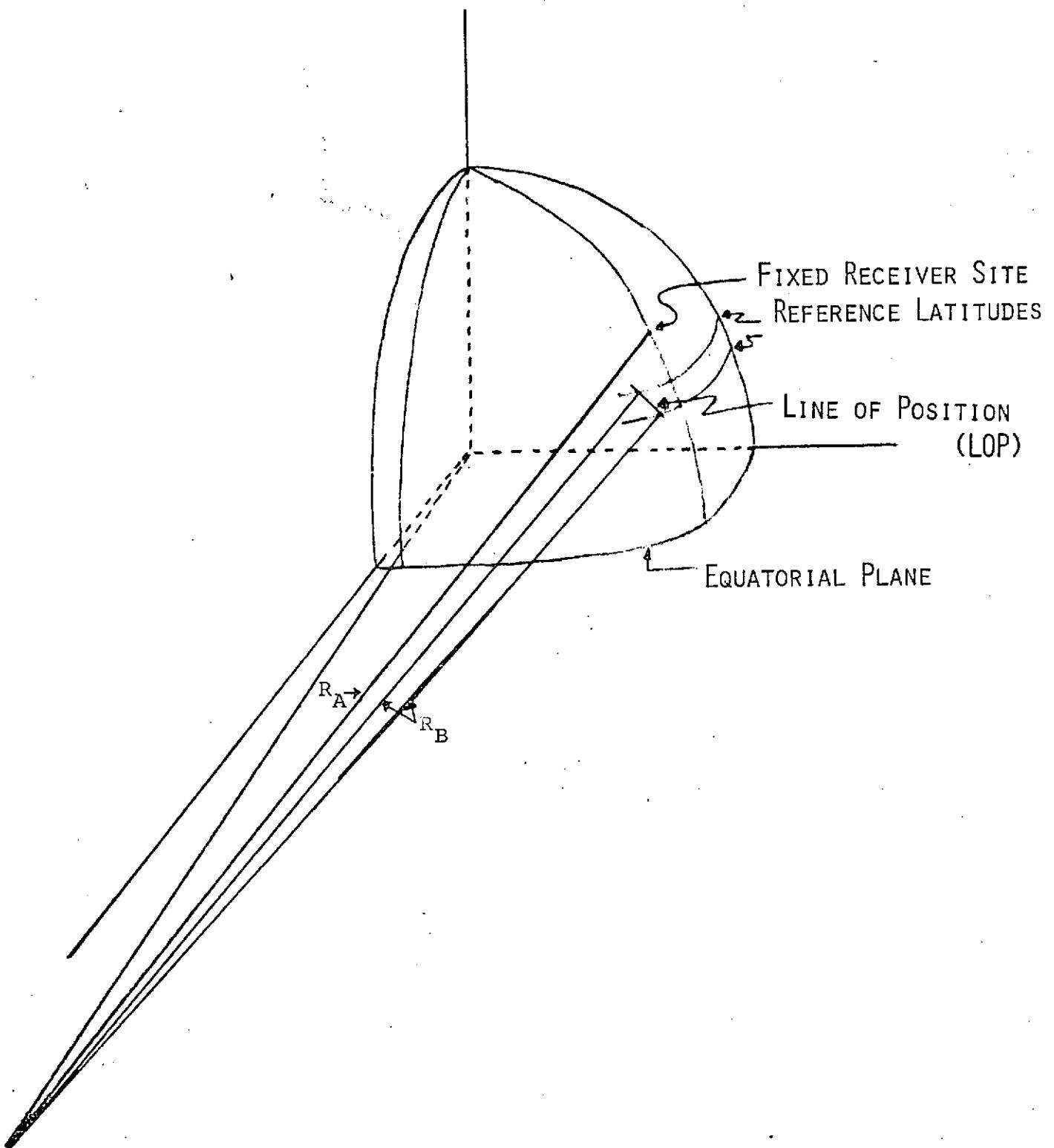
Figure 2-4.   Geometry Used to Determine
Line of Position

Errors contributing to inaccuracies in the ranging measurements arise from either equipment or environmental noise sources and include receiver noise, equipment non-linearity, quantization frequency-standard errors, multipath, ionospheric and tropospheric delays and geometric effects. Errors associated with satellite-position uncertainty represent the present tracking and prediction capability and have been reduced to second order effects by virtue of the method of data reduction used. The equipment noise error (which includes both the receiving system noise and the frequency-standard noise) and the satellite position uncertainty are the two largest error sources contributing to the relative range uncertainty. Table 2-1 summarizes the error sources and the total relative range uncertainty.

The link budget for the experiment is summarized in Table 2-2. This reflects the use of one TWT in the satellite L-band transponder and a 3-foot receiving antenna at the Wallops Station.

TABLE 2-1. ERROR SOURCE SUMMARY

Error Source	Relative Range Uncertainty
Receiver Noise	5.1 feet
Correlator Linearity	2.8 feet
Phase Alignment of Frequency Standards	14.3 feet
Satellite Position Uncertainty	7.0 feet
Other Error Sources	0.8 feet
Range Accuracy (RSS)	17.0 feet
Position Accuracy	21.3 feet

2.4 TEST RESULTS

The average line of position (LOP) for each test period was computed from the individual LOP's. The standard deviation of the individual LOP's about the mean was then determined for each test period. Figure 2-5 summarizes the average LOP's for each test period and Table 2-3 presents the offsets and rms noise for each test.

A test period dedicated to the calibration of the receiver front-end delay yielded a bias of 45 feet between the two receiving systems which is equivalent to an LOP offset of 56 feet when projected through the elevation angle. Calibration of the phase

TABLE 2-2. SUMMARY LINK BUDGET OF ATS-5 SATELLITE
OPERATING IN C-TO-L CROSS-STRAP MODE

Parameter	Rosman to Wallops	
	6214 MHz Up-Link	1551 MHz Down-Link
Net Antenna Gain (dB)*	+76.4	+31.5
ERP (dBW)	+96.5	+24.0
Net Propagation Loss (dB)	-203.8	-189.5 to -191.5
Received Carrier Power (dBW)	-91.4	-147 to -149
Received System Noise Temp (dB - °K)	+30.7	+28.2
Noise Power Density (dBW/Hz)	-197.9	-200.6
Carrier/Noise Power Density (dB-Hz)	+106.5	51.6 to 53.6
Receiver Bandwidth (dB)	+67.8	+32
Carrier/Noise Ratio (dB)	+38.7	19.6 to 21.6
*85-foot Transmit Antenna; 3 and 4-foot receive antennas		

Projection of Line of Sight from Receiver to Satellite

AVERAGE LOP'S FOR TEST PERIODS 2,5,8,12 and 13

Latitude Degrees
37.864343

Remote Site

Test #	Offset
2	6.9 feet
5	8.5 feet
8	1.2 feet
12	4.6 feet
13	4.6 feet

Test Number   2 13   8   12   5

75.507600   75.507500

Longitude, Degrees
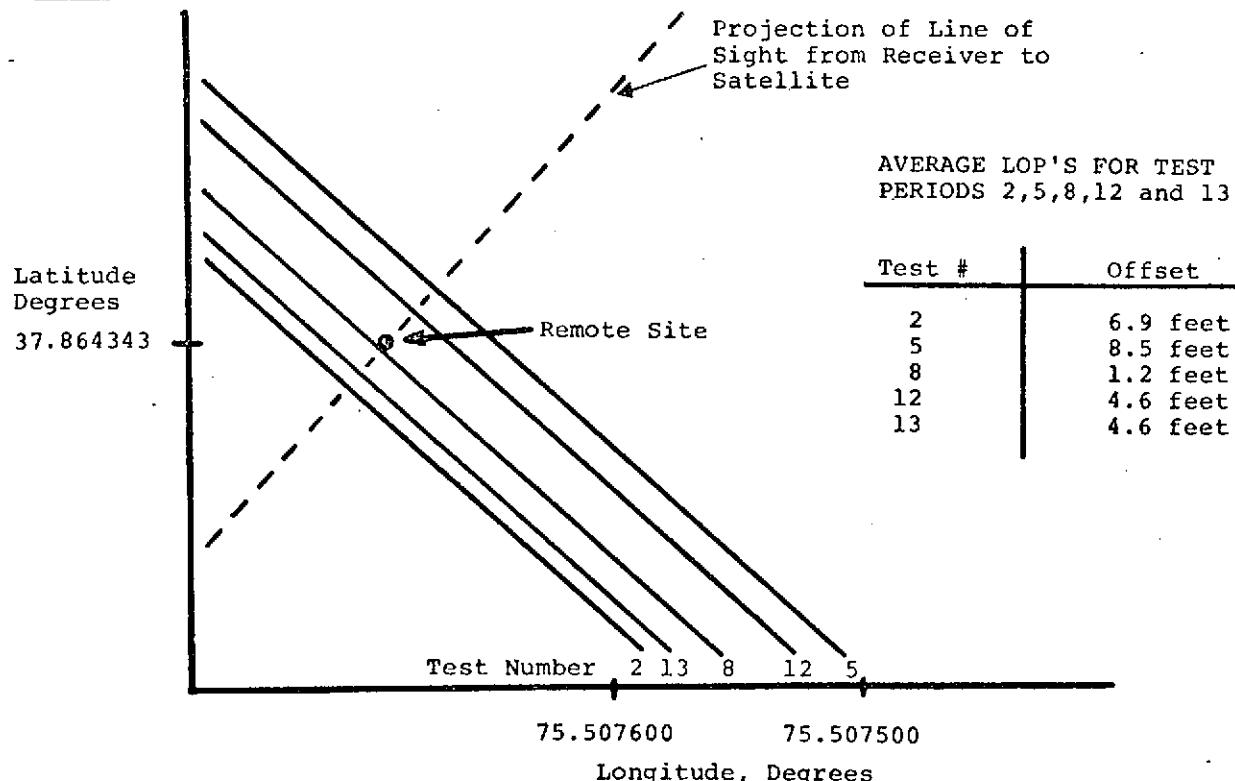
Figure 2-5. Average LOP's for Test Periods
2, 5, 8, 12 and 13

TABLE 2-3. SUMMARY OF THE TEST DATA

Test	Date	Offset of Average LOP (feet)	Rms (feet)
2	July 12	6.9	25.88
5	July 15	8.5	31.63
8	July 21	1.2	16.77
12	July 27	4.6	33.26
13	July 28	4.6	30.52

drift in the rubidium frequency standards by fitting the pre- and post-test calibration data to a straight line resulted in a correction term of approximately 600 feet per hour.

The noise on the LOP's was analyzed by comparing the data from several test configurations. This enabled a noise value of 12 to 15 feet to be determined for both frequency standards. The noise error of an individual receiver was determined to be less than 4 feet by removing the above frequency standard noise from the results.

2.5 CONCLUSIONS

The following conclusions are warranted by the results of the study and experiment:

- Communications satellites in synchronous orbit can be utilized as transponders for relay of precision positioning signals.

- Using those signals at L-band, positioning accuracies relative to another receiver of less than 30 feet are achievable even without accurate ephemeris data and on a moving ship. With an integration period of an hour or more, relative positioning accuracies of 8 feet are achievable.

- The major source of errors encountered appears to be the rubidium frequency standard.

SECTION 3

EXPERIMENT DESIGN

3.1 EXPERIMENT TEST CONFIGURATION

The objective of this study was to demonstrate the technical feasibility and level of accuracy of precise range measurements at L-band via synchronous satellite for application to oceanographic and geophysical position-fixing. The demonstration test was required to operate with the spinning ATS-5 satellite and interface with NASA-supplied equipment and facilities. The experiment design was, of course, dictated by the test objectives, the equipment capabilities, and the constraints of the proposed test site.

To accomplish the experiment objectives, a test configuration employing a fixed and a transportable receiver, and operating in conjunction with a NASA transmitter and the ATS-5 satellite, was designed (see Figure 3-1). The demonstration test profile consisted of calibration of both receivers in close proximity, followed by ranging measurements through the ATS-5 satellite, and generation of the line of position (LOP) on the surface of the Earth upon which the transportable receiver was located. By knowing the precise locations of the two receivers through first-order survey markers, the repeatability and precision of the ranging measurements could be established. The use of two proximate stations enabled most of the errors caused by propagation effects and lack of knowledge of the satellite's position to be cancelled.

As shown in the test configuration of Figure 3-1, an AII ALPHA II modulator was used to drive the C-band up-converter and transmitter system located at the NASA Rosman, North Carolina, station. (C-band transmission to the ATS-5 satellite was necessitated by the temporary inoperative condition of the ATS-5 L-band receiver during the test period.) The 10-megabit PN-code-modulated signal was transponded by the ATS-5 satellite while operating in the C-band to L-band cross-strap mode, which has a 1-dB bandwidth of 6 MHz. The identical and independent L-band down-converters located at the Wallops facility translated the received signal to a 70-MHz IF frequency. The IF signals were then processed by identical code correlators and decoded by PN code generators operating from separate rubidium frequency standards. To accommodate the data collection function, the range readings from the code correlator were transmitted to a tape control unit, formatted and recorded on 7-track magnetic tape.
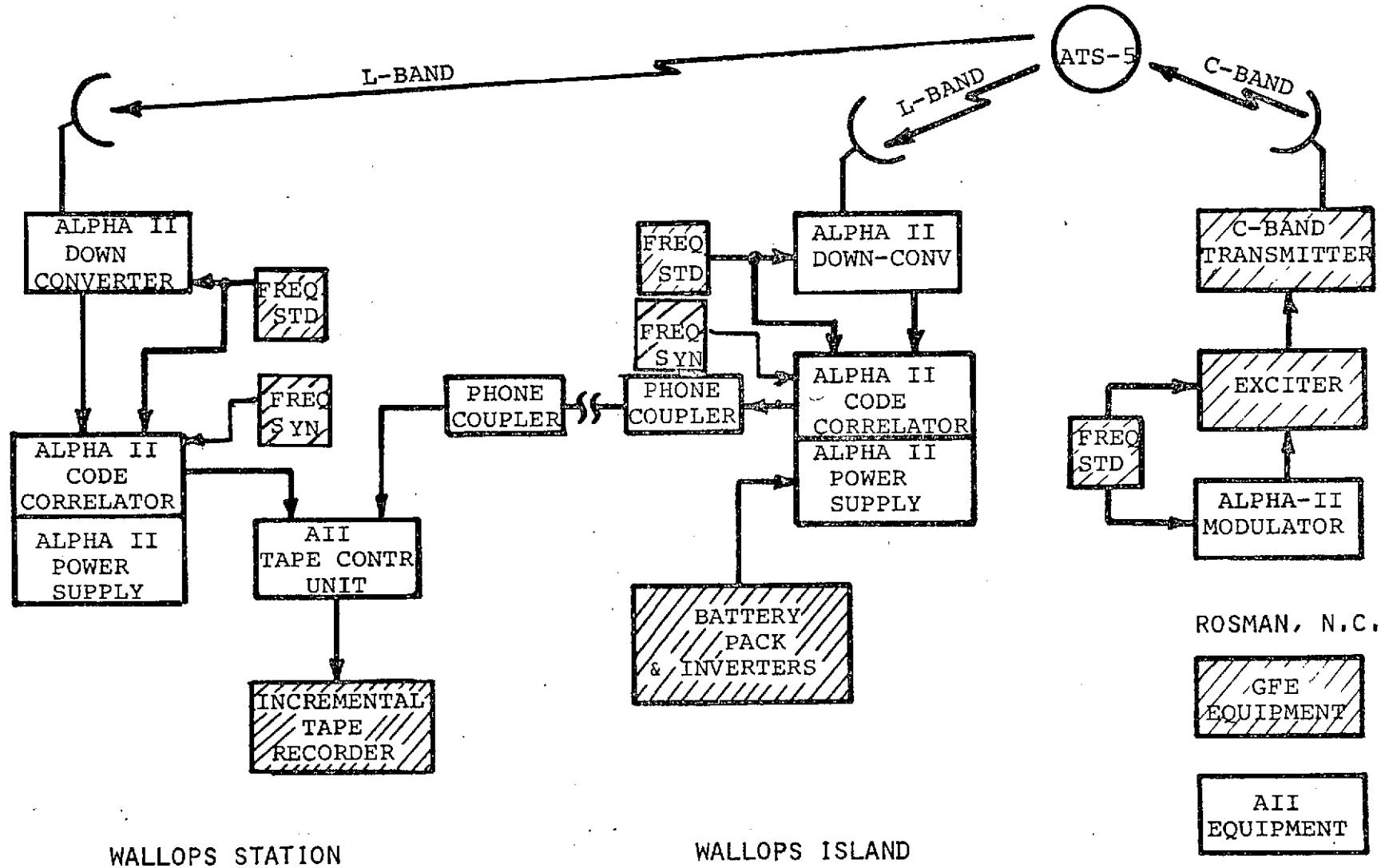
Figure 3-1. Configuration of Experiment

3.2 EQUATIONS FOR RELATIVE RANGING

The relative ranging technique used in this test is a method which yields a line of position of one receiver (B) relative to another, fixed or reference, receiver (A). The information used consists of the ranges measured by the two receivers, R_A and R_B, at the same instance of time, and a calibration curve describing the behavior of the B frequency standard relative to the A frequency standard, the satellite ephemeris, and the location of receiver A.

The complete derivation of the equations for position determination in a relative ranging environment can be found in Appendix B, and are summarized here.

The position of a point on the surface of the Earth can be defined by latitude, longitude and distance to the center of the Earth. (Refer to Figure B-1 in Appendix B.) These coordinates are denoted by ψ, λ and R. The terms A, B and S (used as subscripts) refer to the fixed and movable receivers and the satellite, respectively. In order for a system using range measurements for positioning purposes to determine these variables, an equal number of satellites is required. Therefore, two of these variables (latitude ψ, and geocentric range R) must be assumed when only one satellite is available.

The measurements M_A and M_B are ambiguous measurements of the sum of up-link distance D and down-link distances D_A and D_B. The sums $D + D_A$ and $D + D_B$ are on the order of 2.46×10^8 nsec. The code D is only 204,700 nsec long. Therefore, M_A and M_B represent the excess above the largest integer multiple of the code length not exceeding the distances D_A and D_B, respectively. The geometric range difference $D_B - D_A$ and the measured range difference $M_B - M_A$ are related by

$$D_B - D_A = M_B - M_A + At + B + 45 \text{ ft} \qquad (3-1)$$

where A and B are calibration constants for the rubidium frequency standards and the 45 ft term is the measured fixed bias due to a difference in front end delay of the receivers.

From spherical trigonometry, the range from each receiver to the satellite is given by

$$D^2 = R^2 + R_S{}^2 - 2R R_S \cos \gamma \qquad (3-2)$$

where

$$\cos \gamma = \cos\psi \cos\psi_S \cos (\lambda_S - \lambda) + \sin\psi \sin\psi \qquad (3-3)$$

The procedure is now as follows. The quantity cos γ_A is
calculated for the fixed site and predicted satellite position
from equation (3-3). D_A is obtained from equation (3-2) while
D_B results from equation (3-1). Next cos γ_B is calculated from
equation (3-2) using the known value of R_B. This value, together
with assumed ψ_B permits the determination of λ_B from equation
(3-3). A slightly different value of ψ_B leads to a different λ_B.
Two such pairs of latitude and corresponding longitudes define
the line of position.

The accuracy with which λ_B is determined and in particular the
effect of the uncertainty associated with satellite position are
considered in Section 4. It is shown that the uncertainty in
satellite position, i.e., a 10 x 10 x 10 km box centered at the
predicted satellite position, will introduce a maximum error of
12 feet. If the deivation of predicted position from true
satellite position is consistently in one direction, the differ-
ence will introduce a bias factor. An alternate method of LOP
computation is discussed in Appendix F.

3.3 DATA REDUCTION METHODS

A typical test period consisted of three distinct time periods:

    (a)   Pre-calibration,

    (b)   Ranging on the satellite, and

    (c)   Post-calibration.

Receiver outputs were compared in the satellite mode and in the
local calibration modes. During the calibration modes, when the
two code correlators were co-located, a laboratory modulator
simulated the link from the Rosman transmitter site to the two
code correlators. The modulator was driven by the frequency
standard of receiver A and its code output fed both to correlators
A and B. The initial range values measured by the correlators
reflected the code positions that the correlators were required to
search through, starting from an aribtrary value in the range
counters. This starting value was a random number within the
length of the code, zero to 204,700 nsec (201,337.02 feet). Range
measurements made during the calibration mode were used to model
the phase and frequency drifts between the two rubidium standards.
Interpolation of this curve at the times for which measured
satellite ranges were available yielded a correction factor to
those measurements describing the long-term drift of the standards.
The correlators also acquired their references during this pre-
calibration mode ("reference" being the initial reading of the
code generator at lock-on).

During the periods that ranging data with the satellite were
collected, receiver B was located at the test site near Wallops
Island, while receiver A remained in the laboratory as the fixed
site.

3.3.1 System Calibration

Site Layout

The fixed receiver was located in a building designated F-160 on the main Wallops base. The transportable receiver was located in Building U-15 near the gate to Wallops Island. Table 3-1 summarizes the geodetic position coordinates of these two sites based upon the Fischer Earth Model.

The indicated-altitudes are the sum of local altitudes of the sites above mean sea level and the antenna heights.

Rubidium Standard Calibration

The rubidium standard drift which occurred during any one of the test periods was determined using range data collected during the pre- and post-calibration periods. These data and the times at which the individual data points were collected, were fit to a parabola and to a straight line using a least squares fit. Evaluation of two special 3-hour continuous calibration runs and the individual pairs of calibration sets showed that the straight line fit was preferred. (See Section 4.)

Meaningful calibration of the rubidium standards and evaluation of the ranging measurements on the satellite resulted only when both receivers maintained their code reference during the test period. Loss of reference occurred several times during transportation of the rubidium standards to or from the remote site. It was caused by an interruption in the power or frequency standard feeding the correlator and resulted in a different range number appearing in the range counters. Since the new range difference was not related to the previous range differences, the drift between the standards could not be properly modeled from the data taken.

TABLE 3-1. GEODETIC POSITION COORDINATES OF
RECEIVER SITES (FISCHER EARTH MODEL)

Parameter	Building F-160	Buidling U-15
North Latitude (deg)	37.936409	37.864341
West Longitude (deg)	75.473952	75.507593
Altitude Above Mean Sea Level (ft)	43.52	45.44

Front End Calibration

When each system was switched from the local pre-test calibration mode to ranging on the satellite, bias errors from antennas, receivers and cables connecting each pair of subsystems were introduced.

Tests were conducted on July 16 to assess the additional delay difference due to these error sources. Thus, no absolute measurement was made on the individual antenna-to-receiver links; rather, the difference in delays through these two links was determined.

During those tests, the antennas were co-located on the roof of Building F-160. Care was taken to insure that the elevation and azimuth headings of the antennas were identical and that the antennas were aligned along the same perpendicular (LOP) to the line-of-sight to the satellite. A regular test period was then executed. The data collected was analyzed in the same manner as data resulting from other test periods. When the straight-line fit to the calibration data was removed from the range differences observed on the satellite, a residual of 45 feet remained which represents the delay difference between the two receiver front ends. This fixed bias was removed from all satellite ranging data so that the same internal points on the code correlator were referenced throughout the analysis.

3.3.2 Computer Programs

The range data generated by the two receivers during the entire test period was recorded by an incremental tape recorder (Kennedy Model 1510) on magnetic tape. The data was then analyzed by computer using two programs specifically written for the relative navigation experiment.

The first computer program, the Raw Tape Decoder Program, was used to read and decode the records, one at a time, and convert the binary data to decimal form suitable for further analysis. A standard format data tape was generated at this time containing a listing of the data for preliminary analysis. In particular, the following items were printed out: time, coarse and fine range for both receivers, the range difference, and status data. Measured range is the sum of coarse range, in hundreds of nanoseconds, and fine range, in nanoseconds. Status data recorded consisted of search/track mode, threshold level detected, station and channel number, and calibration or track data.

The second computer program, the Line of Position (LOP) Program, operates on the computer tape generated by the Raw Tape Decoder program. Initially, the LOP program translates the indicated time of each ranging data record, which represents the elapsed time since turn-on of the tape recording system, to Greenwich

Mean Time. All pre-test and post-test calibration range differences are then read and fit to a straight line. Next, sets of approximately 20 consecutive range differences of satellite data are fit to parabolas. Each such parabola is evaluated at its center point in time. The smoothed range difference value is reduced by the calibration line interpolated at this point in time. The remainder is then used to calculate a line of position using the equations described in Section 4. A flow diagram of the Line of Position Program is shown in Figure 3-2.

3.4 SATELLITE CHARACTERISTICS

The spinning ATS-5 satellite is the only satellite of the ATS series containing an L-band transponder and, thus, provided the only vehicle for performing testing in the allocated band for marine/aeronautical service. The ATS-5 satellite is rotating with its directional antennas scanning the Earth approximately once every 780 milliseconds. The 3-dB beamwidth of the satellite antenna provides joint illumination of the transmitting and receiving sites for approximately 52 milliseconds every revolution. This scanning illumination limits the period during which the satellite can relay the up-link signal to approximately 52 milliseconds out of every 780-millisecond rotational period. This is true for both the L-band and C-band transponders.

During the test, a malfunction in the reciever of the L-band transponder necessitated operating the satellite system in a C-band to L-band cross-strap configuration. Normally, the satellite is capable of operating in either a C-band to C-band or L-band to L-band frequency translation mode with a bandwidth of 25 MHz. The cross-strap mode provides reception on either frequency and transmission on the opposite frequency. However, in the cross-strap mode, the bandwidth is limited to approximately 6 MHz. Figure 3-3 illustrates the actual passband characteristic of the satellite when operating in the C-band to L-band cross-strap mode. The measurements were conducted by NASA at the Mojave ground station. The horizontal axis is the transmitter IF frequency and the vertical axis is the output power level normalized to full output power in the L-band, wideband frequency-translation mode.

The ALPHA II down-converter system was designed to receive exactly 1550.0 MHz. The equivalent Rosman transmitter IF frequency for an ATS-5 down-link transmission of 1550 MHz is 69.0495 MHz and examination of the passband characteristics of Figure 3-3 indicate that operation at this frequency would result in a output power approximately 12 dB below normal. Therefore, the Rosman transmitter was required to operate at an IF frequency of 70.1 MHz and the ALPHA II down-converters were offset by slightly more than 1 MHz using a government-supplied frequency synthesizer in the local oscillator injection chains.

INITIALIZE

READ: FIXED STATION COORDINATES
SATELLITE EPHEMERIS
EARTH MODEL, REFERENCE LATITUDES

WRITE: INPUT PARAMETERS

OPERATE ON CALIBRATION DATA

READ: MEASUREMENT DATA, TIME

STOP TIME OR END OF FILE — YES → STOP

NO

UPDATE SATELLITE EPHEMERIS
CORRECT RANGE DIFFERENCE FOR
FREQUENCY STANDARD DRIFT

COMPUTE LONGITUDE GIVEN LATITUDE

LIST OUTPUT

TWO LAT, LONG POINTS ? — NO / YES

Figure 3-2. Flow Chart for Line of Position Calculations
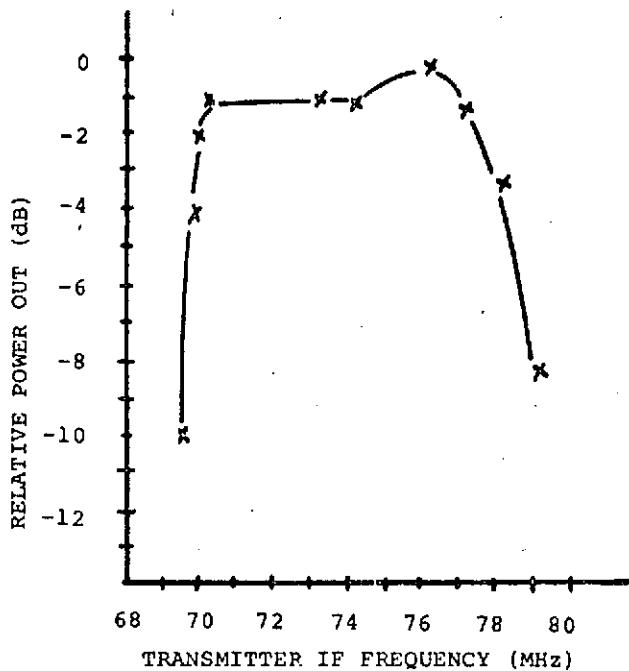
Figure 3-3.   ATS-5 Bandwidth Characteristic in C- to L-band
             Cross-strap Mode

The ATS-5 satellite is in a near-synchronous Earth orbit with a
daily in-orbit excursion between ±2° in latitude, coupled with a
slow drift westwards and a geocentric range variation on the
order of 30 nautical miles. The satellite thus oscillates about
a point near 106°W longitude. The errors in the quoted satellite
position are governed by the accuracy to which its range can be
measured from the NASA Mojave and Rosman tracking stations.

3.5 EXPERIMENTAL PROCEDURE

The experiment hardware configuration at NASA Wallops Station
consisted of two identical receiving systems, a data recording
system and a duplicate of the modulator installed at the NASA
Rosman STADAN transmitting site. A simplified functional diagram
of a single receiving system is shown in Figure 3-4.

The satellite RF signal received by the antenna is applied to
the L-band receiver where the signal is down-converted from 1551
MHz ±12.5 MHz to an IF frequency of 70 MHz ±12.5 MHz and amplified
to a nominal level of 0 dBm. The code correlator demodulates the
signal, extracting the range information. This range data is
processed by the tape control unit of the data recording system
and recorded on magnetic tape. Three identifiable equipment
biases exist which had to be calibrated in order to assure mean-
ingful range readings. These are: (1) the RF front-end bias,
(2) the PN code generator offset, and (3) the frequency standard
drifts.
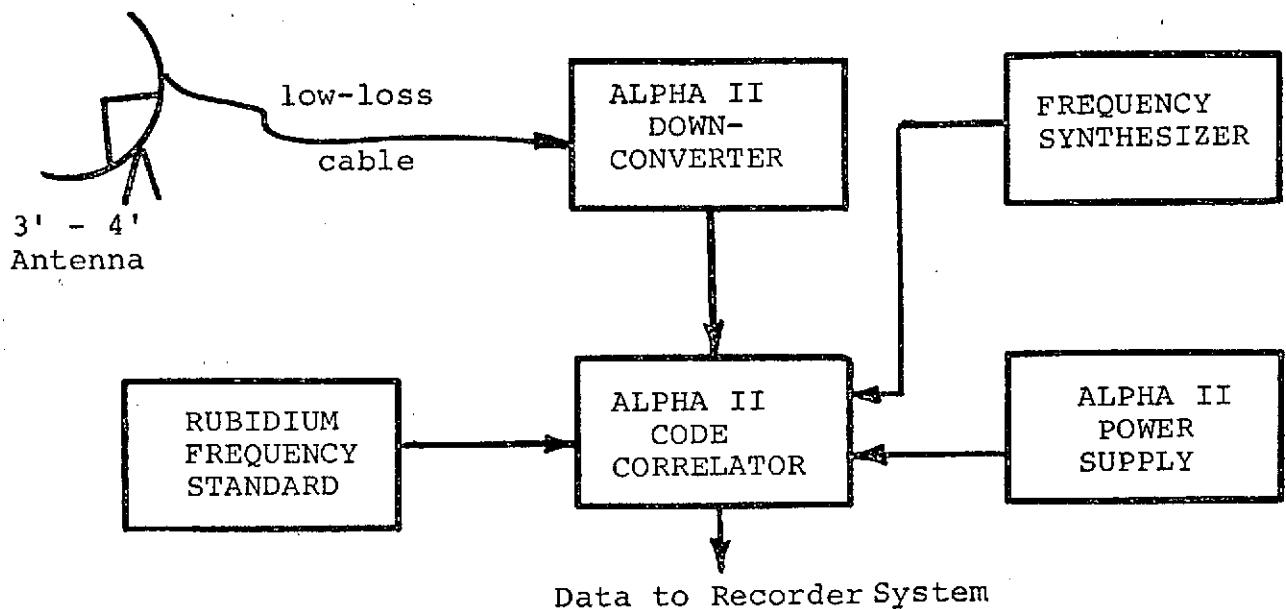
Figure 3-4. Simplified Functional Diagram of
ALPHA II Receiving System

The front-end bias encompasses the difference in signal path
delay from the antenna feed to the input of the code correlator.
This bias is fixed throughout the experiment provided the physical
integrity of the equipment is maintained. The RF front-end bias
can be calibrated, as shown in Figure 3-5, by operating both
receiving systems at the same site with both antennas physically
located with their feeds adjacent on the same line of position.
The resulting data is then processed to determine the magnitude
of the bias.

The bias produced by the PN code generator offset is a random
offset due to the positions of the code-generating shift registers
when power is applied during each test period. This bias is fixed
and will not change if the integrity of the power source and the
frequency source is not violated. However, the two independent
frequency standards drift with respect to each other as a function
of time and, therefore, produce a time dependent bias which must
also be calibrated. The calibration configuration used to deter-
mine both of these biases is shown in Figure 3-6.

The internally generated PN codes are derived from the 14-bit
shift registers in each correlator and the modulator. The cali-
bration mode enables a determination of the daily phase discrep-
ancy between each receiving system. As can be seen in Figure 3-5,
the ALPHA II modulator is used to simulate the transmitted RF
signal. Since the System "A" frequency standard is used to pro-
vide the reference clock to the modulator, the System "A" calibra-
tion reading drifts in direct proportion to the drift between the

```
                        ┌──────────────┐
                        │   ALPHA II   │
                        │  MODULATOR   │
                        └──────────────┘
                               │
                               ▼
                        ┌──────────────┐
                        │    POWER     │
                        │  SPLITTER    │
                        └──────────────┘
                        ┌──────────────┐
                        │  FREQUENCY   │
                        │ SYNTHESIZER  │
                        └──────────────┘

┌────────────┐   ┌────────────┐         ┌────────────┐   ┌────────────┐
│ RUBIDIUM   │   │    CODE    │         │    CODE    │   │ RUBIDIUM   │
│ FREQUENCY  │──▶│ CORRELATOR │◀──    ──▶│ CORRELATOR │◀──│ FREQUENCY  │
│ STANDARD   │   │     A      │         │     B      │   │ STANDARD   │
│    A       │   └────────────┘         └────────────┘   │    B       │
└────────────┘                                            └────────────┘

                        ┌──────────────────┐
                        │ TAPE CONTROL UNIT │
                        │       AND         │
                        │  TAPE RECORDER    │
                        └──────────────────┘
```
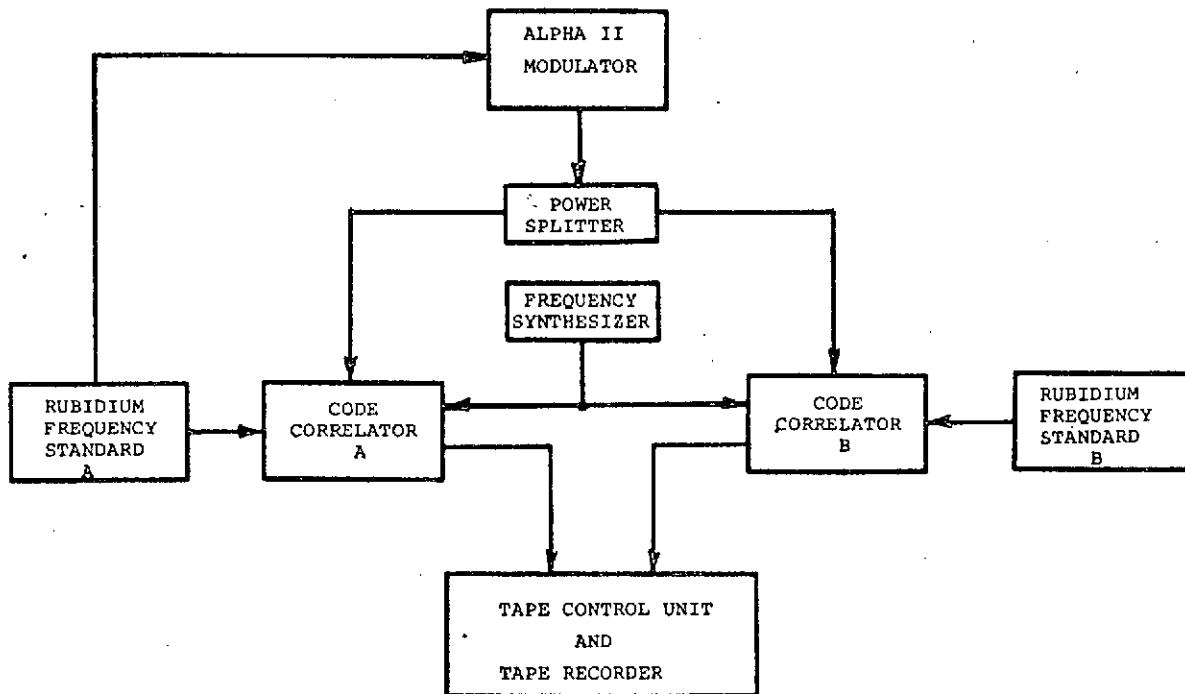
Figure 3-5. Calibration Configuration for Frequency
Standard Drift and Code Offset

two frequency standards, provided power and clock integrity are
not violated. To insure this integrity, the System "B" standard
is operated from its own battery supply and the System "B"
correlator is powered from batteries and DC to AC solid-state
inverters.

At the beginning of each test day the operating condition of
each receiving system was verified. Once normal operation was
demonstrated, both systems were configured in the calibration
mode. After recording the intial system offsets and drift for
approximately fifteen minutes, System "B" was transported to the
remote site just prior to satellite transmission. The first few
minutes of each satellite test period consisted of CW trans-
mission, which was used to maximize signal strength by manually
"tuning" the frequency synthesizer to compensate for the ATS-5
master oscillator offset and drift. The code was then transmitted
to obtain the precision ranging data. Following the transmission
period, System "B" was returned to the fixed site and a second
calibration was performed to determine the total drift of the
frequency standards. Table 3-2 summarizes the events of each
scheduled test day. Tests were performed for 14 out of 16
scheduled test periods for a total satellite use time of 33 hours
10 minutes. The first six completed test periods were conducted
in mid-afternoon, the next four just prior to sunrise and the
remaining tests near 2400 hours local time.
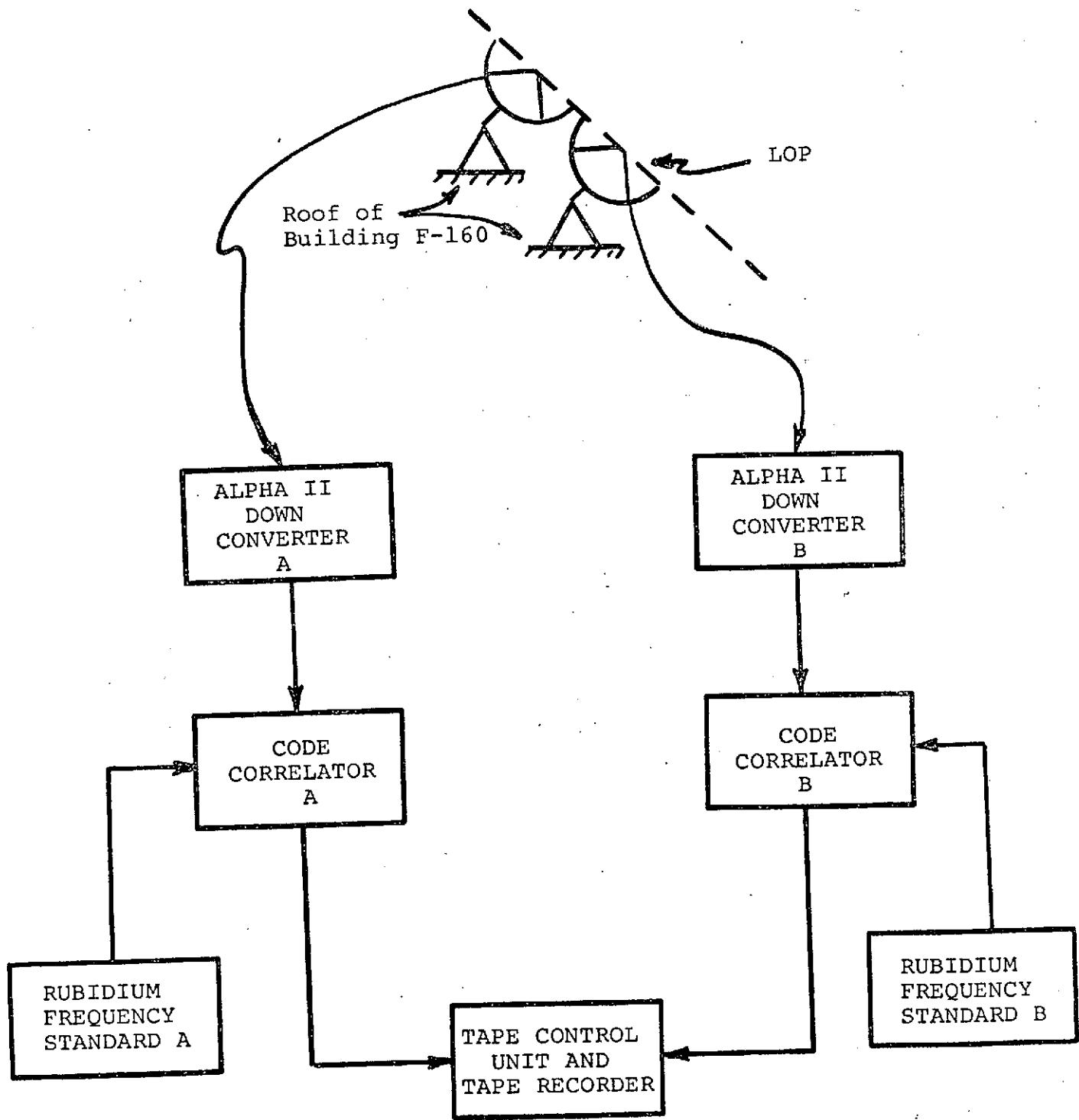
Figure 3-6. RF Front End Bias Calibration Configuration

TABLE 3-2. SUMMARY OF WALLOPS PRECISION POSITIONING TEST PHASE

TEST NO.	DATE/DAY	SCHEDULED TIME (GMT)	ACTUAL TIME	WEATHER	PRE-CAL READINGS A/B (NANOSECONDS)	POST-CAL READINGS A/B (NANOSECONDS)	TIME BTWN CAL.RDNGS (HRS)	OFFSET OF AVG LOP (FEET)	# OF TWTs	CW S/N dB (1.6KHz)	ATS-5 MAST.OSC. FREQ.DRFT (HZ/HR)	SPECIAL NOTES
-	7-7-71-Wed.	2200-0100	CANCELLED -- NASA PRIORITY									
1	7-8-71-Thur	1630-1930	1750-2030	Clear	8290/202047	N.A.	--	--	1	NA	750	1.No remote site 2.Circuit Breaker interruption
2	7-12-71-Mon	1630-1930	1645-1935	Clear	127061/ 45115	127069/47397	3.1	6.9	1	NA	6500	1.Heaters on for one hour before test in ATS-5 2.3-hr rubidium std calibration run
3	7-13-71-Tues	1630-1930	1815-2130	Clear	127070/ 129920	127070/ 116323	8.0	--	1	+18.4	250	1.Heaters on in ATS-5 overnight 2."B" lost reference
4	7-14-71-Wed	1630-1930	1700-2030	Clear	5399/82943	181092/85442	5.0	--	1	+19.8	<250	1.5MHz line to n' Correlator interrupted
5	7-15-71-Thur	1630-1930	1850-2030	Clear	39523/89701	39522/91342	2.8	8.5	1	+16.4	<250	
6	7-16-71-Fri	1630-1930	1700-1930	Clear	140574/ 100779	91597/102875	3.0	45*	1	+16.4	<250	1.Conducted front end bias calibration 2."A" lost reference during remote site test
7	7-20-71-Tue	0630-0830	0730-0830	Clear	196369/ 38330	80498/128446	N.A.	--	1	+18.6	<250	1.Modulator reference lost during test 2.Power down at remote site 3.Phone coupler difficulty.

TABLE 3-2. SUMMARY OF WALLOPS PRECISION POSITIONING TEST PHASE (Continued)

TEST NO.	DATE/DAY	SCHEDULED TIME (GMT)	ACTUAL TIME	WEATHER	PRE-CAL READINGS A/B (NANOSECONDS)	POST-CAL READINGS A/B (NANOSECONDS)	TIME BTWN CAL.RDNGS (HRS)	OFFSET OF AVG LOP (FT)	# OF TWTs	CW S/N dB (1.6KHz)	ATS-5 MAST.OSC. FREQ.DRFT (HZ/HR)	SPECIAL NOTES
8	7-21-71-Wed	0630-0830	0700-0845	Clear	196722/ 131649	196722/ 134074	3.5	1.2	1	+17.6	4750	1.Heaters were NOT on in advance of test in ATS-5
9	7-22-71-Thur	0630-0830	0700-0845	Clear	101265/ 78496	101268/ 23159	3.25	--	1&2	+18.6	300	1."B" ref lost
10	7-23-71-Fri	0630-0830	0700-0845	Clear	149222/ 203669	149233/ 77240	2.33	--	1	+18.8	<100	1."B" ref lost
11	7-26-71-Mon	1300-1600	1300-1600	Cloudy	195624/ 74941	195624/9435	3.85	--	1&2	N.A.		1.Sys "A" would not maintain lock -- no data
12	7-27-71-Tue	1300-1600	1300-1600	Clear	62029/ 143253	62033/145842	4.1	4.6	1&2	+20.6	<250	1.3-hr rubidium std calibration run
13	7-28-71-Wed	1300-1600	1300-1600	Cloudy	135300/ 94875	135299/ 97645	4.5	4.6	1&2	+19.2	<250	
14	7-29-71-Thur	1300-1600	0330-0600	Rain	102965/ 154360	141760/ 166589	3.75	--	1	N.A.		1.Sys "A" reference lost
-	7-30-71-Fri	1300-1600 CANCELLED--NASA PRIORITY--										

*NOTE: The difference in antenna cable lengths and front end delays = 45 feet.

TOTAL ACTUAL ATS-5 TEST TIME = 33 Hours 10 Min

The entries of Table 3-2 are generally self-explanatory. The number in the OFFSET OF AVERAGE LOP column is calculated elsewhere in this report. The S/N measurement was recorded during the CW transmissions for the peak signal strength observed during the burst of signal. The SPECIAL NOTES COLUMN indicates that during six test periods the power and/or frequency integrity of either system A or B or the modulator, which was always the reference, was violated. This was due to either operator error or mechanical deficiency during the transportation of system B to the remote site.

The range reading was measured by the digital subsystem of the receiver code correlator consists of a pulse count which is generated by enabling a counter to accumulate standard clock pulses when the reference PN code is at a specified phase point and stopping the counter when the received PN code is at the same phase point. The resultant count accumulated in the counter is then representative of the time phase difference or the range between the transmitted signal and its point of origin and the received signal and its point of reception. This count can be converted to any suitable unit of measurement by knowing the value contained in the counter and the clock rate which was being accumulated. The lane width of the 10-megabit ALPHA II system is 30 meters (100 nanoseconds). As described in Section 5, a special four-phase clock allows this bit interval to be divided into quarters, giving a granularity of 7.5 meters (25 nanoseconds). Range differences finer than 7.5 meters are resolved by digitizing the D-C voltage appearing at the phase detector output of the correlator with an A/D converter. The complete system is capable of quantizing range readings down to one nanosecond. A front panel display indicates the resultant range reading as it is being measured. The displayed number is indicative of the range in nanoseconds, which is approximately the range reading in feet. The range reading is then formatted and buffered to the magnetic tape control unit for recording.

The tape control unit performs a parity check on the data received from either code correlator. The tape control unit also generates a time signal from the 5-MHz frequency standard which is recorded with each data record. The time signal is an elapsed time measurement from the beginning of the test. The time is expressed in minutes, seconds and tenths of seconds and the total accumulation overflows at 59 minutes, 59.9 seconds. The data record is not written if parity errors are detected in the words received from either correlator.

The first 5 bytes of the 13-byte data record contain the range reading of the fixed receiving site; the second 5 bytes contain the range reading of the remote receiving site, and the last 3 bytes are the time code. Following the 13 bytes, an inter-record gap is generated which will contain the standard LRC check

character. The magnetic tape format for the individual bytes described above is shown in Table 3-3. The range readings are recorded as 8-4-2-1 positive convention BCD digits. The composite "FINE" reading will assume values between 0 and 99 nanoseconds. The composite "COARSE" reading will assume values between 0 and 2,046; this value must be multiplied by 100 to convert to nanoseconds. The total reading is then the decimal sum of the "FINE" and "COARSE" values.

3.6 EXPERIMENTAL ERROR ANALYSIS

The following paragraphs systematically identify and evaluate the various error sources which contributed to the ranging inaccuracy in the position determination experiment. The error calculations are based upon actual measurements or equipment characteristics whenever possible. Certain error sources, e.g., delays due to the troposphere and ionosphere, have effects which can only be estimated. Table 3-4 contains the ATS-5 C-band to L-band link budget calculations based upon the actual equipment used, with the exception that it does not consider the 6 dB loss of signal strength due to the satellite passband constraint. The equivalent S/N ratios observed each day in the CW mode at the fixed receiver site are tabulated in Table 3-2.

The important error sources identified during the experiment include: (1) receiver noise, (2) equipment nonlinearity, (3) quantization, (4) phase alignment of the rubidium standards, (5) multipath, (6) tropospheric delay uncertainty, (7) ionospheric delay uncertainty, (8) atmospheric and galactic noise, (9) satellite position uncertainty, and (10) fixed receiver position uncertainty. These, of course, are further subject to Geometric Dilution of Precession (GDOP).

3.6.1 Signal-to-Noise Ratio

Measurements on the received CW signal indicated that the signal-to-noise ratio (S/N) varied between 16.4 and 20.6 dB in the 1.6-kHz IF bandwidth, which is about 3 dB less than the calculations of the link budget. The tracking loop filter in which the range measurement is made is 50-Hz wide. The S/N of the modulated signal in this filter varied between 21.4 and 25.6 dB. The 10 dB discrepancy is due to a loss of roughly one dB in the transponder output power and about 3 dB due to the satellite antenna rotation. The additional 6 dB loss was due to the 6-MHz filter in the C-band to L-band cross-strap mode in the satellite which had to pass the 10 megabit PN code.

TABLE 3-3.   MAGNETIC TAPE DATA FORMAT

Byte No.	B	A	8	4	2	1	
1	F/40	F/80	Spare B3	Spare B2	Ch.1=1 Ch.2=0	1	Channel A Data
2	F/1	F/2	F/4	F/8	F/10	F/20	
3	C/1000	C/2000	C/4000	C/8000	C/10000	CAL = 1 NORM = 0	
4	C/40	C/80	C/100	C/200	C/400	C/800	
5	C/1	C/2	C/4	C/8	C/10	C/20	
6	F/40	F/80	Spare B3	Spare B2	Ch.1=1 Ch.2=0	0	Channel B Data
7	F/1	F/2	F/4	F-8	F/10	F/20	
8	C/1000	C/2000	C/4000	C/8000	C/10000	CAL = 1 NORM = 0	
9	C/40	C/80	C/100	C/200	C/400	C/800	
10	C/1	C/2	C/4	C/8	C/10	C/20	
11	M/2	M/4	M/8	M/10	M/20	M/40	Time Data
12	S/4	S/8	S/10	S/20	S/40	M/1	
13	S/.1	S/.2	S/.4	S/.8	S/1	S/2	

F/X = Fine Range/BCD X   (X = nanoseconds)

C/Y = Coarse Range/BCD Y   (Y = 100 nanoseconds)

M/A = Minutes/BCD A   S/B = Seconds/BCD B

S/.C = Seconds/BCD.C   All BCD are positive
                                      convention, 8-4-2-1 code.

TABLE 3-4. LINK BUDGET FOR THE ATS-5 SATELLITE, IN THE C-BAND
TO L-BAND CROSS-STRAP MODE

Parameter	6214-MHz Up-Link (85 ft Antenna)	Rosman to Wallops 1551-MHz Down Link	
		3 ft Antenna	4 ft Antenna
Transmit Antenna Gain (dB)	+62.0	+ 14.3	+ 14.3
Transmit Network Loss (dB)	- 1.5	- 1.3	- 1.3
Receive Antenna Gain (dB)	+16.3	+ 20.0	+ 22.6
Receive Network Loss (dB)	- 0.4	- 1.5	- 1.5
Net Antenna Gain (dB)	+76.4	+ 31.5	+ 34.1
Transmitter Power Out (dBW)	+36.0	+ 11.0	+ 11.0
ERP (dBW)	+96.5	+ 24.0	+ 24.0
Free Space Loss (dB)	-199.9	-188.0	-188.0
Atmospheric Loss (dB)	- 0.2	- 0.2	- 0.2
Polarization Loss (dB)	- 3.0	- 0.5	- 0.5
S/C Antenna Point Loss (dB)	- 0.5	-0.3 to -2.3	-0.3 to -2.3
Ground Antenna Point Loss (dB)	- 0.2	- 0.5	- 0.5
Net Propagation Loss (dB)	-203.8	-189.5 to -191.5	-189.5 to -191.5
Received Carrier Power (dBW)	-91.4	-147 to -149	-144.4 to -146.4
Receiver Noise Temp ($^\circ$K)	890°	600°	600°
Receive Antenna Noise Temp ($^\circ$K)	290°	55°	55°
Receive System Noise Temp (dB - $^\circ$K)	30.7	28.2	28.2
Noise Power Density (dBW/Hz)	-197.9	-200.6	-200.6
Carrier/Noise Power Density (dB-Hz)	106.5	51.6 to 53.6	54.2 to 56.2
Receiver Bandwidth (dB)	67.8	32	32
Carrier/Noise Ratio (dB)	38.7	19.6 to 21.6	22.2 to 24.2

NOTE: There is a 6 dB loss in signal not considered in this link budget,
see paragraph 3.4

3.6.2 Internal Errors

Receiver Noise

The correlation function "Z" curve represents the error between received and locally generated codes. This curve is shown in Figure 3-7.

As derived in Appendix D,

$$\sigma_N = \frac{50}{\sqrt{S/N}}$$

The resulting range error corresponding to a signal-to-noise level of 23 dB is then

$$\sigma_N = 3.5 \text{ nsec}$$

$$\approx 3.6 \text{ ft.}$$

Since two receivers were used, the resulting noise error increases by a factor of $\sqrt{2}$, thus $\sigma_N \approx 5.1$ ft.

Correlation Curve Nonlinearity

The correlation curve of Figure 3-7 in reality exhibited certain nonlinear characteristics, as opposed to the idealized characteristics shown. This resulted in a prevalence of certain fine range readings (between zero and 99 nanoseconds) and a relative shortage of other fine range readings. This characteristic was noticeable near the terminal points of the analog-to-digital converter intervals, i.e., (0 and 24), (25 and 49), (50 and 74) and (75 and 99). The values 0 and 24 were recorded much more often than the values 21, 22 and 26. The same situation was observed at 49, 74 and 99 nanoseconds. The error due to this behavior is difficult to determine theoretically. However, laboratory tests indicate that a 2% nonlinearity of the "Z" curve is reasonable. Therefore, $\sigma_c \approx 2$ feet for one receiver or 2.8 feet for two receivers, as used in the test.
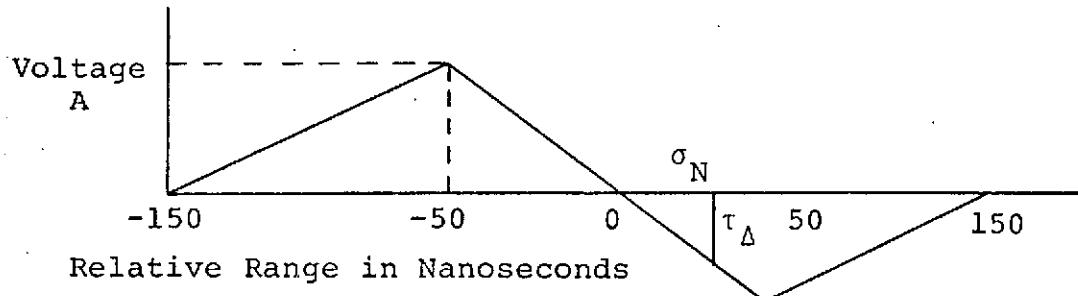
Figure 3-7. Correlation "Z" Curve

Quantization Error

Quantization error refers to the inability to determine the exact location of the correlation maximum which occurs somewhere within the smallest resolvable interval. This interval is 1-nsec wide and represents the nearest value to which range is resolved. Since the correlation maximum can occur anywhere within the $\pm.5$ nsec interval around the measured fine range value, then

$$\sigma_q = \frac{q}{\sqrt{12}}$$

$$= .29 \text{ (ft)}$$

where q = 1 ns.

The $\sqrt{12}$ term results from the assumed uniform distribution over the 1-nsec interval. Since two receivers are used, the error increases by the $\sqrt{2}$, thus

$$\sigma_q = .42 \text{ feet}$$

Phase Alignment Error

In the test configuration, the two rubidium standards drift apart in phase as well as in frequency. The noise on the rubidium standards was estimated on the basis of the typical stability of these standards, 5 parts in 10^{10} per day. The resulting drift per day would then be $5 \times 10^{-10} \times 8.64 \times 10^{13}$ (nsec/day) or 4.32×10^4 nsec/day. The corresponding drift per minute would be 30 nanoseconds, a portion of which is clearly correctable.

Results of 3-hour noise-free calibration runs on July 12 and July 27, yield rms values of 15.9 and 13.2 feet, respectively. These rms values result from the deviations observed about the least squares parabolic fit. However, the rms values are contaminated by the error resulting from the nonlinear correlator. When 2.8 feet is removed from the observed rms values to account for this nonlinearity, the remaining rms due to the two rubidium standards is 15.7 and 12.9 feet for the July 12 and July 27 tests, respectively. The average of the two test periods is 14.3 feet, which is in reasonable agreement with published test data (see Figure 3-8 taken from Reference 3-5). From Figure 3-8 it can be seen that a single frequency standard would yield an error of about 10 feet if the nearest calibration point were an hour and a half away. Thus, with two standards, an error of $\sqrt{2} \times 10$ feet, or about 14 feet, would be expected. Therefore, although the error due to the rubidium standards is clearly dependent on the time from the test to the closest calibration point, it was decided to account for this with a non-time-varying term.
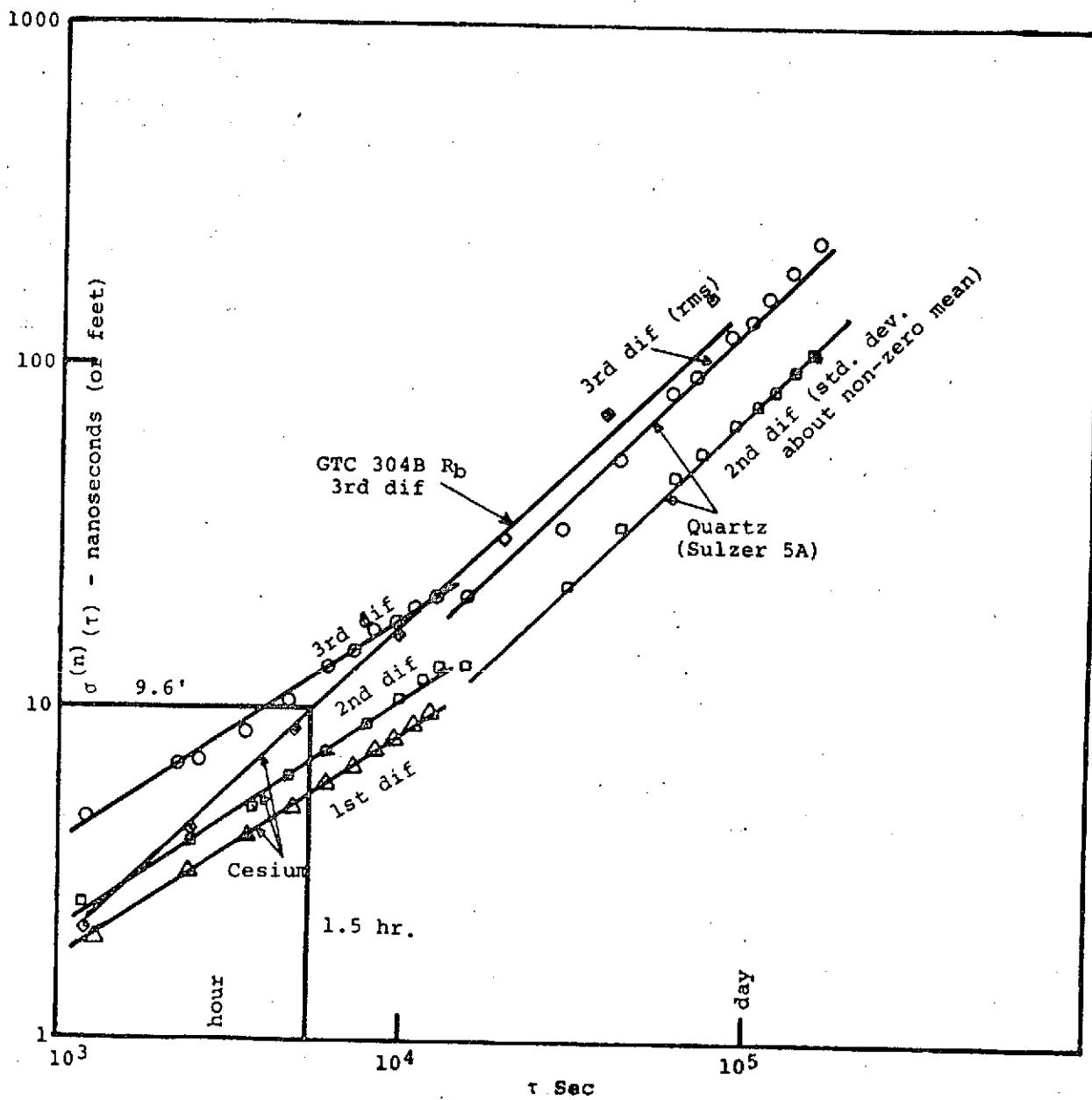
Figure 3-8. Barnes' Variate Difference Data and GTC 304B Rubidium Oscillator Test

3.6.3 Environmental Errors

Multipath

Error due to multipath is caused by the simultaneous reception of the signal over more than one path. One is the direct path, while the others result from reflections. The multipath at Wallops Station is stationary since the reflections are caused by land.

The rms on the range measurement due to multipath is given by (Reference 3-1)

$$\sigma_m = \frac{\rho \ h \ sinE}{\sqrt{G_{SR}}}$$

where ρ is the surface relfectivity (30%), h is the height of the receiving antenna (20 feet for the fixed receiver, 3 feet for the remote receiver), E is the elevation angle (36 degrees) and G_{SR} is the power ratio of main lobe response to side lobe response in the direction of the reflected ray (20 dB). Thus, σ_m is .36 feet for the fixed site, and .05 feet for remote site. In addition, the characteristics of the ranging code itself have a significant effect on reduction of the multipath rejection. However, this effect will not be considered in this analysis.

Tropospheric Delay

The principal measurement error introduced by the ionosphere and troposphere is an increase in the effective path length between the satellite and ground station over the corresponding path length in free space. Part of this refractive delay is predictable, assuming a priori knowledge of the geometry between the ground station and the satellite, time of day and year, sun-spot activity, and surface conditions. A portion of the effect will be unpredictable, varying with anomalies in the ionosphere and troposphere. The following estimates are a condensation of many references which have been reviewed to arrive at a reasonable estimate of both ionospheric and tropospheric delay uncertainties. No attempt has been made to model the tropsopheric delay and, hence, reduce the uncertainty introduced in the range measurements.

The incremental increase in path length due to tropospheric effects is, in comparison with ionospheric effects, quite predictable and independent of carrier frequency in the range of 100 MHz to 10 GHz. The refractivity of the troposphere is given by

$$N = 77.6 \left(\frac{P}{T}\right) + 3.73 \times 10^5 \left(\frac{e}{T^2}\right)$$

where P is total atmospheric pressure in millibars; e is water vapor pressure in millibars; and T is temperature in degrees Kelvin.

The Central Radio Propagation Laboratory of the National Bureau of Standards developed an Exponential Reference Atmosphere model and adopted this model for prediction of refraction phenomena in the troposphere. The results of this model are plotted in Figure 3-9 for two extremes of surface refractivity (N_S) versus elevation angle.

The incremental increase in path length due to downlink tropospheric delay, at an elevation angle (E) of 36°, is

$$\Delta L_T = 14 \text{ feet}$$

The rms variation on this path length is typically taken as 10% of path delay. Hence

$$\sigma_{\Delta L_T} = 1.4 \text{ feet}$$

Both ionospheric and tropospheric inhomogeneities tend to be correlated over small distances with the result that nearly parallel paths tend to suffer equal range-error fluctuations which tend, therefore, to cancel in terms of range difference.
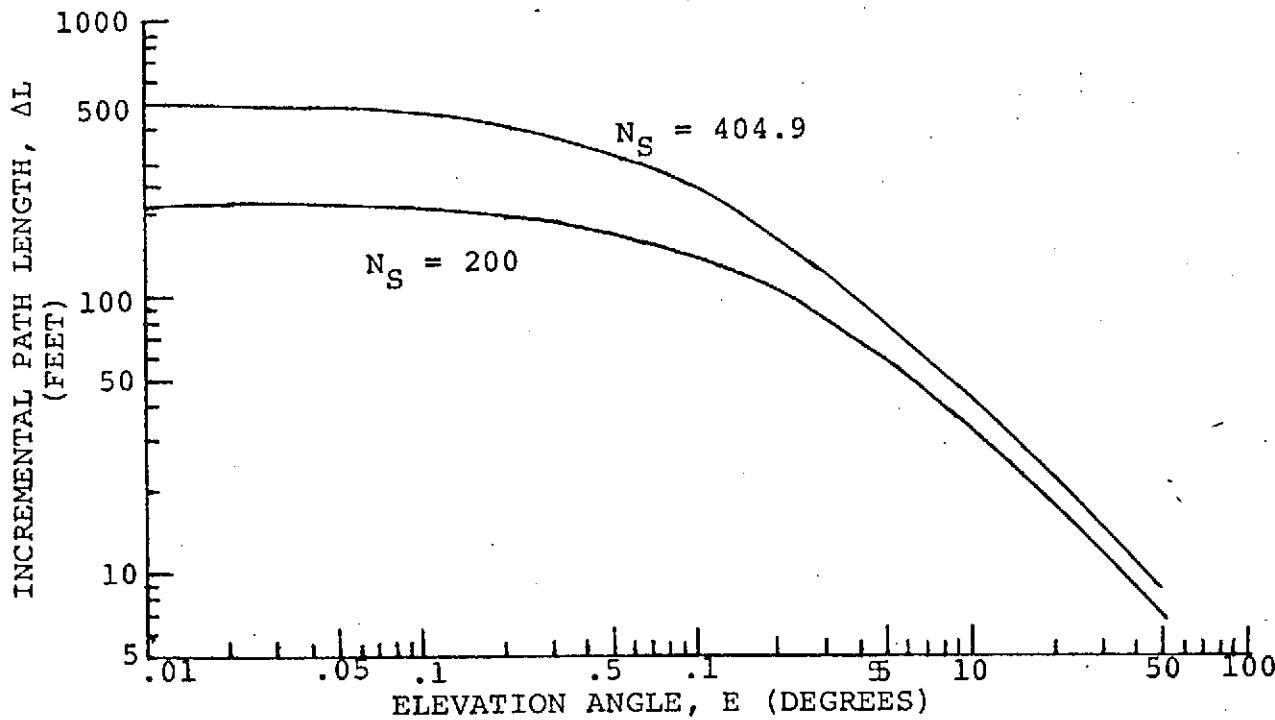
Figure 3-9. Tropospheric Effects; Incremental Path Length vs Elevation Angle

Figures 3-10 and 3-11 indicate the extent of this correlation or range-difference error reduction factor as a function of the range separation. These data were recorded as a part of the National Bureau of Standards series of Maui experiments (Reference 3-7). Figure 3-10 is a plot of interferometer angular error ($\Delta\phi$) due to tropospheric fluctuations. The data is taken in a bandwidth of the order of 10 Hz, but tends to be dominated by very low frequencies below approximately .002 Hz for baselines of interest. For the normal baseline, the angular fluctuations ($\sigma\phi$) is directly related to range difference fluctuation (σ_{RD}) through the baseline B.

$$\sigma_{RD} = B \cdot \sigma_\phi$$

For baseline length of 8 kilometers, $\sigma_\phi \approx 1.5$ µrad so

$$\sigma_{RD} \approx .012 \text{ meters}$$

Figure 3-11 is the range difference directly taken from a similar experiment and indicates for a baseline length of 8 kilometers, $\sigma_{RD} \approx .03$ meters.

The path for these measurements is that from Haleabrela beach on Maui to the island of Lanai and is intentionally chosen as one highly subject to cloud and high wind turbulence, probably among the most inhomogeneous type of air that could be encountered. Similar measurements in Colorado have shown almost an order of magnitude smaller fluctuations.

Thus we conclude that the errors due to the troposphere are negligible in this experiment.

Ionospheric Delay

The incremental path-length difference (ΔL_I) between effective path length and free-space path length, due to ionospheric refraction is

$$\Delta L_I = \frac{40.25 \ N_T \ Q(E)}{f^2} \quad \text{(feet)}$$

where N_T is the total electron content (number/m^2); $Q(E)$ is the obliquity factor, a function of elevation angle (E) to the satellite; and f is the carrier frequency.

The total electron content (N_T) varies about its approximate mean of $10^{17}/m^2$ by at least 30% in the course of a day and also from day to day. Figure 3-12 presents a plot of the variation in incremental path length versus elevation angle for a nominal
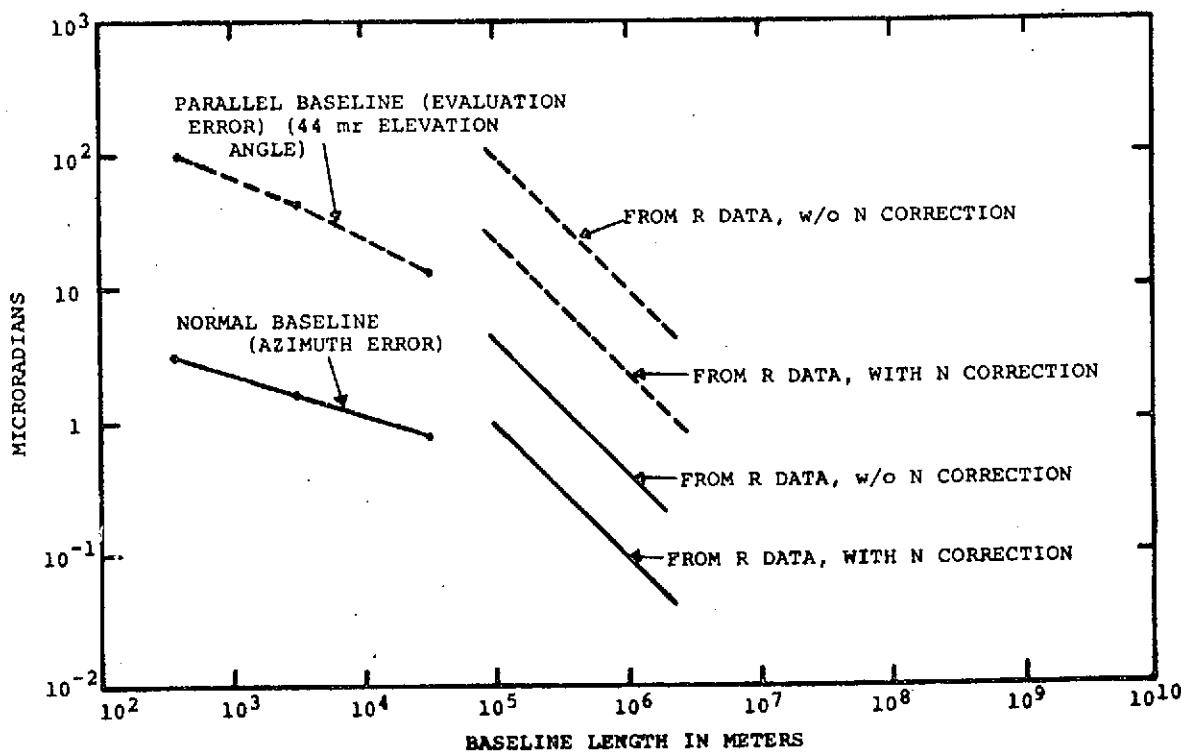
Figure 3-10.   RMS Angular Position Variation vs Baseline Length
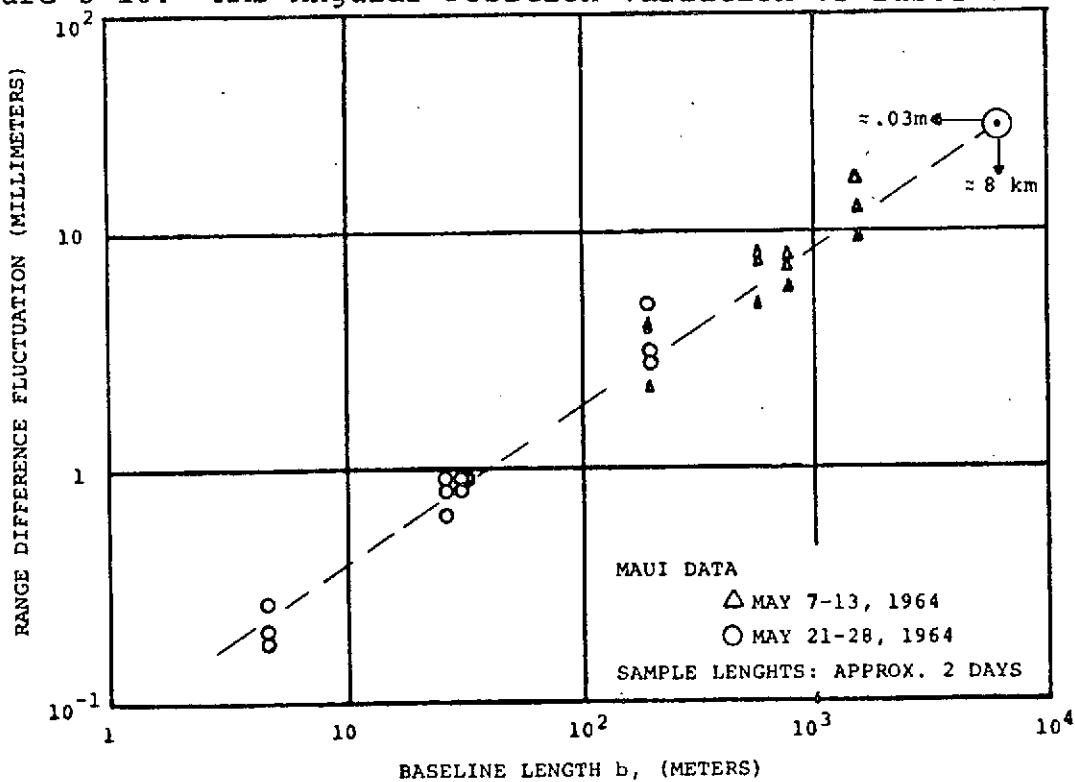
Figure 3-11.   Range Difference Fluctuation versus Baseline Length

value of N_T and extreme N_T values of 0.7×10^{16} and 1.3×10^{18}. The principal variation of N_T in the ionosphere is due to the sun spot number, time of day, season and latitude. In addition, there are day-to-day fluctuations, simultaneous spatial variations due to ionospheric irregularities, and short-term (order of minutes) variations due to motion of the irregularities.

·The uncertainty in N_T at a particular time and placesis estimated to be approximately 30%. This uncertainty includes a $\pm20\%$ day-to-day variation and the uncertainty in smoothed sun spot number. The minimum, nominal and maximum path lengths errors on the down-link can be obtained from Figure 3-12.

$$\Delta L_I = .5 \text{ ft. minimum}$$

$$= 7 \text{ ft. nominal}$$

$$= 100 \text{ ft. maximum}$$

In addition, at any one time there will be a random spatial variation of N_T due to the presence of irregularities in the ionosphere, which is dependent on the distance between the points through which the signal passes, as indicated in Figure 3-13. For this experiment, the fluctuation can be seen to be $\approx 0.1\%$, a negligible value.
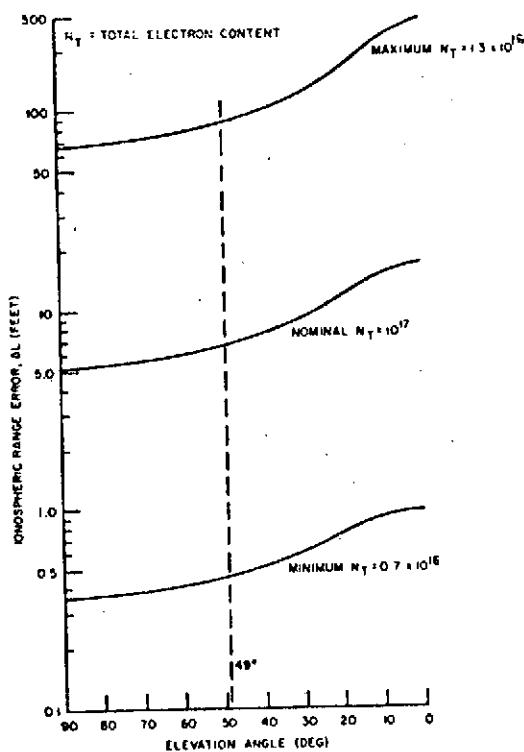
Figure 3-12. Ionospheric Effects at 1600 MHz
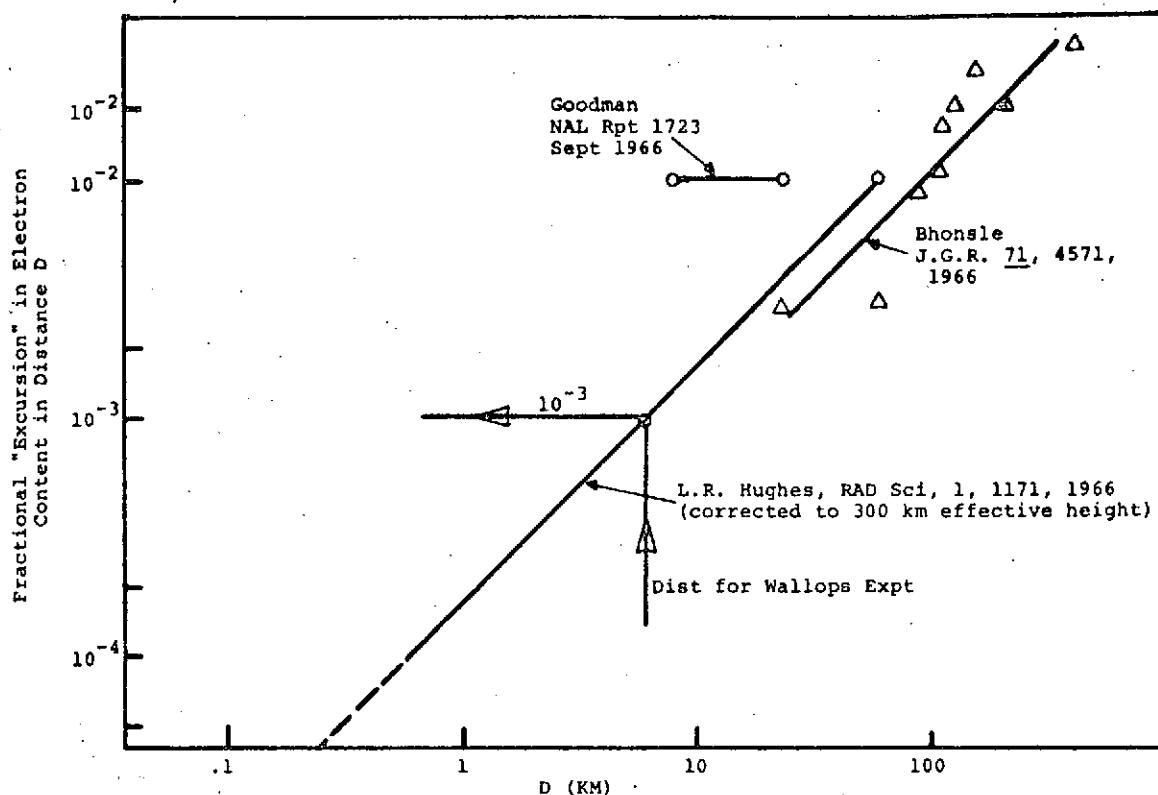
Figure 3-13.   Short Distance Fluctuations in Electron Content

Atmospheric and Galactic Noise

In addition to receiver noise, noise also originates in the
atmosphere from lightning discharges, as well as from electrical
machinery (see Reference 3-3).   However, since receiver noise is
usually the dominant noise source at frequencies above 300 MHz,
atmospheric and galactic noise are neglected in this analysis.

3.6.4   Geometric Errors

Satellite Position Uncertainty

Errors in satellite position are governed by the accuracy to which
the ranges are measured from the Mojave, Calibornia, and Rosman,
North Carolina, ground stations.   The present NASA tracking
procedure can estimate the position of the satellite within a
10 km x 10 km x 10 km box, centered at the predicted point.   The
motion of the satellite relative to the predicted orbit is not
known.

The 10 x 10 x 10 km box would produce an error vector of 8.7 km
from the predicted position to the farthest corner of the error
cube. The angle subtended at the satellite by the 4.7-nmi distance

between the receiver sites is 2.4×10^{-4} radians. Hence, the maximum error due to satellite position is 7.13 feet (8.7 km x 3281 ft/km x 2.4×10^{-4} rad).

Position Error of the Fixed Receiver

The range measurements from the fixed and movable receiver to the ATS-5 satellite, denoted by M_A and M_B, respectively, are ambiguous measurements of the true ranges D_A and D_B. In order to determine the location of the movable receiver with respect to the fixed one, M_A, M_B and D_A are used, with D_A calculated from the geometry. However, the location of the fixed receiver must be accurately known, as well as the location of the satellite. Errors due to uncertainty in satellite position have already been discussed. Since the receivers are located in areas for which type I surveys are available, it is assumed that no new errors are introduced into the relative range measurements by the position of the fixed receiver.

Geometric Dilution of Precision (GDOP)

Geometric dilution of precision refers to the attenuation or amplification of range errors. These range errors contribute to horizontal errors in the computation of receiver position to an extent determined by the relative geometry of the receivers and satellite. GDOP thus is not an error source itself, but represents an error multiplication.

The magnitude of the GDOP is given by 1/cosE, where E is the elevation angle of the satellite. For Wallops Station, the elevation of the ATS-5 satellite is 36 degrees. Hence, the GDOP is 1/cosE, or 1.25.

If σ_R is the rms range error due to all contributing error sources, the rms position error is given by

$$\sigma_{pos} = \sigma_R \times 1.25$$

3.6.5 Position Error Summary

The error sources and the resulting uncertainties are presented in Table 3-5.

Range accuracy is determined as the square root of the sum of the squares of the individual range errors. The position accuracy is then found by multiplying the range accuracy by the GDOP factor. Thus,

$$\sigma_{pos} = 21.3 \text{ feet}$$

TABLE 3-5.   RELATIVE RANGING ERRORS AT WALLOPS STATION

Error Source	Relative Range Uncertainty (ft)
Receiver Noise	5.1
Nonlinear Correlator	2.8
Quantization	0.42
Rubidium Frequency Standard	14.3
Multipath	0.4
Troposphere	Negligible
Ionosphere	Negligible
Satellite Position Uncertainty*	7.0
Survey Error	Negligible
Range Accuracy (RSS)	17.0

*This would be the result of a 10 x 10 x 10 km error which we believe to be high.

REFERENCES

(3-1) Barton, D.K., <u>Radar System Analysis</u>, Prentice-Hall, Inc. 1965, p. 376.

(3-2) <u>Final Report, Phase Difference Navigation Satellite Study</u>, RCA, SEER, NASA ERC, Contract No. NAS-12-509.

(3-3) Davies, K., <u>Ionospheric Radio Propagation</u>, National Bureau of Standards, 1965, p. 310

(3-4) <u>System 621B/ATS-5 Signal Demonstration Test Final Technical Report</u>, Applied Information Industries, USAF SAMSO, Contract No. F04701-70-C-0281.

(3-5) Mollinchrodt, A.J. and Otten, D.D., <u>Oscillator Error Statistics for NAVSAT</u>, TRW Report 08710-6005-T000, August 22, 1967.

(3-6) TRW internal correspondance "Ionospheric Scintillation" A.J. Mallenchrodt, 25 February 1971.

(3-7) Janes, H.B. and Thompson, M.C., <u>An Experimental Study of Atmospheric Errors in Microwave Range and Range Difference Measurements</u>, National Bureau of Standards Report No. 7908.

SECTION 4

EXPERIMENTAL DATA AND ANALYSIS

The experimental test data was measured by the ALPHA II receiving
systems in several test configurations, as described in the
previous section. The calculation of the position of the remote
receiver relative to the fixed known site necessitated calibration
of several equipment characteristics. The results of the calibra-
tion tests, the satellite ranging tests and the resulting calcu-
lated lines of position describing the location of the remote
receiver are presented in this section. An evaluation of the
contribution of several external error sources is also included to
explain the data reduction method.

4.1 SUMMARY OF THE TEST RESULTS

A summary of the complete test cycle is given in Table 4-1, showing
valid LOP test data measured during six test periods. During five
of these test periods the B receiving system was located at the
remote site and data suitable for relative position determination
was collected during those periods.

The sixth fully successful test period was used to calibrate the
receiver front-end delay bias by co-locating the two systems with
the antennas mounted on the same line of position. The average
LOP calculated for this test was 56 feet removed from the fixed
site. Thus, the delay bias between the two systems is 45 feet.

The average calculated LOP's for the five successful test periods
with receiver B located at the remote site are summarized in
Figure 4-1. A statistical summary of these tests is given in
Table 4-2.

The offsets of the average LOP's in Figure 4-1 were measured by
using the scaling factor of one inch equal to 18.23 feet. The
standard deviation (σ) of the LOP's about the average LOP for
each test is also given in Table 4-2.

The estimate of (σ) is obtained from the detailed LOP plots in
Figures 4-6 to 4-10 as follows. The number of individual LOP's
to one side of the average LOP are counted and the LOP corres-
ponding to 2/3 of this total is singled out. The same procedure
is repeated for the LOP's on the opposite side of the average
and the distance between the two selected LOP's is measured. This
distance is assumed to be 2σ.

TABLE 4-1.   SUMMARY OF EXPERIMENTAL TEST CYCLE

July 1971	Test Number	Test Disposition
7		Cancelled - NASA priority
8	1	Circuit breaker interrupt at fixed site - co-located test
12	2	Valid data
13	3	Receiver B lost reference
14	4	Receiver A lost reference
15	5	Valid data
16	6	Front end calibration, co-located test
20	7	Battery of rubidium standard B low; Power failure at remote site, no data link.
21	8	Valid data
22	9	Receiver B lost reference
23	10	Receiver A lost reference
26	11	Equipment problems with receiver A
27	12	Valid data
28	13	Valid data
29	14	Receiver B lost reference
30		Cancelled

Test #	Offset
2	6-9 feet
5	8-5
8	1-2
12	4-6
13	4-6

Latitude
Degrees

37.864343

37.864300

37.864253

Remote Site

Test Number   2 13   8   12   5

75.507600   75.507500   75.507400   75.507300
Longitude, Degrees
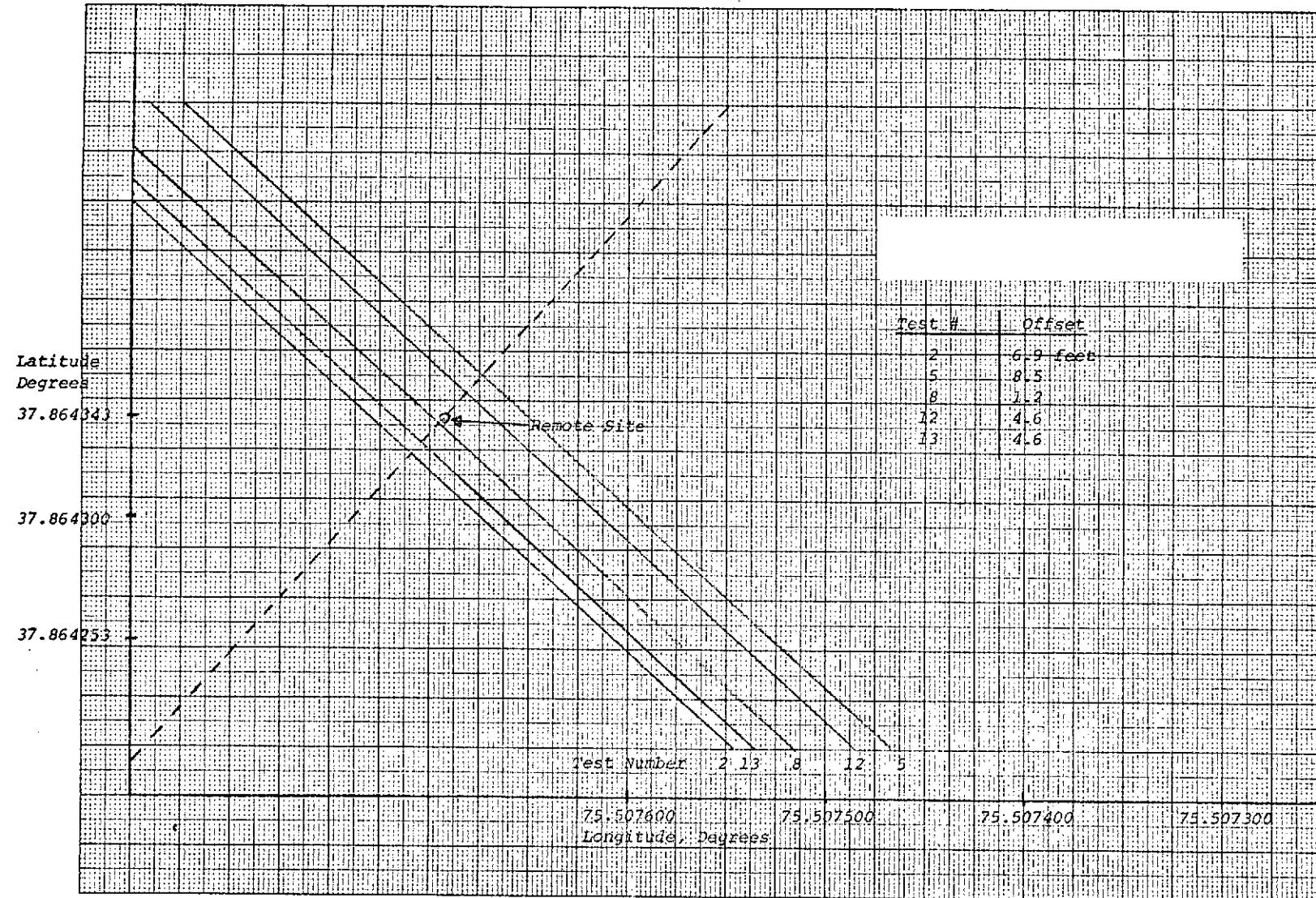
Figure 4-1.   Average LOP's for Test Periods 2, 5, 8, 12 and 13

TABLE 4-2. SUMMARY OF TEST DATA

Test	Date	Offset of Average LOP (ft)	Rms (ft)	GMT
2	July 12	6.9	25.88	1856-1930
5	July 15	8.5	31.63	1702-1734
8	July 21	1.2	16.77	0759-0845
12	July 27	4.6	33.26	0131-0403
13	July 28	4.6	30.52	0200-0402

4.2 CALIBRATION OF RF FRONT END BIAS

On July 16, both complete receiver systems, including antennas, were co-located at the fixed site in order to determine the relative delay due to the front ends. This test was important since any delay resulting from these systems, if uncorrected, would affect the determination of the lines of position, resulting in a bias on the LOP's.

The antennas were placed on the roof of Building F-160 and physically aligned along the same perpendicular (LOP) to the line of sight to the satellite and matched in azimuth and elevation. A normal satellite test period was then performed.

The pre- and post-calibration periods were fit to a straight line in the least squares sense. The average difference in feet between the data taken on the satellite and the calibration line was then determined. This average was 45 feet, with a spread from 30 feet to 61 feet. The corresponding lines of position in Figure 4-2 were obtained by projecting the observed differences just defined through the elevation angle along the line of sight to the satellite. Since the position predictions of the ATS-5 satellite were not used in determining the receiver front-end delay bias, inaccuracies associated with the ephemeris are eliminated.

4.3 CALIBRATION OF THE FREQUENCY STANDARD DRIFT

Proper modeling of the relative drift in frequency and phase between the two rubidium standards is the most important step in the determination of the lines of position. Prior to the tests, it was assumed that the relative drift in frequency was significant. Since measurement of distance was sought, it was decided to model the relative behavior of the rubidium standards by a least squares
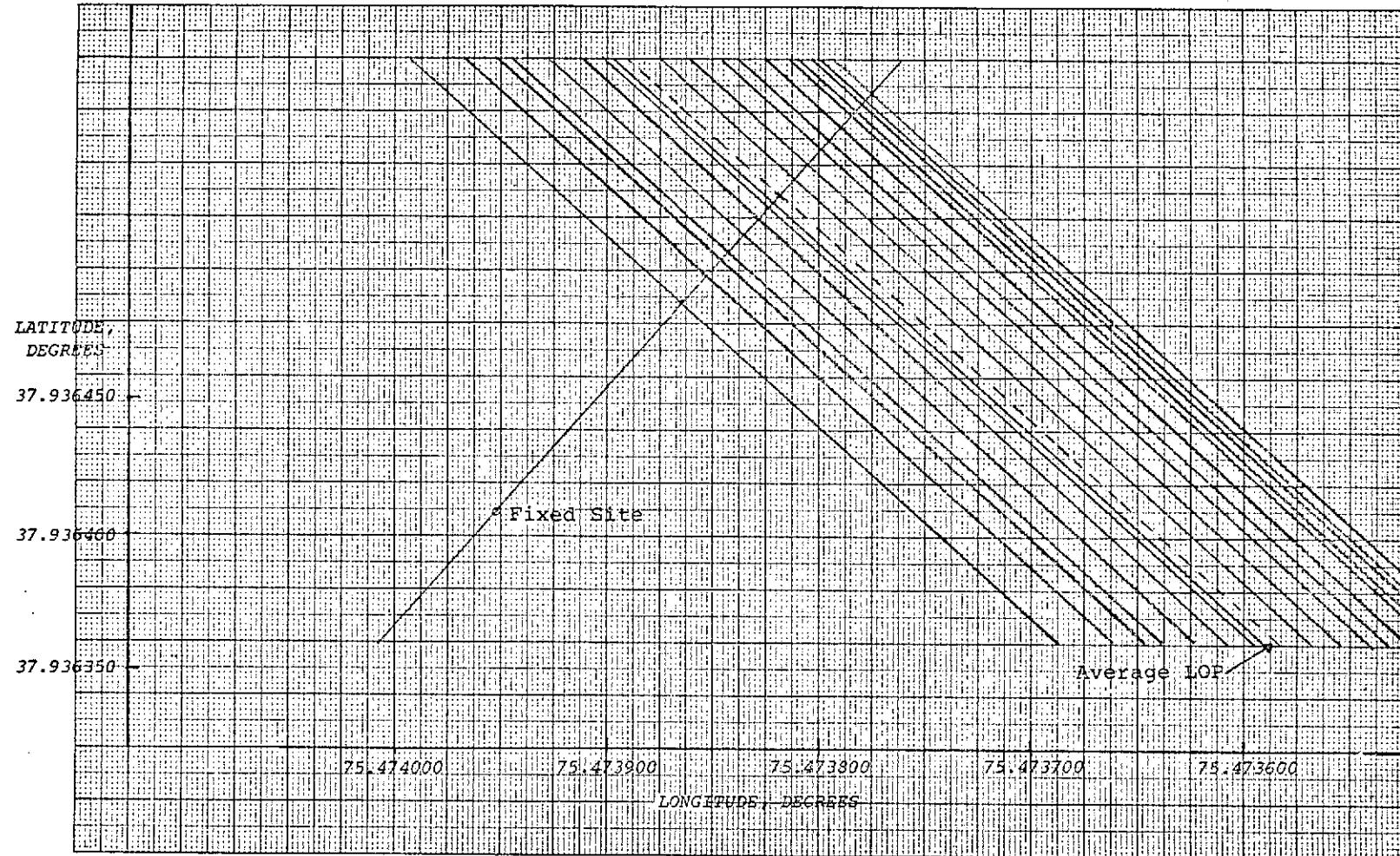
Figure 4-2.   Test 6 LOP's RF Front End Bias Calibration

parabola ($At^2 + Bt + C$), where the quadratic term in time represents the frequency drift, the linear term in time the phase drift, and the constant represents the initial offset between the range measurements of the two receivers. In order to test this hypothesis, two special 3-hour calibration test periods were conducted on July 12 and July 27, respectively. The parabolas were based on 4789 and 5000 contiguous points, respectively. The resulting coefficients calculated from the test results are presented in Table 4-3.

These test results show that the quadratic coefficients were very small compared to the linear coefficient, being 4.5 and -6.3 feet in three hours, versus -1644.9 and -1952.4 feet. It is, therefore, concluded that the rubidium standards did not drift relative to each other in frequency.

The same model was also used to fit the calibration data of the various experimental test periods. A typical test resulted in the following parabola.

$$P_2 (t) = 10.3t^2 - 732.8t + 93217.0$$

(Test 2 based on 712 points)

On both July 12 and July 27, a normal satellite test period was executed in addition to the special 3-hour calibration runs. The quadratic coefficient observed in the satellite test was two orders of magnitude larger than for the 3-hour calibration runs.

To understand the cause of this conflicting result and obtain a better model, the 3-hour calibration run of July 27 was subjected for further analysis. To simulate a satellite test sequence, the first 38 data points of the calibration run were entered as time and observed range difference, and 94 points, beginning almost 3-hours later, were entered into the curve-fitting routines, thus simulating the discontinuity that occurs in an actual satellite

TABLE 4-3. COEFFICIENTS OF LEAST SQUARES FIT PARABOLA*
FROM SPECIAL 3-HOUR CALIBRATION TESTS OF
RUBIDIUM STANDARDS

Date	Number of Points	A	B	C	Rms (ft)
July 12	4789	.5	-548.3	78114.0	15.9
July 27	5000	-.7	-650.8	62877.0	13.2
*At^2 + Bt + C, where t is in hours					

test period. The total number of points entered (132) was typical for an average satellite test period. The time interval between sets was smaller than for a typical satellite test period. The least squares parabola and least squares straight line were then calculated based upon this set of 132 points. The continuous data resulting from the three-hour test was also entered. All three functions, namely,

- the least squares line - L(t) $\quad = \quad 62,876.6 - 650.92t$

- the least squares parabola - P(t) $\quad = \quad 62,878.5 - 733.31t + 27.48t^2$

- and the 3-hour parabola - O(t) $\quad = \quad 62,877.0 - 650.8t - .7t^2$

were evaluated for a continuous set of points for which difference readings were available. The selected set was near the center of the time interval. The results are given in Table 4-4. Time and difference readings are given in Columns 1 and 2. The parabolic fits, namely the ones based on 5000 and 132 points are given in Columns 3, 4, 5 and 6. The deltas from the observed range differences are also given. The last two columns represent the straight line fit.

The P(t) parabola differs from the observed range differences by 40 to 70 feet but the straight line fit and the original parabola based upon the continuous data set do not differ from the observed range difference readings by more than about 15 feet. Thus, it was concluded that the parabola is not a good fit to drift characteristics of this standard.

The data points collected in the pre- and post-calibration periods were then fit to a straight-line model of the frequency standard drift. The individual lines are summarized in Table 4-5.

The rms values about the moving mean are also shown in Table 4-5. The rms noise for Test 8 is large. The pre- and post-calibration periods are shown in Figures 4-3 and 4-4, respectively. The pre-calibation is very noisy due to an improper threshold setting in code correlator B. The rms for Test 13 is also larger than expected; however, in this case the range difference did not decrease at a near-constant rate. The range difference remained nearly constant for periods as long as two minutes in some instances, while during other 2-minute time spans the range difference decreased at nearly 1000 nsec/hour.

Figure 4-5 shows the pre-calibration data for Test 2. The calibration line is also shown. This figure is typical of the calibration data observed during the other satellite test periods.

TABLE 4-4. LINEAR AND PARABOLIC LEAST SQUARES FITS TO TEST DATA FROM THE THREE-HOUR JULY 27 CALIBRATION RUN

| Time | Difference Reading | Parabolic Fits | | | | Linear Fit | |
| | | 5000 Points | | 132 Points | | 132 Points | |
hr min sec	8 ft	Value	Observed -O(t)	Value	Observed -P(t)	Value	Observed -L(t)
1 27 48.4	61920.7	61923.1	-2.37	61864.2	56.54	61924.0	-3.26
1 27 49.5	61948.2	61922.9	25.33	61864.0	84.24	61923.8	24.44
1 27 50.0	61944.3	61922.8	21.52	61863.9	80.43	61923.7	20.63
1 27 50.5	61941.4	61922.7	18.71	61863.8	77.62	61923.6	17.82
1 27 51.1	61919.7	61922.6	-2.88	61863.7	56.03	61923.5	-3.77
1 27 52.6	61924.6	61922.3	2.29	61863.4	61.20	61923.2	1.40
1 27 53.2	61931.5	61922.2	9.30	61863.3	68.21	61923.1	8.40
1 27 54.2	61986.6	61922.0	64.58	61863.1	123.47	61922.9	63.69
1 27 55.3	61929.6	61921.8	7.78	61862.9	66.69	61922.7	6.88
1 27 56.3	61935.5	61921.7	13.86	61862.7	72.77	61922.6	12.97
1 27 57.4	61934.5	61921.5	13.06	61862.5	71.97	61922.4	12.16
1 27 59.5	61931.5	61921.1	10.44	61862.2	69.25	61922.0	9.54
1 28 00.0	61934.5	61921.0	13.53	61862.1	72.44	61921.7	12.63
1 28 01.6	61937.4	61920.7	16.72	61861.8	75.63	61921.6	15.82
1 28 02.1	61927.5	61920.6	6.91	61861.7	65.92	61921.5	6.11
1 28 03.7	61918.7	61920.3	-1.60	61861.4	57.31	61921.2	-2.50
1 28 04.2	61921.7	61920.2	1.49	61861.3	60.40	61921.1	.59
1 28 04.7	61905.0	61920.1	-15.12	61861.2	46.80	61921.0	-16.02
1 28 06.8	61904.0	61919.8	-15.73	61860.8	43.18	61920.7	-16.64
1 28 08.9	61898.1	61919.4	-21.25	61860.5	37.66	61920.3	-22.16
1 28 09.4	61919.7	61919.3	.44	61860.4	59.35	61920.2	- .47
1 28 10.5	61917.8	61919.1	-1.26	61860.2	57.65	61920.0	-2.17

TABLE 4-4. LINEAR AND PARABOLIC LEAST SQUARES FITS TO TEST DATA FROM THE THREE-HOUR JULY 27 CALIBRATION RUN (Continued)

Time hr min sec	Difference Reading .8 ft	Parabolic Fits				Linear Fit	
		5000 Points		132 Points		134 Points	
		Value	Observed -0(t)	Value	Observed -P(t)	Value	Observed -L(t)
1 28 13.6	61900.0	61918.5	-18.50	61859.6	40.41	61919.4	-19.41
1 28 14.1	61916.8	61918.4	-1.61	61859.5	57.30	61919.3	-2.52
1 28 15.7	61910.9	61918.1	-7.22	61859.2	51.69	61919.0	-8.13
1 28 16.2	61928.6	61918.0	10.57	61859.1	69.48	61919.0	9.66
1 28 16.8	61922.7	61917.9	4.78	61859.0	63.69	61918.8	3.87
1 28 17.8	61898.1	61917.8	-19.64	61858.9	39.27	61918.7	-20.55
1 28 18.3	61904.0	61917.7	-13.65	61858.8	45.26	61918.6	-14.56
1 28 18.9	61917.8	61917.6	.26	61858.7	59.17	61918.5	- .56
1 28 19.9	61917.8	61917.4	.44	61858.5	59.35	61918.3	- .47
1 28 20.4	61897.1	61917.3	-20.17	61858.4	38.74	61918.2	-21.08
1 28 21.0	61911.8	61917.2	-5.36	61858.3	53.55	61918.1	-6.27
1 28 21.5	61915.8	61917.1	-1.27	61858.2	57.64	61918.0	-2.18
1 28 23.1	61910.9	61916.8	-5.88	61857.9	53.03	61917.7	-6.79
1 28 23.6	61915.8	61916.7	- .89	61857.8	58.02	61917.6	-1.80
1 28 25.2	61913.8	61916.4	-2.60	61857.5	56.31	61917.3	-3.51
1 28 25.7	61920.7	61916.3	4.39	61857.4	63.30	61917.2	3.48

TABLE 4-5.   STRAIGHT LINE FIT* TO THE CALIBRATION DATA

Test	Date	A	B	Rms (ft)
2	July 12	-547.54	89660.22	14.02
5	July 15	-618.84	-38074.84	18.43
8	July 21	-673.28	68018.83	75.13
12	July 27	-605.74	-79019.48	10.45
13	July 28	-638.78	39765.47	10.25
*At + B (t in hours)				

4.4   CALCULATED LINES OF POSITION

The data for the satellite test periods are tabulated in Appendix
A and the resultant lines of position are plotted in Figures 4-6
through 4-10.   These figures are Mercator projections; thus, any
measurement of length made on these figures is directly related
to change in latitude.   The scale used is one inch in latitude
(.000050 degree) equals 18.23 feet.

In each figure, the remote site is indicated at latitude 37.864343
degrees and longitude 75.507593 degrees.   The two other latitudes
shown are the assumed reference latitudes of 37.864300 and 37.864253
degrees used in the calculations.

The longitudes of the LOP's were calculated for each of these
latitudes.   The average LOP for the complete test period is
indicated as the dashed line.   This average LOP results from
averaging the sets of longitudes pertaining to each reference
latitude.   The azimuth heading from north for all LOP's is
approximately 132 degrees.   The line perpendicular to the LOP's
is the line of sight to the satellite.

The LOP's presented in Figures 4-7 through 4-10 are based on
approximately twenty successive range differences which were fit
to a parabola.   Thus, the noise on the range differences has been
smoothed to some extent.   Any reference to time has been lost in
these figures in that they show latitude versus longitude.   Since
the headings of the LOP's are all approximately 132 degrees from
true north, any LOP is equally well defined by the longitude at,
for example, the reference latitude of 37.864253 degrees.   The
longitude at the other reference latitude of 37.864300 degrees
exceeds the first longitude by .000063 degree.   It is then possible
to plot longitude versus time as is done in Figures 4-11 through
4-15 for Tests 2, 5, 8, 12 and 13 for the first 30 minutes of each
test.   The indicated longitudes are still the result of smoothing

4-10
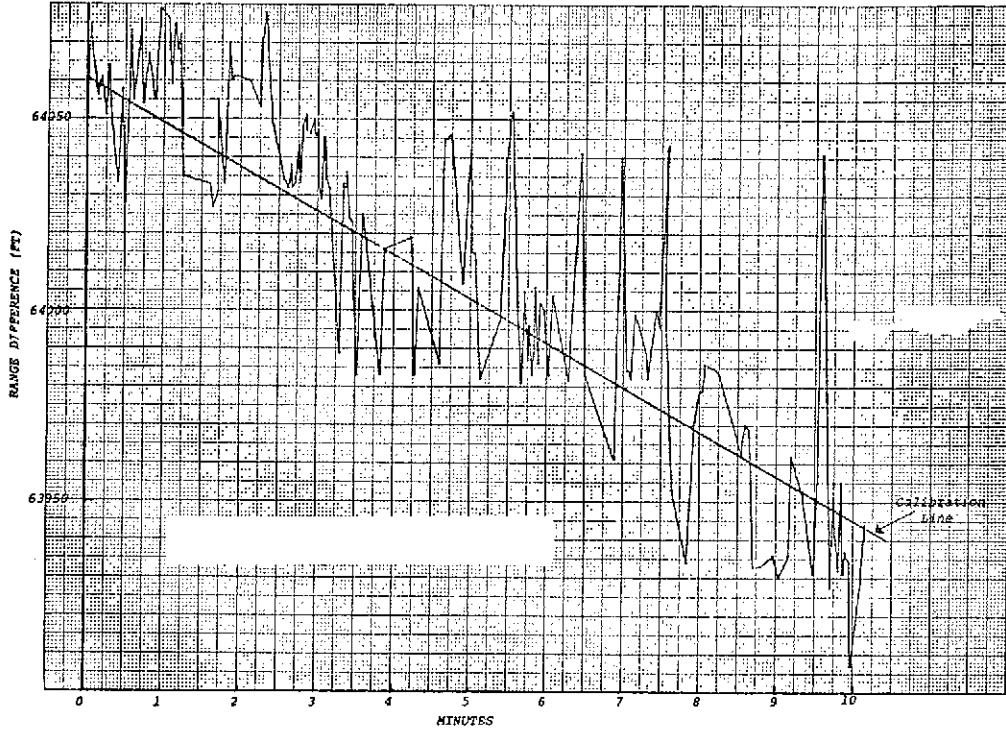
Figure 4-3.   Test 8 Precalibration Data
Reference Time: 0 = 5:50:09.2 GMT
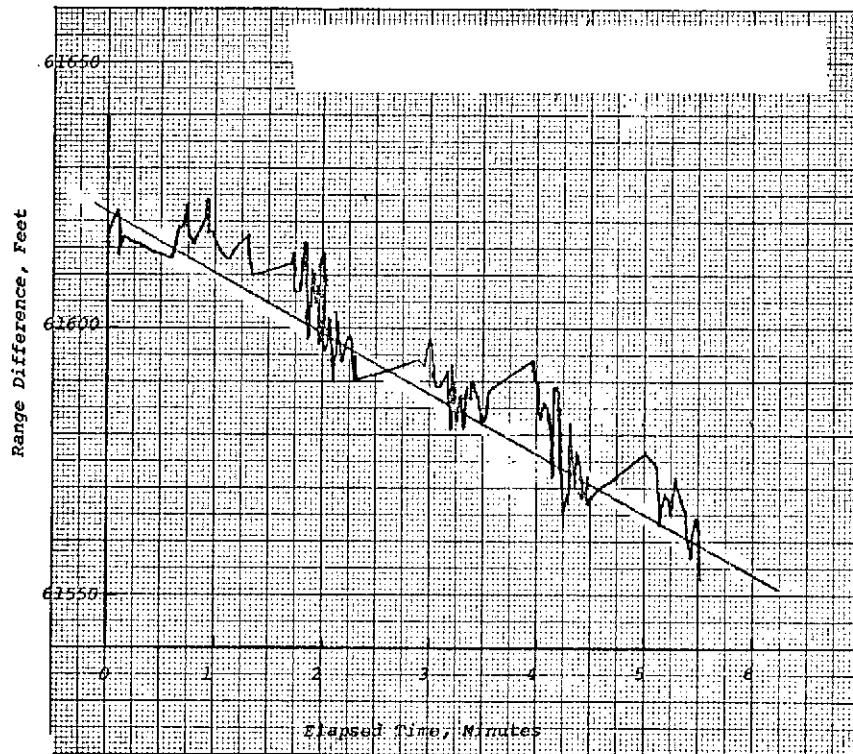
Figure 4-4.   Test 8 Post-Calibration Data
Reference Time: 0 = 9:25:54.3 GMT

Figure 4-5.   Test 2 Pre-Calibration Data
Reference Time: 0 = 16:31:37.9 GMT

a group of successive measured range differences (ΔR).   Figures
4-16 and 4-17 are also plots of longitude versus time.   However,
each longitude indicated is the result from one range difference.
Hence, no smoothing was done on this data.   A set of successive
ΔR's were analyzed for Test 2 (Figure 4-16) and two sets of
successive ΔR's for Test 12 (Figure 4-17).   Twenty successive
longitudes in these figures describe the structure within one LOP
or longitude in Figures 4-11 and 4-15.   The data for all these
figures is presented in Appendix A.

Consider now a configuration in which a user wishes to determine
his position (LOP's relative to one or two satellites) in a short
period of time.   In particular, we are addressing relative navigation
for a ship.   If σ_R represents the position error on the surface of
the Earth, while σ_S represents the permissible error in the LOP's
and if

$\sigma_S \geq \sigma_R$ then one measurement suffices; or if

$\sigma_S < \sigma_R$ then N = $\dfrac{\sigma_R^2}{\sigma_S^2}$ measurements are required.

The reduction in error as a function of integration time or number
of samples is schematically depicted in Figure 4-18.

4-12
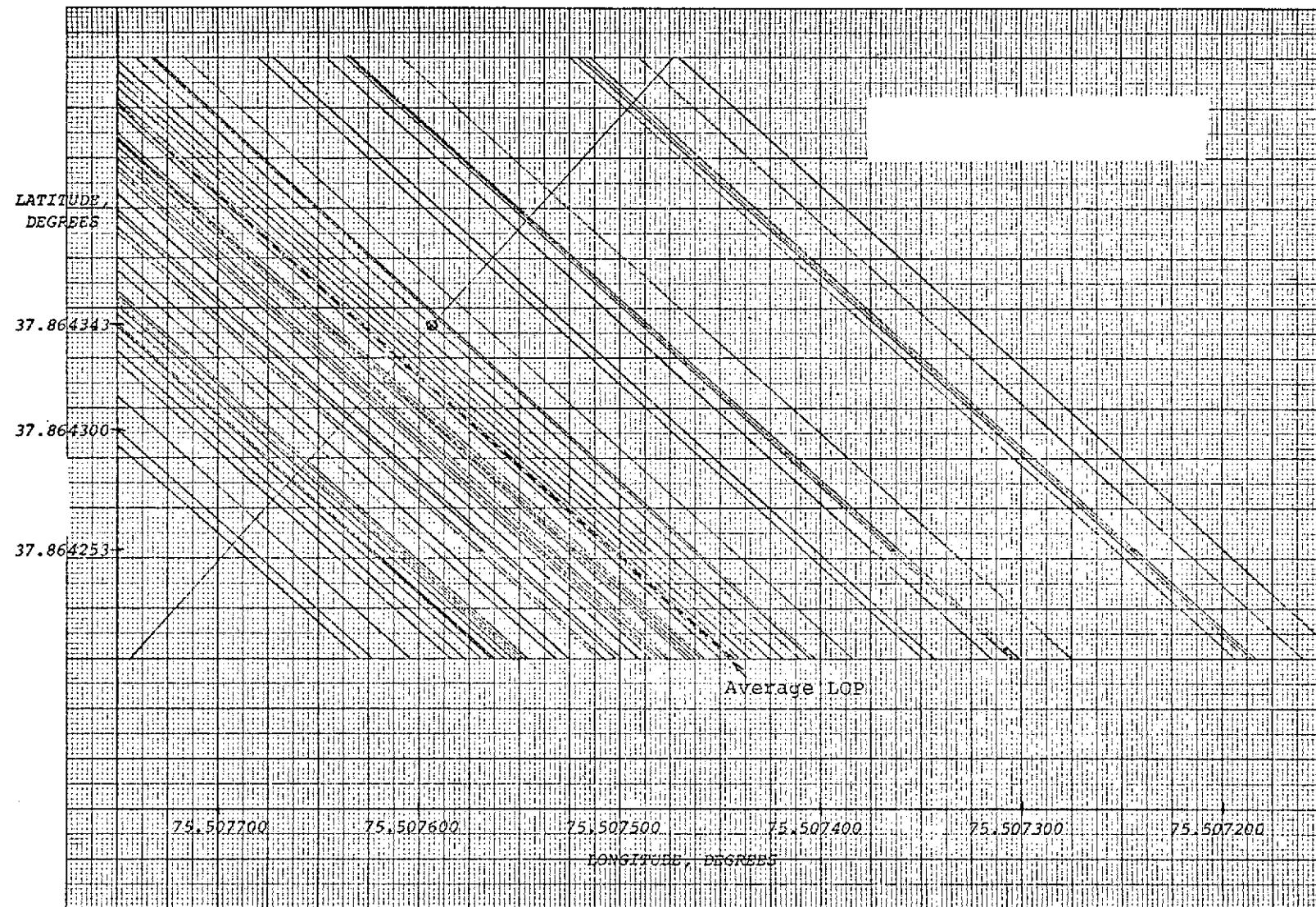
Figure 4-6. Test 2 LOP's; Remote Site = ⊙
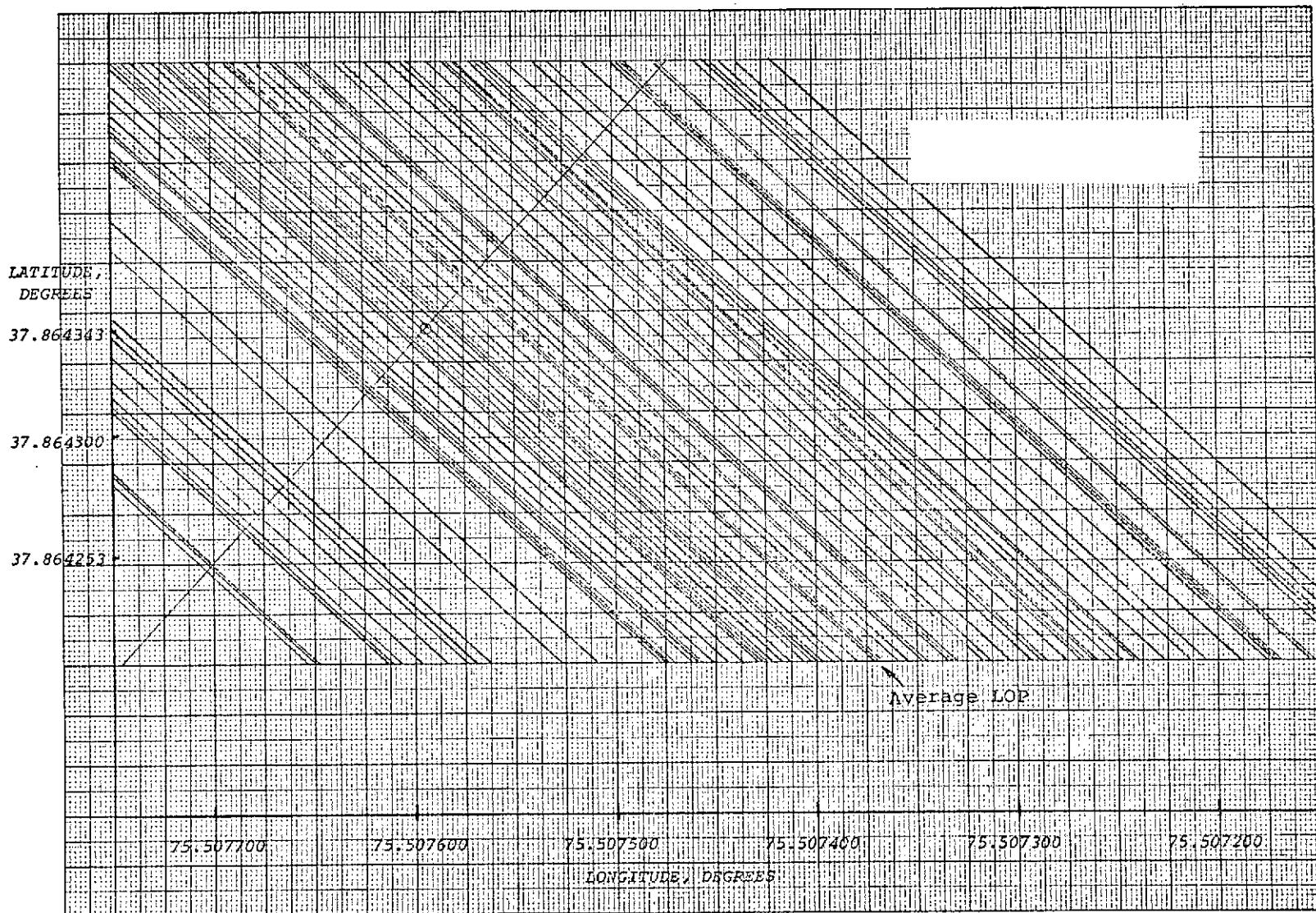
Figure 4-7.   Test 5 LOP's; Remote Site = ⊙
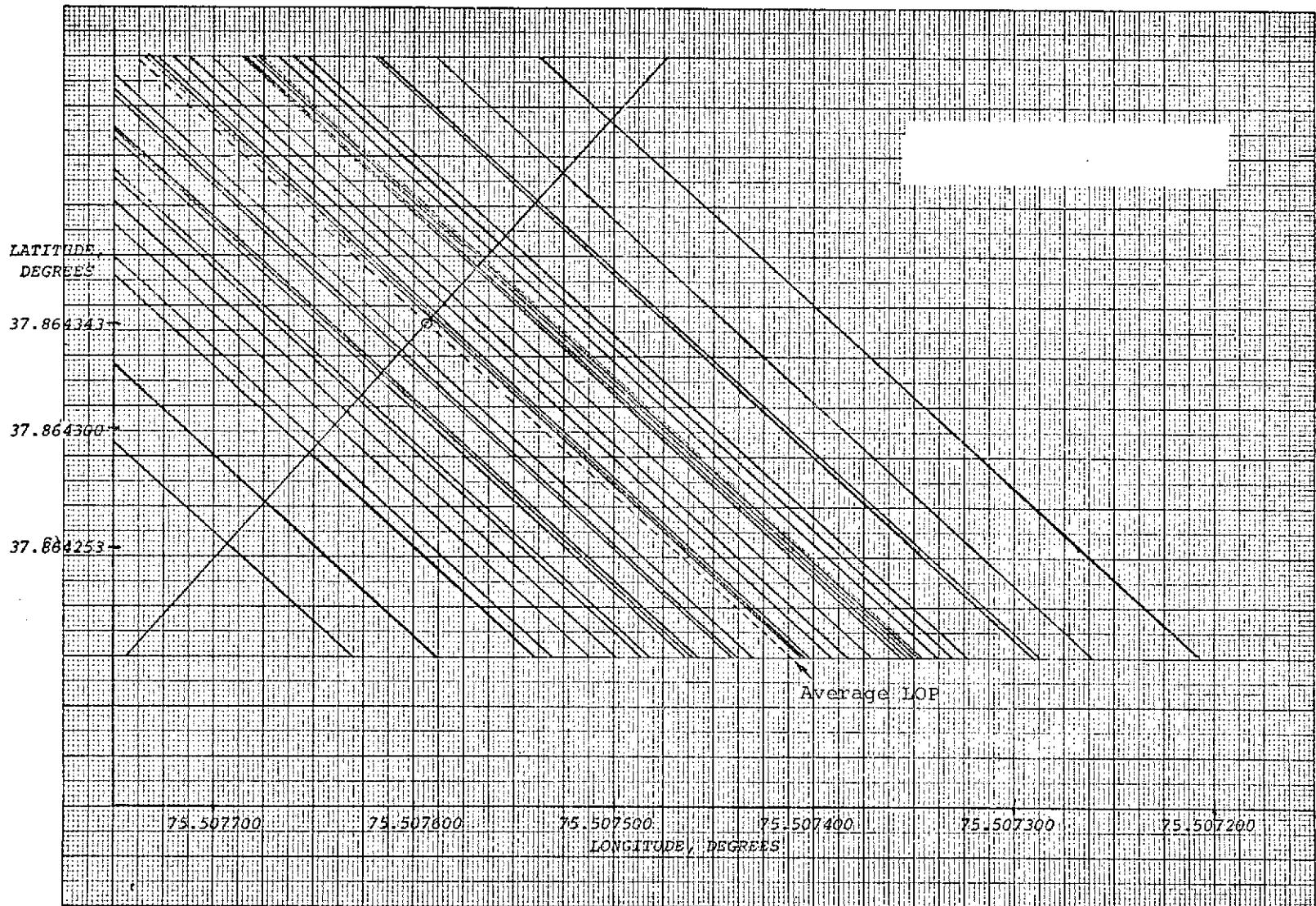
Figure 4-8. Test 8 LOP's; Remote Site = ⊙
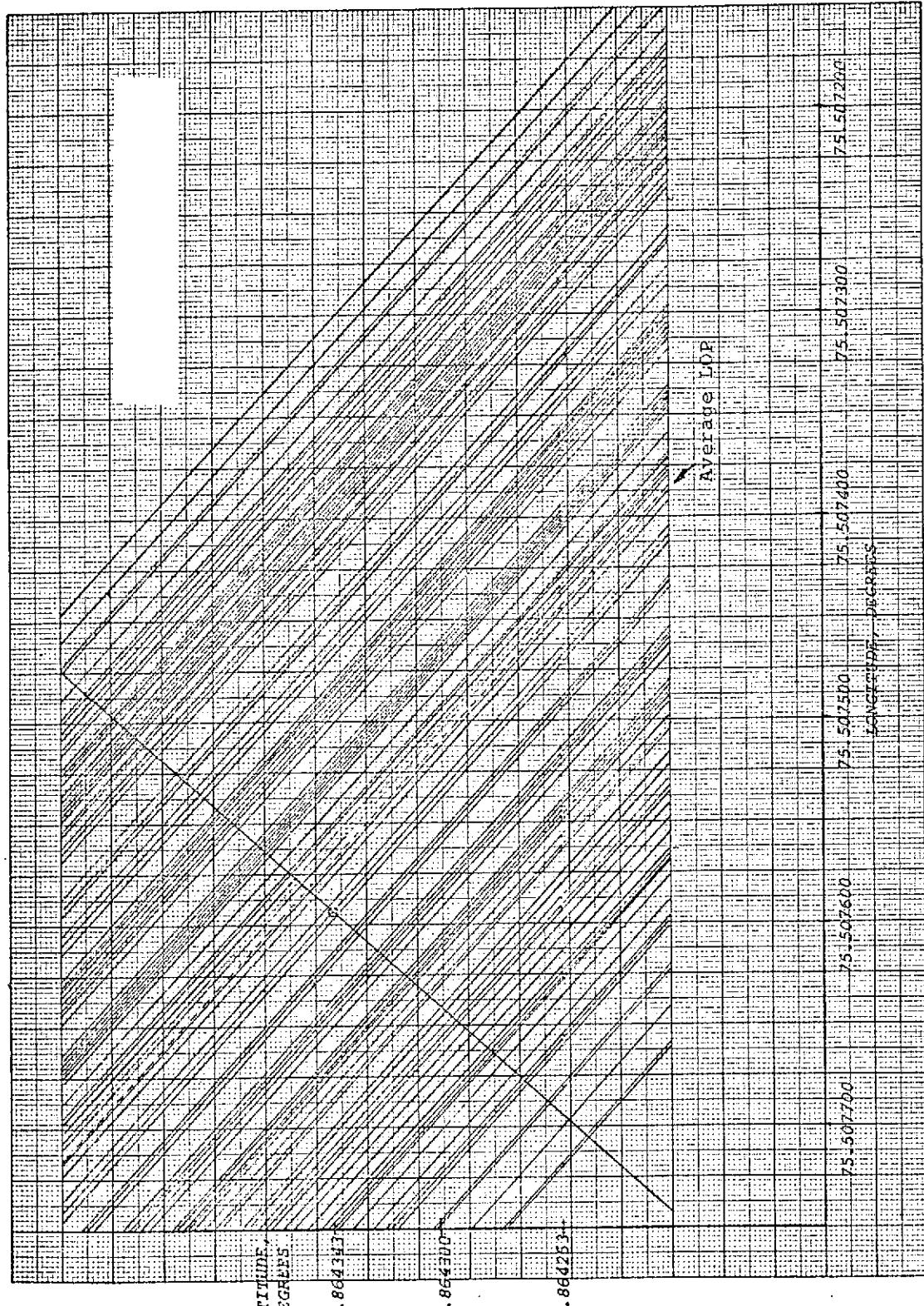
Figure 4-9. Test 12 LOP's; Remote Site = ⊙

LATITUDE,
DEGREES

37.864343

37,864300

37.864253

Average LOP

75.507700   75.507600   75.507500   75.507400   75.507300   75.507200

LONGITUDE, DEGREES
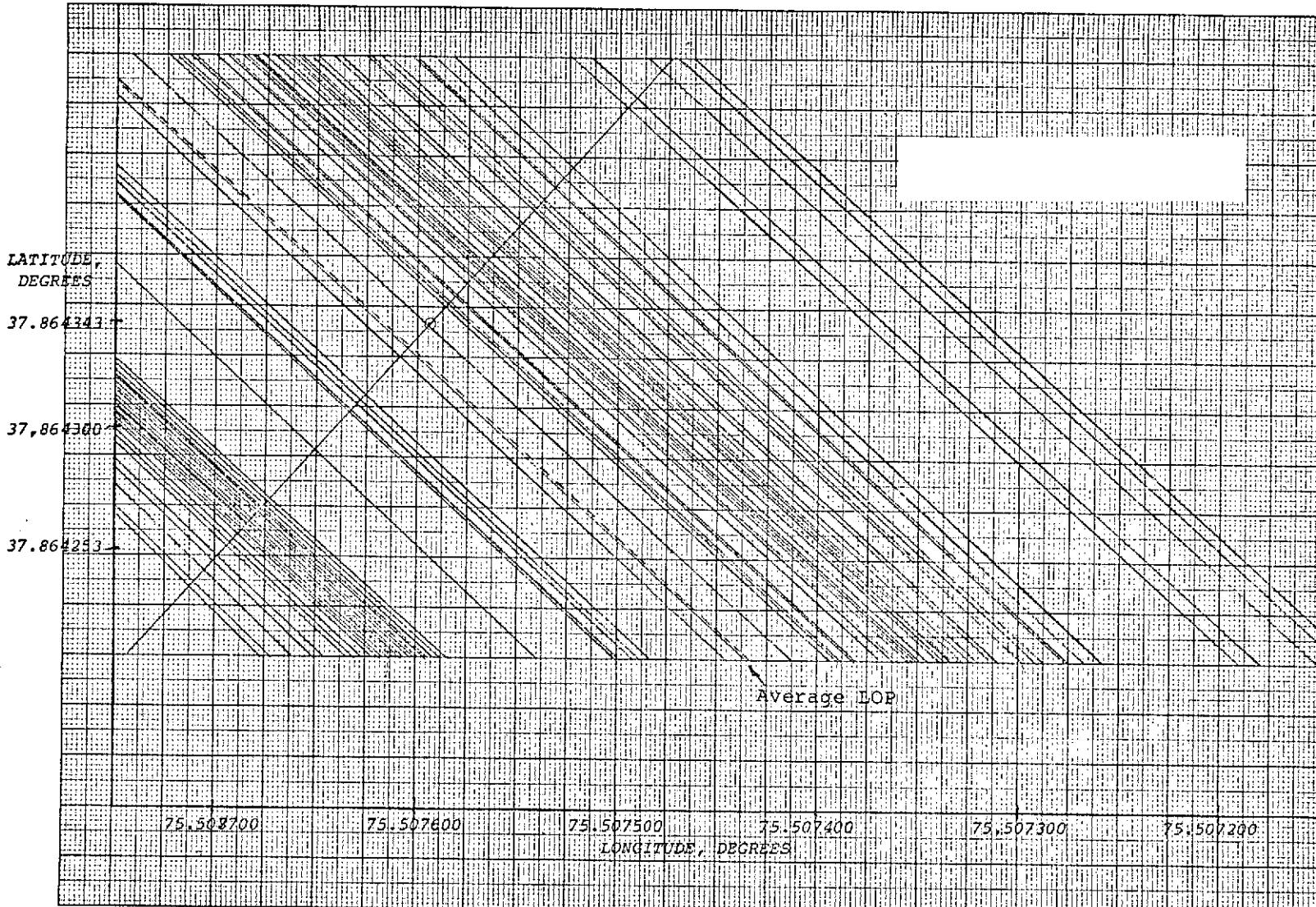
Figure 4-10.   Test 13 LOP's; Remote Site = ⊙

Thus, initially the residual error decreases as $\dfrac{\sigma_R}{N}$ when N samples are integrated. However, if integration is increased above a certain limit, no further reduction in σ can be obtained. This constant level is due to inherent noise sources in the system, e.g., short term noise due to the frequency standard.

The results from the Wallops tests indicate that σ can be reduced to about 30 feet if 20 data points are smoothed. The time from measurement to measurement is 0.8 second due to satellite rotation while each measurement lasts 20 microseconds. The 16 seconds could be considerably reduced without loss in accuracy if the navigation signals originated from non-spinning satellites.

4.5 LOP ERRORS FROM EPHEMERIS PREDICTS

In order to determine a line of position, the position of the ATS-5 satellite at that instance of time must be known. NASA ephemeris predictions for the ATS-5 satellite yield the geocentric range, latitude and longitude at 30-minute intervals. Typically, five or six consecutive ephemeris points are required over a test period. The sets of latitude, longitude and range points are fit to least squares parabolas. These parabolas are then evaluated at the points in time corresponding to the ranging test data.
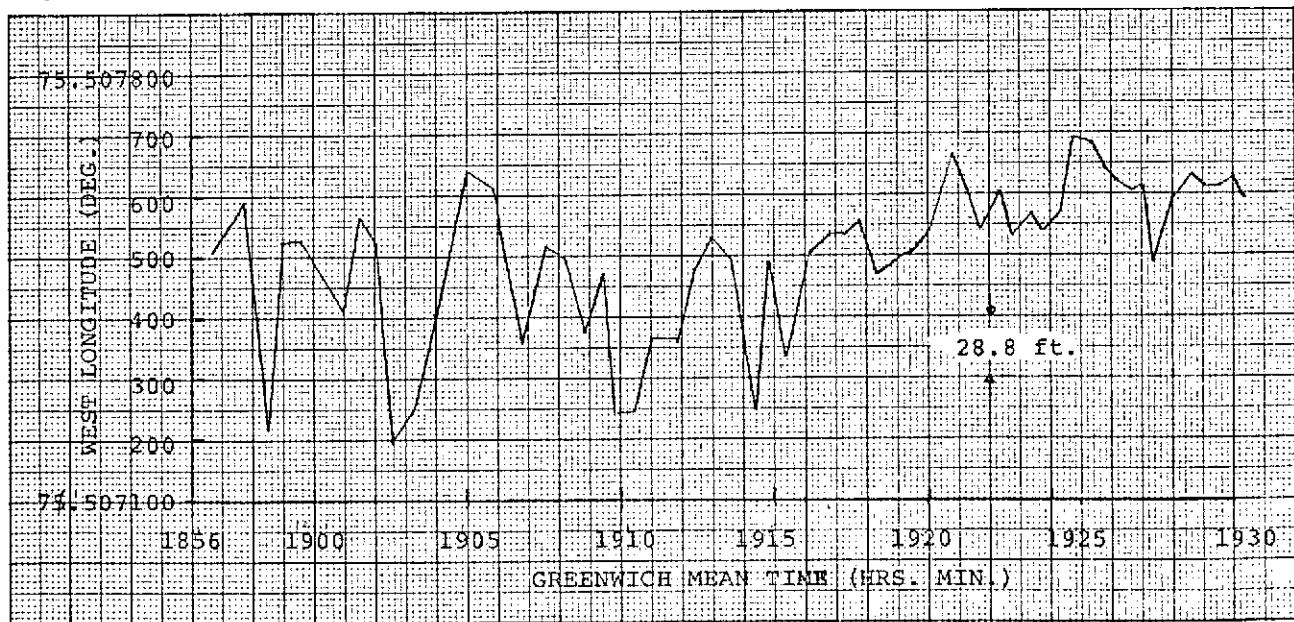
Figure 4-11.   West Longitude of Test 2 LOP's at
Latitude 37.864253 Degrees
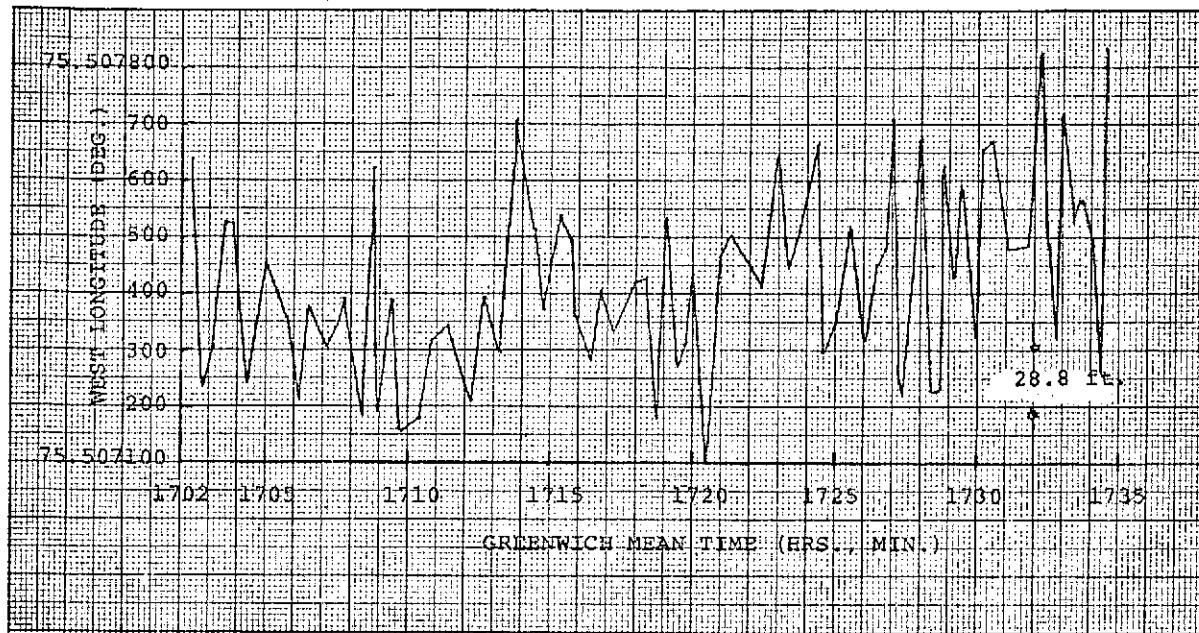
Figure 4-12.   West Longitude of Test 5 LOP's
                at Latitude 37.864253 Degrees
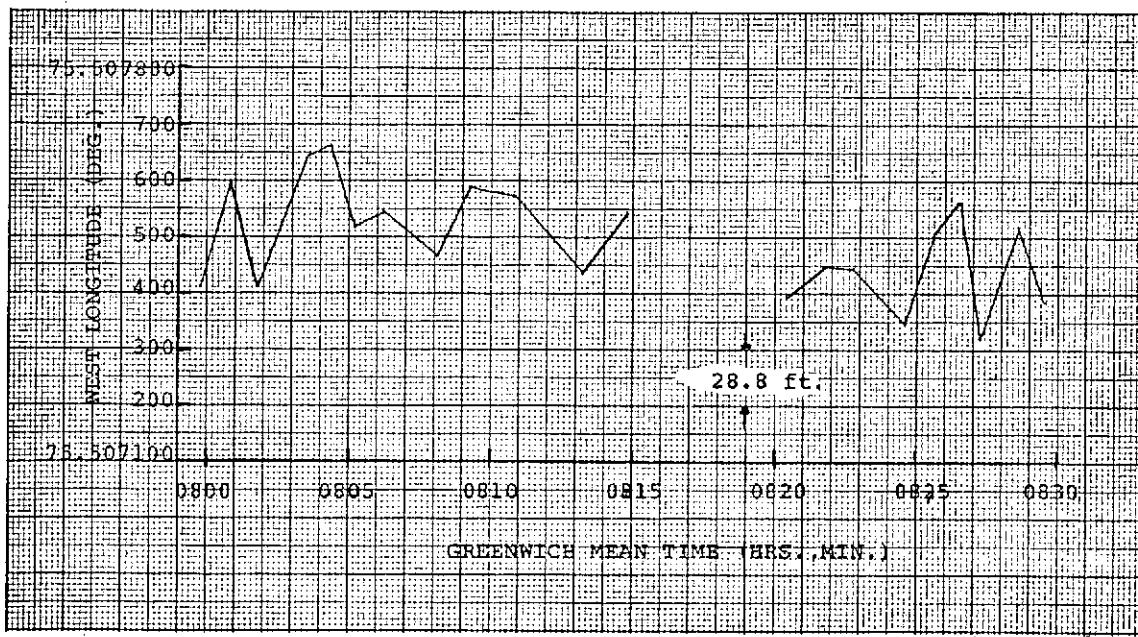
Figure 4-13.   West Longitude of Test 8 LOP's
                at Latitude 37.864253 Degrees
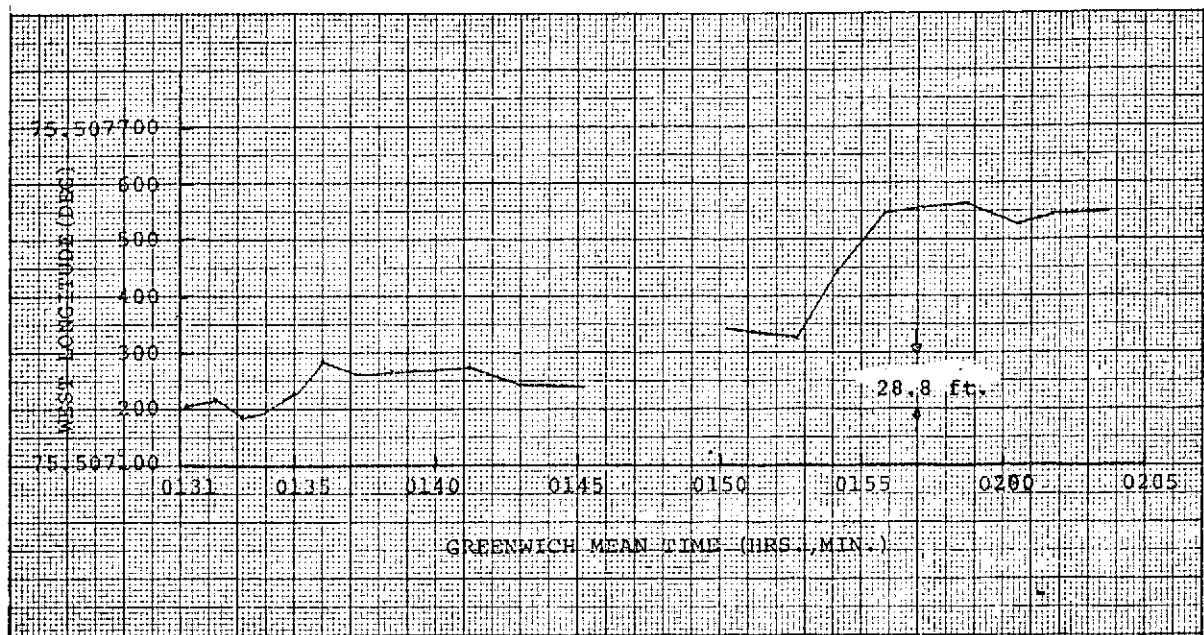
Figure 4-14.   West Longitude of Test 12 LOP's
              at Latitude 37.864253 Degrees
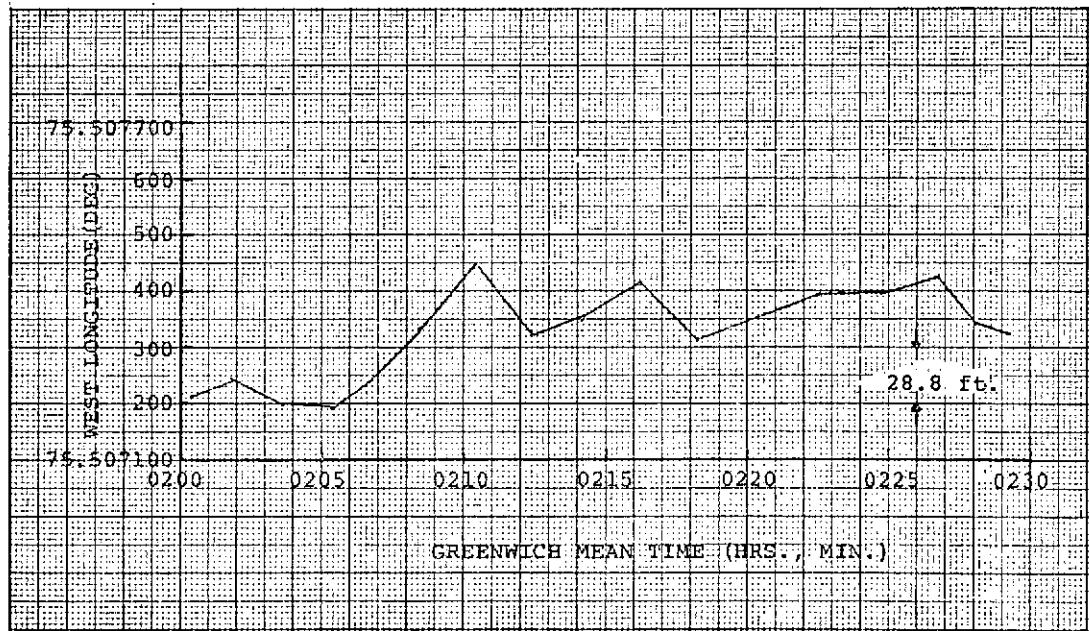
Figure 4-15.   West Longitude of Test 13 LOP's
              at Latitude 37.864253 Degrees
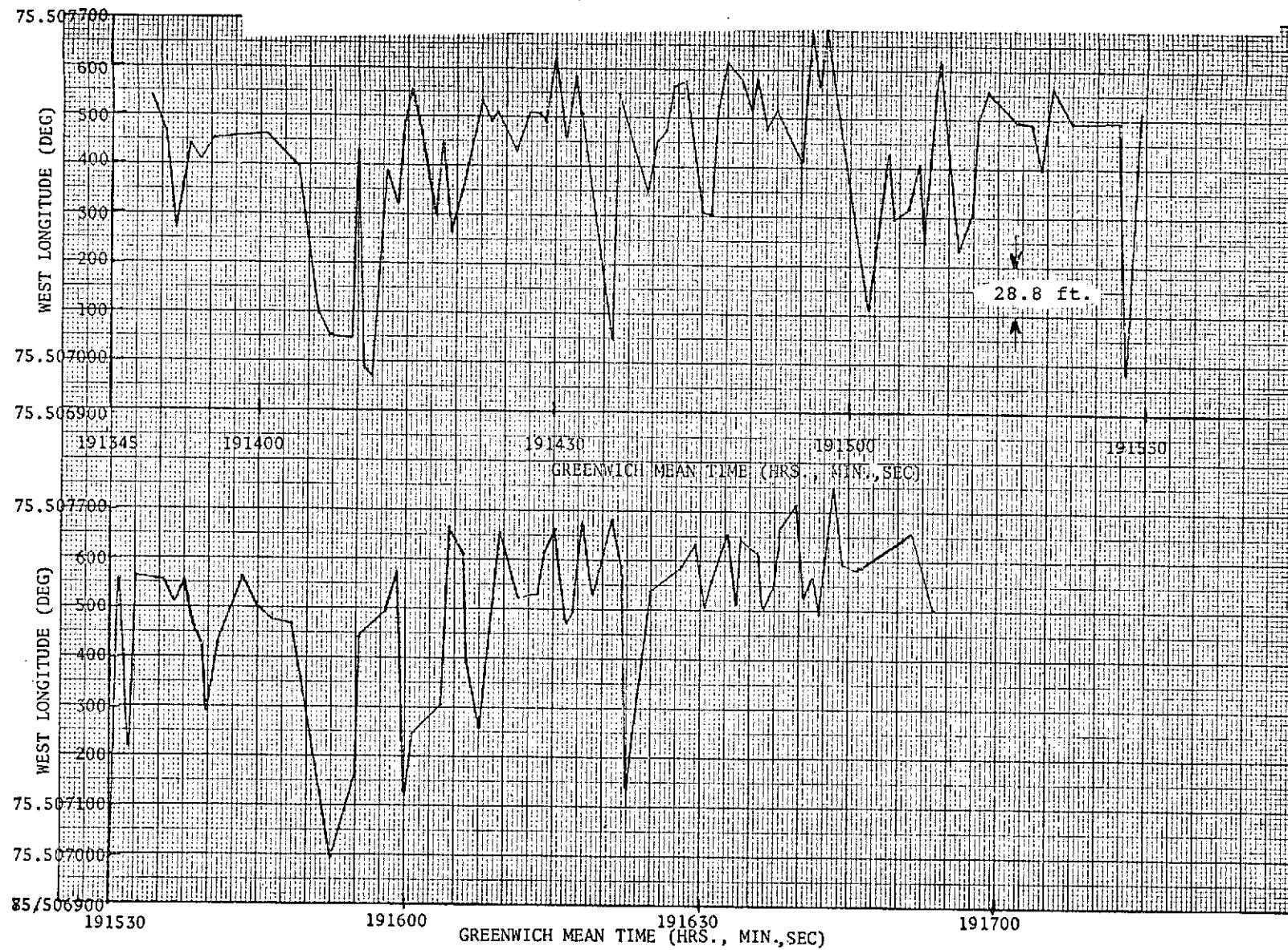
Figure 4-16. West Longitude Crossing Points at Latitude
37.864253 Degrees for Test 2
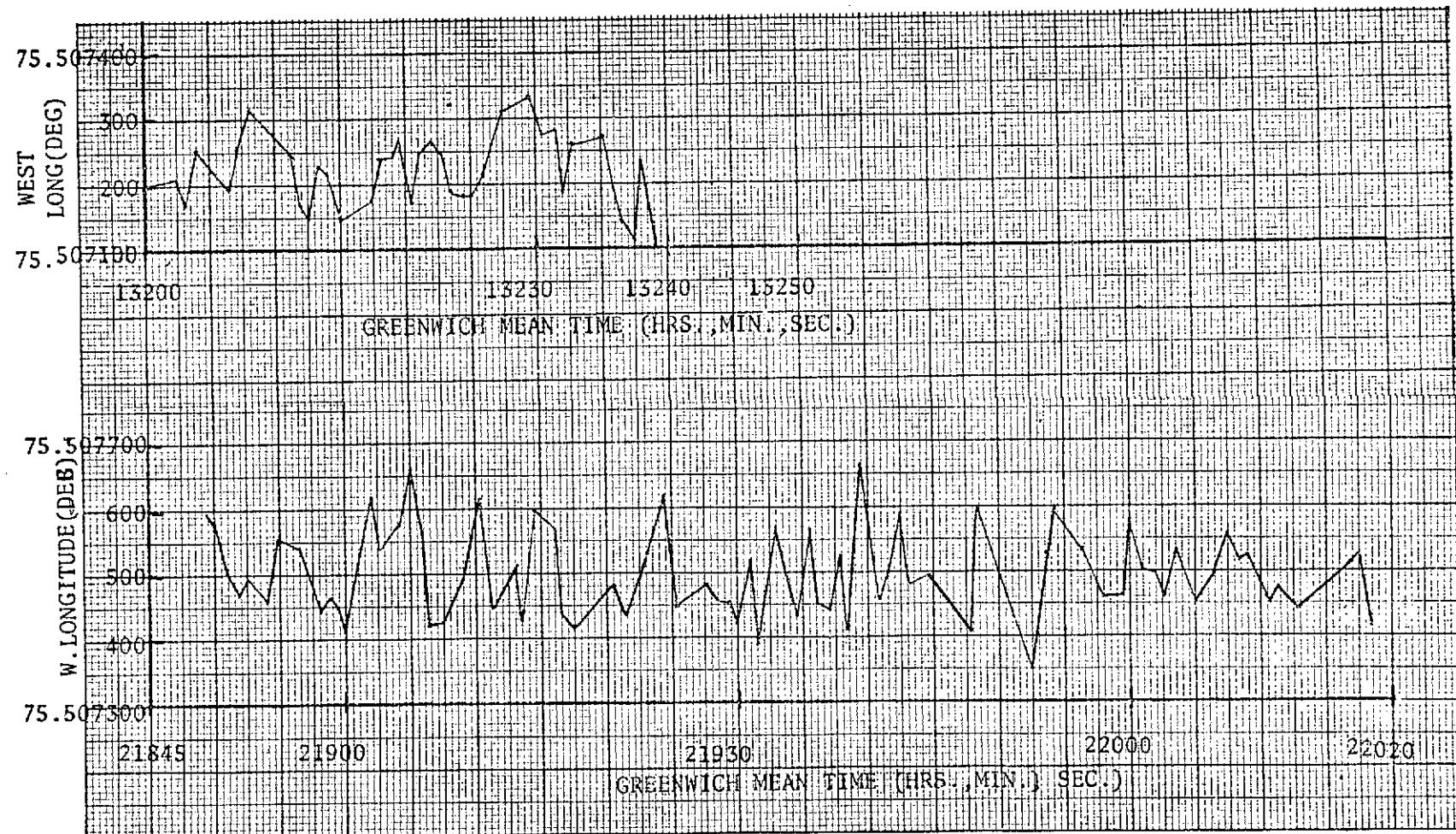
Figure 4-17. West Longitude Crossing Points at Latitude
37.864253 Degrees for Test 12
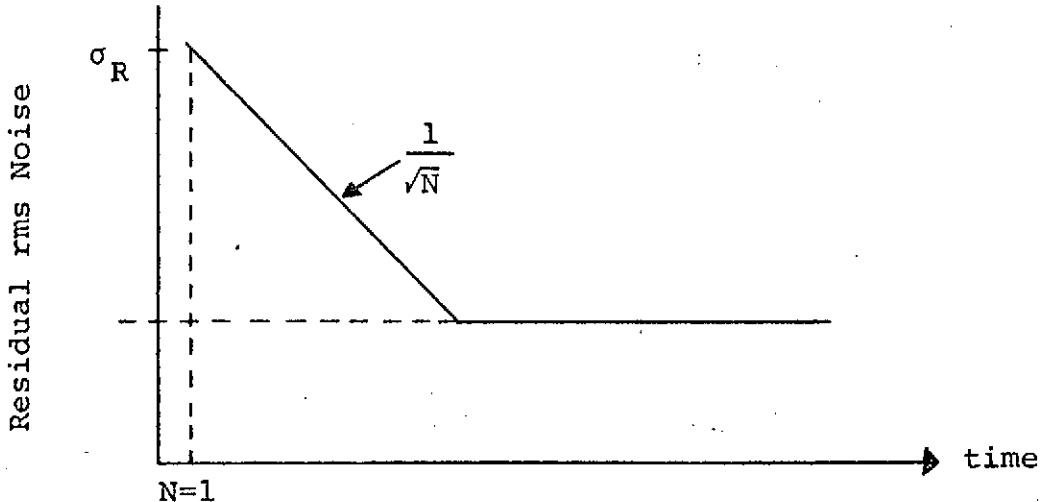
Figure 4-18. Residual Error Following
Smoothing of N Samples

Two possible errors result from this approach. The first is due
to the inaccuracies associated with the predicted satellite
positions; the second is due to the selection of the parabolic
model of the orbit, which is insignificant, as shown below.

According to NASA (see reference 3-5), the position of the satellite
is true within a cube of 10 x 10 x 10 km centered at the predicted
point. This inaccuracy in ephemeris prediction is sufficient to
effect the relative position determination. Thus, it was neces-
sary that the latitude and longitude of the fixed site be known
to six decimal places with the Type I survey.

To determine the effect of a satellite position error within the
confines of the ephemeris uncertainty cube, the predicted satellite
position on July 21 at 2100 GMT was selected and the position per-
turbed in range, latitude and longitude individually. The range
was perturbed by +5 km and the latitude and longitude were per-
turbed by +.016 degrees (5 km at 22,000 nmi). The results are
summarized in Table 4-6.

The degree to which LOP longitude changed is a nearly linear
function of the variation in ephemeris. Therefore, individual
component errors can be root sum squared. It should be noted
that the effect of change in range is very small compared with the
effects of change in angle. It is not known in which manner the
true position of the satellite differs from the predicted position,
but the deviation was probably periodic. If so, over a short

TABLE 4-6. LOP ERROR AS A FUNCTION OF SATELLITE
POSITION ERRORS

| Parameter | Change in Longitude | |
	Deg	Feet
Range ±5 km	±0.000002	± 0.4
Latitude ±0.016 deg	±0.000023	± 4.6
Longitude ±0.016 deg	±0.000059	±11.4

period of time, the deviation would be consistently in one direction, introducing a bias in the LOP's. This may be the reason the average LOP of any given data set is offset by several feet from the remote site.

The second error source was due to the parabolic fit to the satellite's latitude, longitude and geocentric range values. A parabolic fit was selected to approximate the nearly closed elliptical path of the ATS-5. The rms values of the data points about the parabolas are given in Appendix A. These values are generally two orders of magnitude smaller than the uncertainty in predicted values, indicating very good fits. The rms on the longitude, the major sources of LOP error, was on the order of 0.00020 degree. The interpolated satellite longitude would, at worst, introduce a 3 σ error (0.00060 degree), which corresponds to 1/400 of the errors exhibited in Table 4-6 of 0.029 foot. Therefore, errors resulting from the parabolic fits to the ephemeris data are negligible.

4.6 RUBIDIUM STANDARD NOISE EVALUATION

The 3-hour calibration runs of July 12 and July 27 indicate that the relative drift in frequency of the standards is negligible. These data points were fit to least squares parabolas and continuous data comprising roughly 5000 data points in each run were available. The relative drift in phase of the standards was significant. When the observed phase drift per hour ($\simeq 600$ nsec) was extrapolated to a per day drift and then compared with the total number of nanoseconds in a day (8.64×10^{13}), the relative phase stability was found to be (600×24) (8.64×10^{13}) or 1.5 in 10^{10} per day.

The pre- and post-calibration runs were always conducted in a noise-free environment. Thus, any noise on the data was due to noise generated by the frequency standards and internally by the correlator non-linearities and logic noise. The rms noise observed on the July 12 data was 15.9 feet versus 13.2 feet for July 27 data. The rms noise observed on the range readings of

code correlator A were typically 3.5 feet. If the range readings of the two correlators are assumed to be independent (which they may not be, see below), rms noise values of 15.5 and 12.5 ft. for July 12 and July 27, respectively, result from the range readings for code correlator B. Removing 3.5 feet of noise for this correlator leaves a noise-component magnitude of 15 feet (July 12) and 12 feet (July 27). This noise then, is due to the instability of the rubidium standards. From the error budget given in Section 3, it is concluded that the noise due to the rubidium standards is a dominant error source.

Figure 4-19 shows the relative, unsmoothed, range difference versus time for data collected during the 3-hour run of July 27. The data gaps are due to absence of readings during those particular time intervals. Figure 4-20 shows the effects of performing minimal smoothing. The arithmetic means of all readings observed in a 30-second interval, i.e., 15 to 25 data points, are given as a function of time. The calibration lines for these three-hour tests are also given in Figures 4-19 and 4-20. The calibration line shown in Figure 4-20 does not pass through all the smoothed range values; however, this is not unexpected considering the time varying nature of rubidium standard errors.

The following implications result for the test data collected. Typically, 10 to 20 range differences (roughly 20 seconds) collected on the satellite were fit to parabolas and evaluated at the center point of the time span, yielding a value, say, ΔR_a. This averaged range difference was reduced by L_a, the calibration line evaluated at the same point in time. Thus $\Delta R_a - L_a$ could be in error by 3 σ. The corresponding LOP would be offset from the remote site by 3 σ times the GDOP or typically 19 to 56 feet.

4.7 RANGE DATA RMS NOISE

All satellite test periods were analyzed in order to obtain estimates of the noise on the range measurements. The results of these analyses are presented in Table 4-7. The rms noise on the five drift calibration lines calculated from the pre- and post-calibration tests are shown, as are the rms noise for each receiver, the range differences between the receivers, and the rms noise on the pre- and post-calibration data.

Two methods were used to determine the standard deviation of the ranging data; both differed from the previously described method of determining the σ of the LOP's. In the first method, small continuous sections of data were fit to parabolas and the σ computed.

In the second method it was assumed that the ranging data was normally distributed. Thus, the formulation to determine σ was that 99.2% of the time not more than 50% of the points deviated
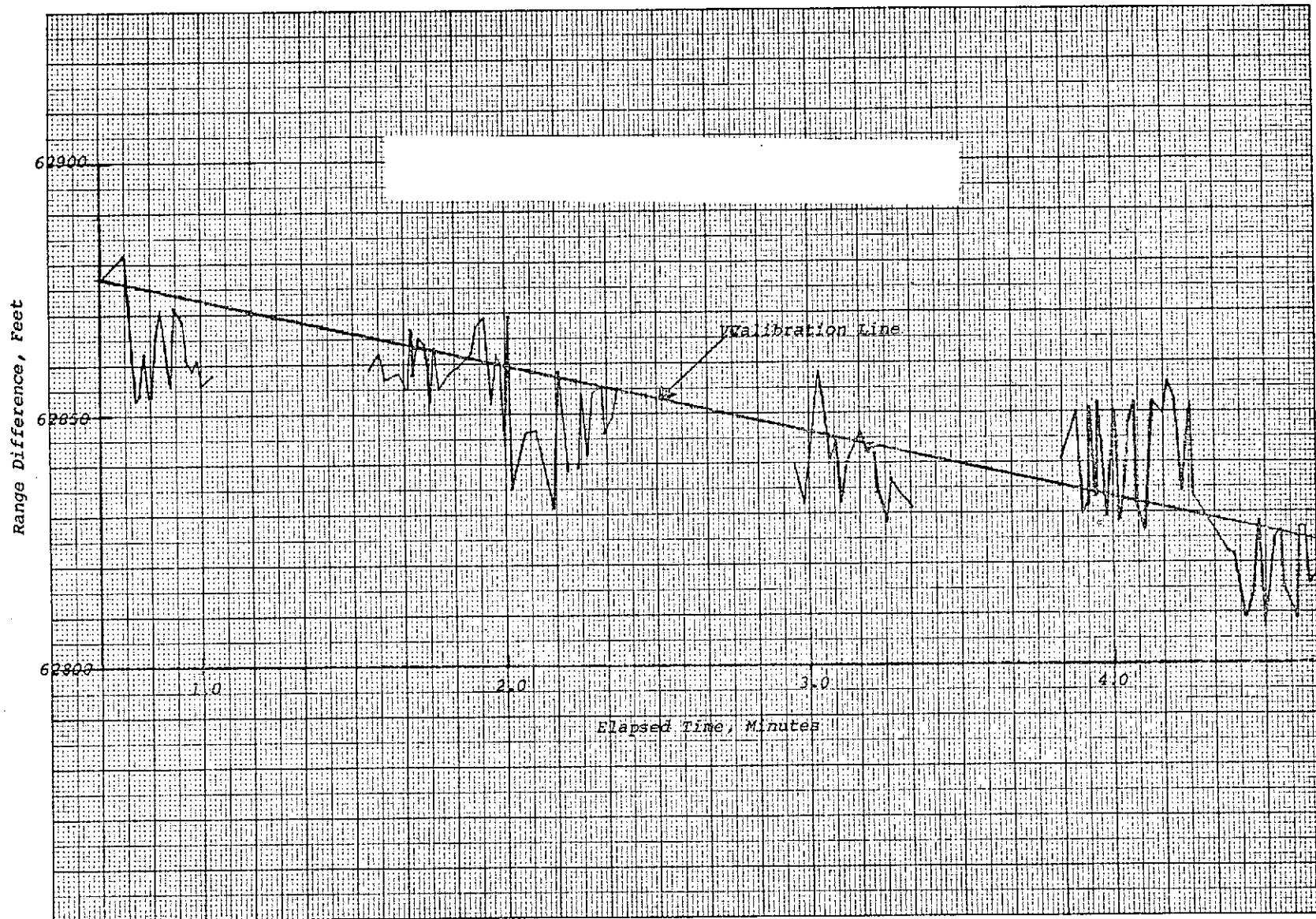
Figure 4-19. Rubidium Frequency Standard Calibration
Three-Hour Test for July 27, 1971
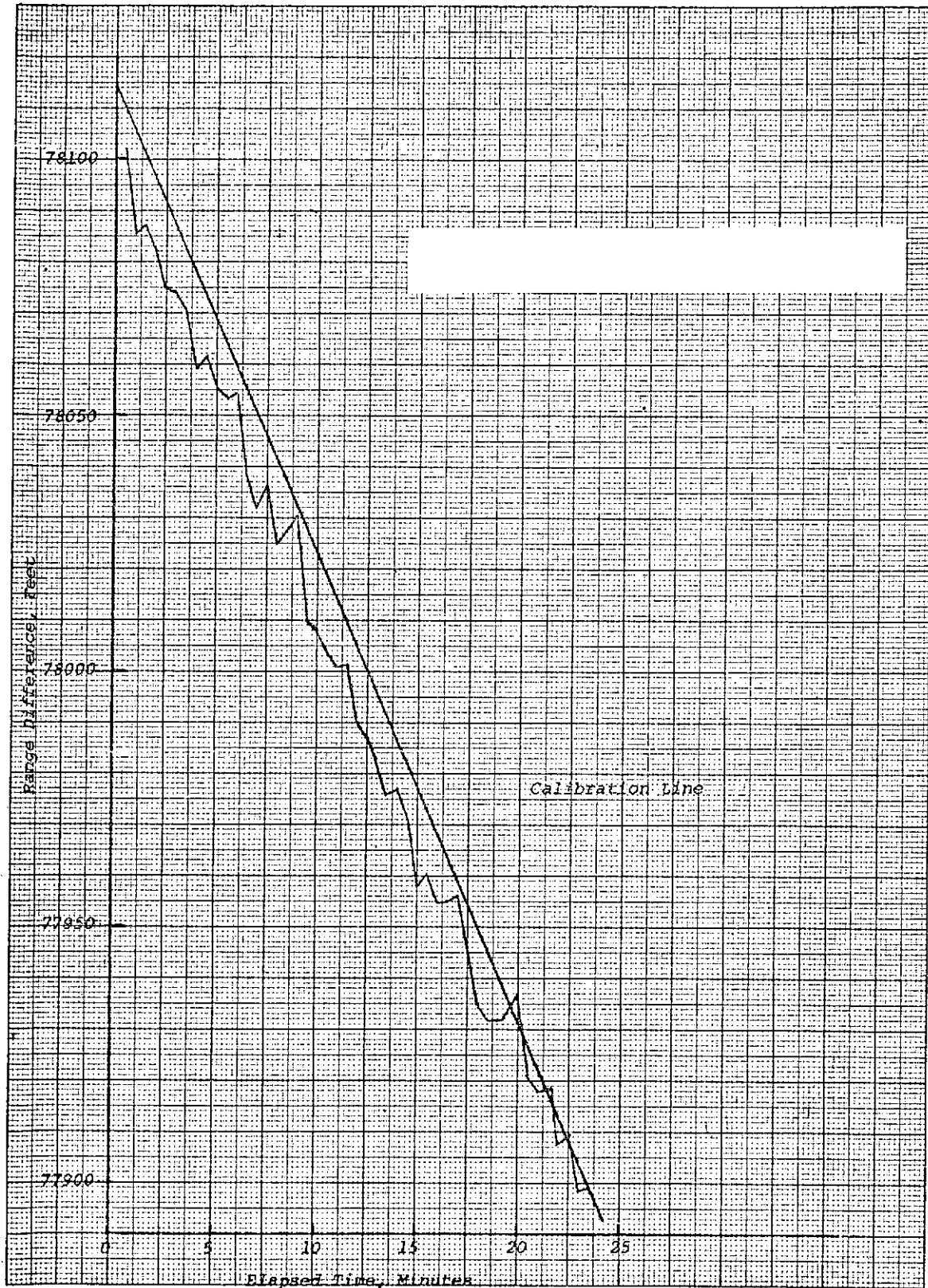
Figure 4-20. Rubidium Frequency Standard Calibration
Three-Hour Test for July 12, 1971

TABLE 4-7.   RMS NOISE (FEET) ON INDIVIDUAL RANGE READINGS

Test No.	Date	Time GMT	Receiver		Range Difference	Measurement Mode
			A	B		
2	7/12/71	1715-1935	–	–	14.02	Drift Calibration Line
			2.1	10.4	10.6	Pre-Calibration
			6	7	7.2	Post-Calibration
			2	4	5.2	Post-Calibration
			4	5	6.1	Post-Calibration
			1.5	2.2	3.9	Post-Calibration
			–	–	13-23	Satellite Ranging
3	7/13/71	1850-2130	3.1	12.5	15.3	Pre-Calibration
			2.0	14.7	14.9	Post-Calibration
			–	–	14-22	Satellite Ranging
4	7/14/71	1700-1945	1.7	11.1	11.3	Pre-Calibration
			3.0	11.0	11.3	Pre-Calibration
			3.1	9.7	10.1	Post-Calibration
			–	–	9-19	Satellite Ranging
5	7/15/71	1645-2030	–	–	18.43	Drift Calibration Line
			2.1	10.0	10.3	Pre-Calibration
			2.1	8.0	8.3	Post-Calibration
			–	–	10-20	Satellite Ranging
6	7/16/71	1640-1930	0.2	7.8	7.8	Pre-Calibration
			0.2	8.1	8.2	Post-Calibration
			–	–	8-14.8	Satellite Ranging
7	7/20/71					No Data
8	7/21/71	0700-0845	–	–	75.13	Drift Calibration Line
			1.0	19.2	24.8	Pre-Calibration
			4.8	16.4	17.2	Pre-Calibration
			1.2	8.2	8.2	Post-Calibration
			–	–	8-17	Satellite Ranging
9	7/22/71	0700-0846	6.7	12.2	13.3	Pre-Calibration
			8.9	11.9	14.0	Post-Calibration
			–	–	8-18	Satellite Ranging

TABLE 4-7. RMS NOISE (FEET) ON INDIVIDUAL RANGE READINGS (Continued)

Test No.	Date	Time GMT	Receiver		Range Difference	Measurement Mode
			A	B		
10	7/23/71	0700-0845	2.8	8.2	8.3	Pre-Calibration
			10.1	14.0	16.8	Post-Calibration
			θ	-	9-18	Satellite Ranging
11	7/26/71					No Data
12	7/27/71	0100-0400	-	-	10.45	Drift Calibration Line
			4.1	9.7	10.3	Pre-Calibration
			3.8	8.1	9.7	Pre-Calibration
			3.7	11.6	12.4	Post-Calibration
			-	-	8-13	Satellite Ranging
13	7/28/71	0200-0400	-	-	10.25	Drift Calibration Line
			3.7	9.0	10.0	Pre-Calibration
			3.5	8.4	9.8	Pre-Calibration
			3.5	9.2	10.0	Post-Calibration
			-	-	0-14	Satellite Ranging
14	7/28/71	0330-0600	3.7	9.0	9.8	Pre-Calibration
			8.4	8.9	12.7	Post-Calibration
			-	-	10-16	Satellite Ranging

from the mean by more than $\pm$ 2.66 σ. Since the number of points outside the mean + 2.66 σ interval is assumed to be small, the distribution of these points is better described by a Poisson distribution. The mean (M) of the Poisson distribution is given by

$$M = pN$$

where

$$p = 1 - q$$

and N is the number of samples observed and q is the probability 99.2%.

The probability that k points fall outside the $\pm$2.66 σ interval centered at the mean is given by

$$P_k = e^{-M} \frac{M^k}{k!}$$

Thus,

$$P_0 = e^{-M}$$
$$= e^{-pN} = 0.5$$

incorporates the 50% chance of any observation being outside the interval. Thus

$$pN = -\ln 0.5$$
$$= .69$$

Since

$$p = .008$$
$$N = 86$$

The probability interval of 4.8 σ about the mean was chosen so that the number of observations would be collected in a relatively short interval. The difference between the smallest and largest range difference observed in 86 points was corrected for the relative drift between the rubidium standards, estimated at 600 nsec/hour. The observed corrected difference divided by 4.8 then yields σ.

The co-located test was considered in detail in order to determine the rms noise due to the receivers. The rms noise on receiver A was 0.2 ft during both calibration periods and 7.8 and 8.1 feet on

receiver B during pre- and post-calibration periods, respectively. The rms on the range difference was 7.8 and 8.2 feet during these calibration periods. Since 257 range readings on the satellite were available, σ is calculated for three intervals of 86, 86 and 85 data points. The average σ_s was 9.53 from the three calculated values of 8, 14.8 and 6.8. When σ_s^2 was reduced by the average noise from the calibration periods (8^2), a remainder of 26.25 resulted. Assuming equal noise generated by the receivers, the rms noise due to each receiver is $\sqrt{26.25/2}$ or 3.62 feet. This agrees closely with the predicted rms of 3.6 feet.

4.8 IONOSPHERIC EFFECTS

The collected data was analyzed in some detail in order to determine if ionospheric effects were discernible. Since the relative ranging tests were not performed with this purpose in mind, definitive conclusions could not be reached. For example, it is not possible to extract information on the ionospheric-induced delays along the paths from ATS-5 to the receivers since such information is inbedded in the noise. Therefore, the only way in which ionospheric effects can be inferred is by considering the distribution of the LOP's as a function of time.

Figures 4-11 through 4-15 show the west longitudes at one of the reference latitudes. The scatter on the points from test 2 and 5 (0700-1930 GMT) is larger than for test 8 (0800-0845 GMT) which, in turn, is larger than for tests 12 and 13 (0100-0400 GMT).

For tests 2 and 5, less than two or three successive LOP's were to one side of the average LOP and, in general, any two successive LOP's were well separated, typically by 10 to 30 feet. This indicated the presence of considerable noise on the measurements. This noise could be due to the rubidium standards, the receivers or the ionosphere. During test 12, thirteen successive LOP's (23 minutes of observation time) were clustered to one side of the average LOP. These LOP's were all displaced by 30 to 50 feet from the mean LOP. Later, in the same test, 29 successive LOP's taken during 30 minutes were all clustered to one side of the mean as shown in Figure 4-21. Test 13 yielded an even more striking result. The first 46 LOP's covering one hour and three minutes were to one side of their mean, while the remaining 34 LOP's representing one hour of data were to the opposite side. This effect may be due to inaccuracy in the slope of the calibration line (overestimating the drift between the rubidium standards in the first half of the test and underestimating it during the concluding half) or due to the motion of the ATS-5 relative to the predicted ephemeris which would introduce a bias-type error.

The spread on the LOP's for tests 2 and 5 was due to considerable noise while most of the spread of the LOP's from tests 12 and 13
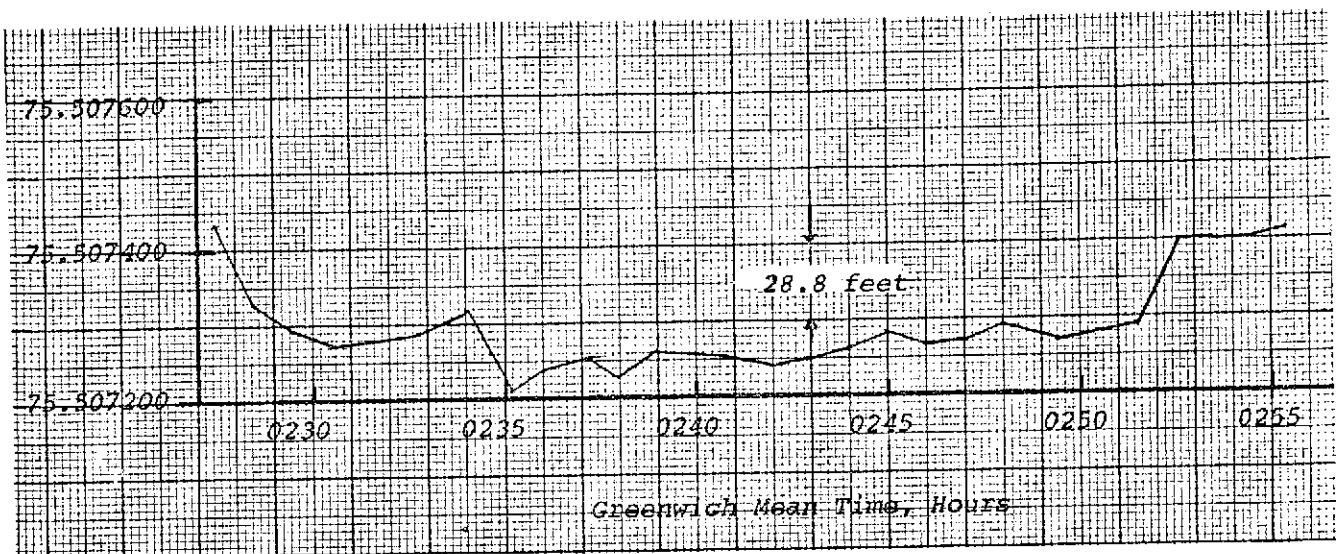
Figure 4-21. Test 12, West Longitude Crossing Points
at Latitude 37.864253 Degrees

resulted from a sequential motion of the LOP's during these tests.
Figures 4-16 and 4-17 from tests 2 and 12 data, respectively,
are illustrative. In these figures a single range difference was
used to determine an LOP. Thus, no smoothing was done. Test 2
data collected over 3 minutes 15 seconds indicates a considerable
spread on the longitudes of approximately 200 feet.

The rms exhibited here can be found by reducing the spread by the
GDOP multiplier of 1.25 leaving 200/1.25 or 160 feet. Equating
this value to approximately 5σ or 66 (133 points) yields a 1σ
value of roughly 30. The spread for the test 12 data is 72 feet.
for the first set and 86 feet for the second set. No dips are
exhibited in test 12 which are exhibited by the test 2 data.

The rms noise data presented in Table 4-7 was also considered.
However, no statistically significant conclusions could be reached
on the basis of that data.

4-32

SECTION 5

EXPERIMENT INSTRUMENTATION

5.1 GENERAL CONSIDERATIONS

The test instrumentation assembled to meet the precise positioning requirements of the experiment included a modulator, two receivers and a data recording system. The design of the ALPHA II receiver system was based on an existing AII L-band correlation receiver used in earlier ATS-5 ranging experiments. This experiment required a receiver with similar precision and ranging capability. The ALPHA II receiver system has the following performance characteristics: (1) 10-MHz PRN code reception and demodulation capability, (2) ability to acquire and track signals from the spinning ATS-5 satellite, (3) computer-oriented format for recording or data-phone transmission, and (4) provision for precision range readout to observe small range fluctuations due to noise.

The technical approach adopted in the ALPHA II receiver design was to demodulate the PRN code from the carrier without phase locking the carrier. The demodulating technique, explained in more detail later in this section, was capable of tolerating the small doppler anticipated due to the movement of the ATS-5 satellite. Severe frequency uncertainties resulting from drift of the satellite master oscillator with temperature were accommodated by manual frequency adjustments. The digital range tracking loop, which is integral with the code generating and control logic circuitry, had natural memory characteristics that enable the signal to be rapidly re-acquired at the beginning of satellite signal burst.

The system design characteristics which govern the ALPHA II receiver operation are summarized below.

5.1.1 Modulation Design

Coherent PSK modulation is used in the ALPHA II system. This implies a carrier system which transmits two signals differing only by a phase reversal of the carrier. The phase reversal represents the mark-space information. The carrier phase reversal produces sequential signals wich are the negative of each other. This means that they have a cross-correlation coefficient of -1, and thus are mutually uncorrelated. This modulation can be demonstrated to be the optimum binary system. It has been shown in many standard references that the coherent PSK system provides the lowest error probability for a given signal-to-noise ratio that one can expect from binary systems, including differential PSK, coherent frequency shift keying (CFSK), and non-coherent FSK.

5.1.2 Detection Design

The ALPHA II receiver system is a correlation design and a full description appears later in this section. Correlation techniques have long been used to extract a signal from noise or to reveal the presence of periodicity in an otherwise completely random signal. Thus, if a signal with the right properties is correlated with a relatively noise-free replica of itself, (i.e., autocorrelation), the random noise component of the signal will rapidly reduce to zero, and any periodic component will be revealed. Similarly, if two signals are cross-correlated, one with the other, an immediate result is the indication of mutual properties which the signals may share.

Communication systems and radar systems apply correlation techniques to optimize performance in the presence of noise and a jamming environment. In the ALPHA II receiver, AII uses a correlation technique in which the code automatically tracks by adjustment of the digital tracking loop. If the filter response of a receiver containing white noise is multiplied by a constant, both the signal and the noise are amplified linearly by the same factor, and the S/N ratio is unchanged. Therefore, to achieve maximum S/N ratio, the signal component must be maximized. The impulse response of the filter which maximizes the signal component and the S/N describes what is known as a matched filter. If the filter output is integrated over a long time period, then the S/N ratio can be very large. Matched filter operation can be obtained in this case with a correlator. The correlator multiplies the incoming signal plus noise by a signal which is identical to the anticipated signal and integrates the result. The result is sampled at a later time and a decision is made concerning its value. The correlation principles adopted are described in the equipment description in this section. Appendix B describes a simple theoretical development of the correlation function in the receiver and demonstrates that the selected approach is truly an optimum system.

5.1.3 Signal Design

The code chosen for the ALPHA II receiver has a clock rate of 10-MHz. The code generator contains a 14-stage shift register capable of being programmed for several maximum length codes. The code length necessary to provide unambiguous ranging of the satellite position is 16,383 bits. A shorter code of 2,047 bits is also available which has excellent multipath rejection and a relatively short search time with a continuous signal. The choice of code is governed by the desired unambiguous range capability, accuracy, the multipath performance, the acquisition time, system performance under doppler conditions and hardware complexity required for code generation.

It is established in Appendix C that maximum-length PN codes of 511 bits or more are theoretically satisfactory to provide greater than 50 dB multipath rejection. Table C-1 of Appendix C shows some of the various code lengths available from the 14-bit shift register code generator. This table provides an insight into the trade-off in search time, multipath rejection and range ambiguity.

The ALPHA II system utilizes a proven correlation technique capable of tracking the ATS-5 L-band signal which is only present for approximately 50 ms out of every 780 ms (one satellite revolution). The utilization of digital loop to track the received PN code provides the memory capability between signal bursts.

5.2 CODE CORRELATOR

The receiver code correlator shown in Figure 5-1, compares the PRN code modulating the received signal with a locally generated duplicate of that PRN code. The modulation code is a pseudo-random, maximum-length code having transitions at a 10-megabit per second rate. The spectrum occupancy of the code-modulated signal from the receiver RF front-end assembly, which feeds the correlator, is 20-MHz. The correlator collapses this wideband noise-like signal to a steady carrier when an exact phase match between the incoming code and the locally generated code is produced.
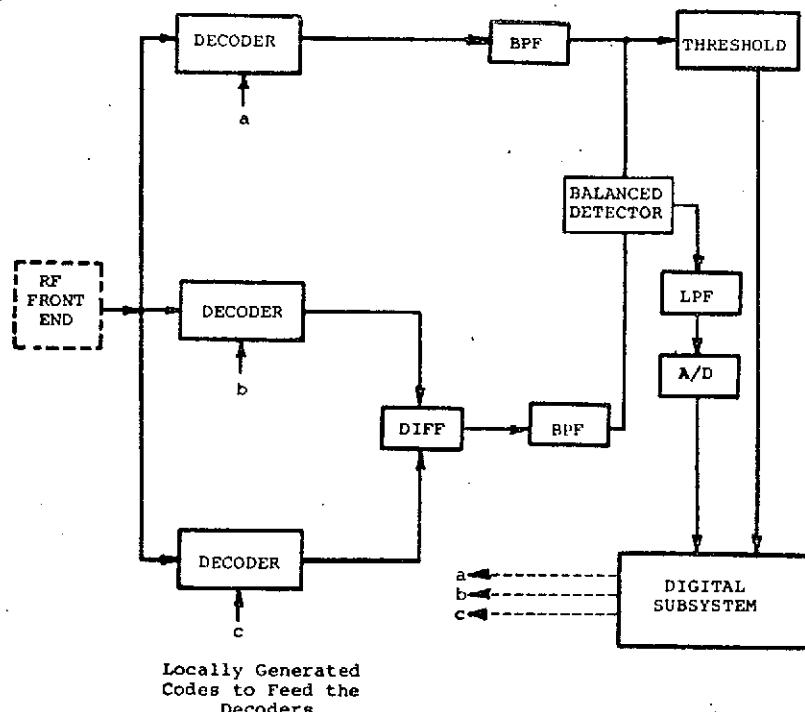
Figure 5-1. Code Correlator

The code correlator multiplies the received PN code modulated
signal by a replica of the PN code and integrates the result.
If a phase error exists between the receive code and the internal
code, a d-c error signal is generated which causes a correction
to be made in the phase of the internal code. When a "match"
occurs, the correlation is complete and the phase difference can
be measured. The code correlator operates in a sample-and-hold
mode making phase corrections only if the decoded received signal
exceeds a predetermined signal-to-noise ratio. The correlator
has a predetection bandwidth of 1.6 kHz and a noise loop bandwidth
of 50 Hz. Operation during the acquisition mode is a time search
through all bit positions of the PN code which is terminated by
an indication that the signal-to-noise ratio has exceeded a pre-
determined threshold, and thus correlation has been accomplished.
The characteristics of the code correlator are summarized in
Table 5-1.

The 70-MHz bi-phase PSK modulated signal is converted to 4.0-MHz
and split into three channels. In the three correlator channels,
the modulated waveform is multiplied with a replica of the PN
code. The code replicas on each of two channels are displaced
in time by plus and minus one-half bit interval from the pseudo-
random code on the third channel. In the channel designated the
in-phase channel, the modulation waveform is centered in time
relative to the PN code in the other two channels. During the

TABLE 5-1. CHARACTERISTICS OF THE CODE CORRELATOR

Parameter	Value
Input	70-MHz
Input Bandwidth	20-MHz
Input Level	-20 dBm
Sensitivity	-30 dBm
Modulation	Bi-Phase, PSK
Coarse Range Granularity	100 feet
Fine Range Quantization	1.0 foot
Code Length	2047 or 16,383
Clock Rage	10 MB/S
Acquisition Bandwidth	1.6 kHz
Control Loop Bandwidth	50 Hz
Multipath Rejection	50 dB
Duty Cycle of Tracking	6% (ATS-5 burst)

acquisition mode, the time difference between the PN code replicas and the received modulation is not known. The function of the correlator is to produce an adjustment of the PN code multiplying the in-phase channel so that it is in time coincidence with the received modulation waveform. This alignment is performed by stepping the local PN code in phase until correlation occurs at one of the three decoders. The output magnitude of the decoder increases at the instant of correlation and its presence is confirmed with a threshold detector. The amplitude increase can occur in any of the three 4.0-MHz channels depending on the time coincidence of the modulation waveform.

The circuit behavior can best be explained by examining the auto-correlation function of each of the three decoders shown in Figure 5-1. When the modulation waveform is matched in any of the three decoders the output amplitude of the decoder increases in level. When it exceeds a preset threshold, the correlator operating mode is switched from code acquisition to range tracking.

Each decoder serves the role of comparing the incoming received code with a similar code locally generated in the digital sub-system. The 2,047 bit code correlator against itself over a full-code period has a single correlation peak and all other time side lobes are down approximately 66 dB below this peak. Maximum-length-code correlation characteristics are illus-trated in Figure 5-2. The triangle identified as A in the
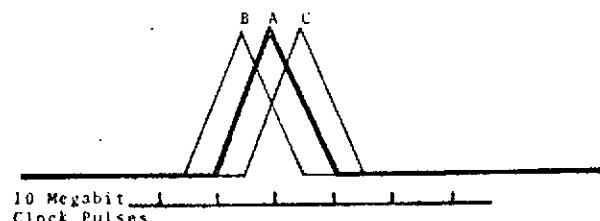
CORRELATION PEAKS OF DECODERS A, B AND C
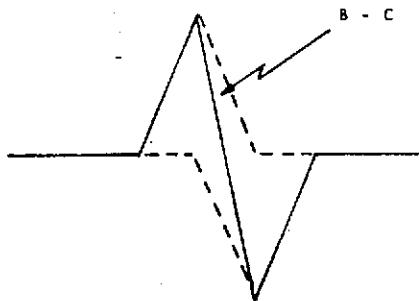
"Z" CURVE GENERATION

Figure 5-2. Correlator Output Characteristics

left diagram is a correlation peak obtained by measuring the amplitude of the decoder output as the locally generated tracking code is moved through a "match" with the incoming code. A match is defined as the relative phase point at which all zeros and ones in the received code are aligned with corresponding zeros and ones in the tracking code. It is noted that the build-up of the correlation peak begins one bit length before the peak and ends one bit following the peak; thus, the correlation peak is two bits wide at the base.

Decoders B and C in Figure 5-1 are identical in action to decoder A. Their peaks, however, are caused to occur one-half bit before (decoder B) and one-half bit later (decoder C). This is accomplished by supplying the locally generated code one-half bit early and one-half bit late, respectively, to these decoders.

The outputs from decoders B and C are shown in Figure 5-1 to be supplied to a differencing circuit. This circuit subtracts the decoder C output from the decoder B output. The resulting characteristic is shown in the right sketch of Figure 5-2. It is referred to as the Z curve. The mid-point of the Z curve, on the zero axis, is the point at which the two codes exactly match. It should be noted that this point coincides with the point at which the output from decoder A reaches its peak.

The 4.0-MHz signals from the quadrature channel and the in-phase channel are filtered with crystal filters having a bandwidth of approximately 1.6 kHz. The in-phase and quadrature channels at the crystal filter outputs contain only the carrier; the modulation sidebands are suppressed by the filter selectivity.

The voltage amplitude of the carrier at the output of the crystal filters contains the information concerning the time coincidence or correlation of the received modulation and the locally generated PN code. When the two range code signals are in time coincidence, the amplitude of the 4.0-MHz carrier in the in-phase channel will be maximized and the 4.0-MHz carrier in the quadrature channel will be minimized.

The processing gain of the system is inversely proportional to the filter bandwidth, and is computed by the ratio of the incoming signal spectrum to the filter bandwidth. Thus, the 20-MHz spread-spectrum signal and the 1.6-kHz filter produces a processing gain of 41 dB.

Other factors influencing the choice of the filter bandwidth are minimum search time and tolerance to frequency uncertainty. The search time is directly affected by the time required to build up a detectable output from the decoders. As the locally generated tracking code is stepped one bit at a time in its search mode, it must remain in each phase position for a time sufficient to integrate the signal in the filter.

The correlator configuration shown in Figure 5-1 performs its decoding independent of the doppler components on the code-modulated carrier. Tolerance to frequency offset extends to a maximum value of +0.8 kHz. The correlator design enables the decoding action to take place despite the presence of small frequency changes on the carrier. The frequency effects are identical in both channels of the correlator and if the carrier falls within the bandpass filters, the decoding is independent of the carrier frequency. Code tracking was demonstrated by this receiver in the operation with the ATS-5 satellite for doppler produced by the satellite motion (approximately 35 feet per second). Severe frequency drifts due to the ATS-5 oscillator (up to approximately 200 Hz/min) were corrected for by tuning of the 2nd L.O. injection signal.

At this point the code phase error information is in the form of amplitude. The ALPHA II correlation system converts this amplitude function into phase information, so that variations in the received signal amplitude will not influence the range measurement accuracy. The quadrature channel is amplified in a limiting amplifier and the in-phase channel signal is amplified in a similar limiting amplifier. The two limiting amplifiers are phase-matched to witin 2° so that their phase response characteristics do not produce range errors. The limiting amplifier outputs are then multiplied in a phase detector which is capable of generating an error voltage proportional to the phase error between the two inputs. The error voltage is integrated in a low-pass filter and amplified. This DC signal contains the sense and magnitude of the alignment error between the local PN code generator and the received range code waveform.

The characteristic which describes the output of the balanced detector as the received code and locally generated code near the optimum tracking position is the Z curve shown in Figure 5-2. The 0 point midway on the Z curve is the balance position where a phase match exists between the two codes. As the phase match changes, a DC output is generated by the Z characteristic. The error signal from the balanced detector is band limited by a low-pass filter and sampled by an analog-to-digital converter. This circuit converts the DC error voltage into digital logic pulses to control the phase positioning of the tracking codes.

5.3 DIGITAL TRACKING SUBSYSTEM

5.3.1 General

A correlation system requires that the receiver have exact knowledge of the code transmitted by the sender. This requirement is met by a reference code generator in the receiver identical to one in the modulator. Under normal circumstances where the receiver is operating independent of the transmitter in a remote location, the

reference code generator in the receiver is driven by its own master clock. The block diagram of the ALPHA II code correlator digital subsystem is shown in Figure 5-3. The system has three basic functions to perform: (1) acquire and lock the internally generated PRN code to the received modulation, (2) measure the phase difference between the received code and the internal reference, and (3) display this measurement to the operator and make it available for external recording.

5.3.2 Operation

Two PRN code generators are used in the ALPHA II correlator. The first is a reference generator, while the second, the tracking code generator, is locked to the incoming signal. Each code generator is a 14-stage shift register with feedback taps configured to generate either 16,383- or 2,047-bit maximum length PN codes. The state (10000...00) is decoded as a synchronization point, and a pulse is produced whenever this state is reached. Since the input clock rate is 10-MHz, the cycle time of the code generators is 204.7 or 1638.3 microseconds, depending upon the selected code length. The tracking code generator develops the three waveforms provided to the decoders. These three versions of the PRN code are offset from each other by one half of a code bit (50 nsec).

The phase selector provides a convenient method of shifting the tracking code generator to provide the equivalent of 40-MHz resolution. This technique, illustrated in Figure 5-4, produces four 10-MHz square waves displaced from each other by 25 nanoseconds (90°). By selecting the waveform nearest the phase of the received signal as the clock for the tracking code generator, the correlation will be within +1/8 bit (+12.5 ns) and the error voltage remains in the linear region of the Z curve.

The phase of the internal code can be easily shifted by changing from one clock stream to another, as the last two waveforms of Figure 5-4 indicate. If the negative edge of the waveform shifts the code generator and phase 2 is the active clock phase, there is a shift at the 0 and 100 nsec points. If the clock switches from phase 2 to phase 3 at 25 nsec, the "retard" waveform results, with shifts at the 0 and 125 nsec points. The subsequent shifts will occur at 100-nsec intervals provided no further clock changes are made. Thus, the effective phase of the code generator has been delayed by 25 nsec or 1/4 of a bit. Similarly, switching from phase 2 to phase 1 produces the "advance" waveform with shifts at the 0 and 75 nsec points and advances the code phase 25 nsec. By successively stepping through the clocks (2,3,0,1,2 or 2,1,0,3,2), the phase of the code can be changed to any desired position.
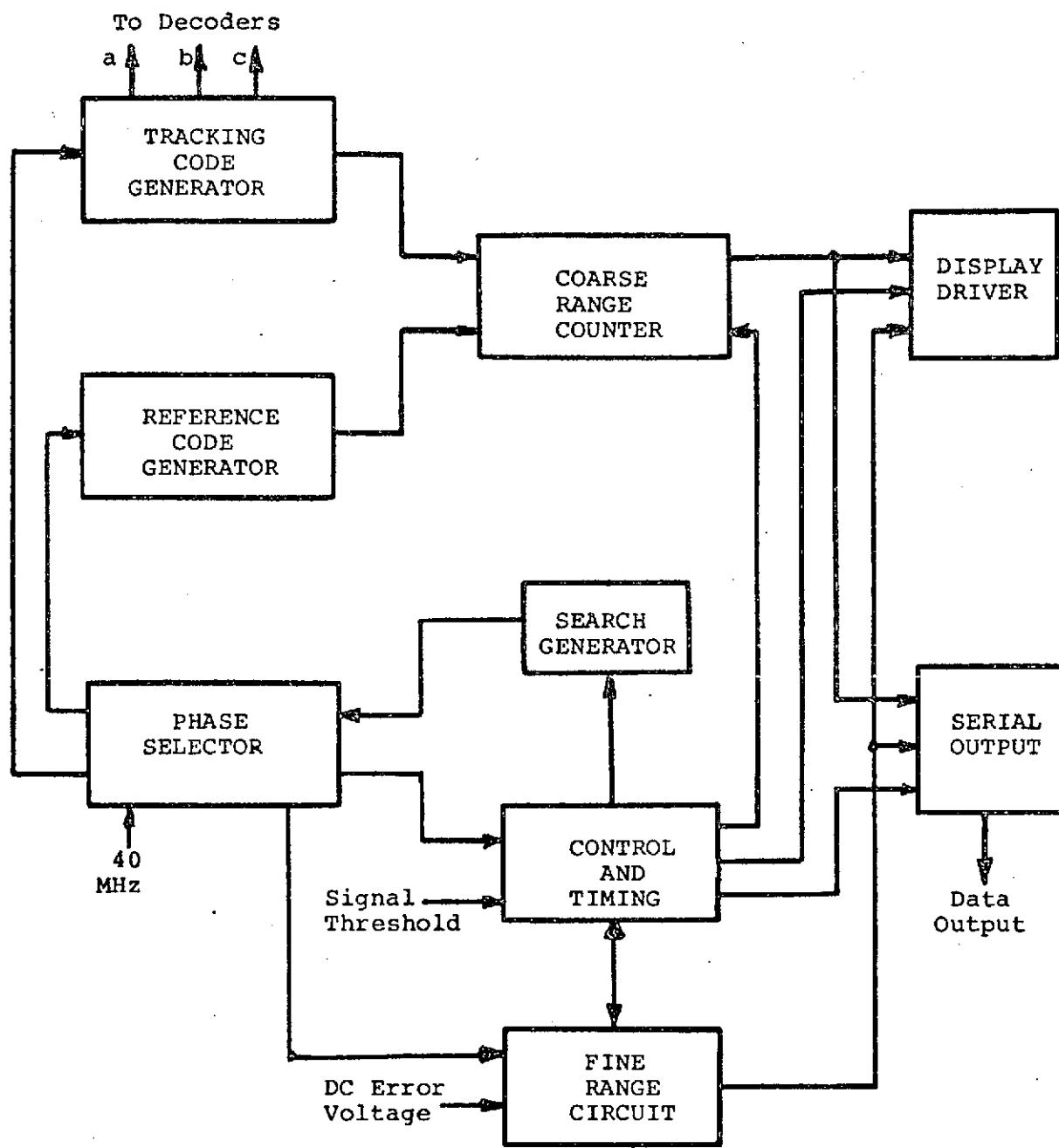
Figure 5-3. Simplified Block Diagram of Digital Subsystem
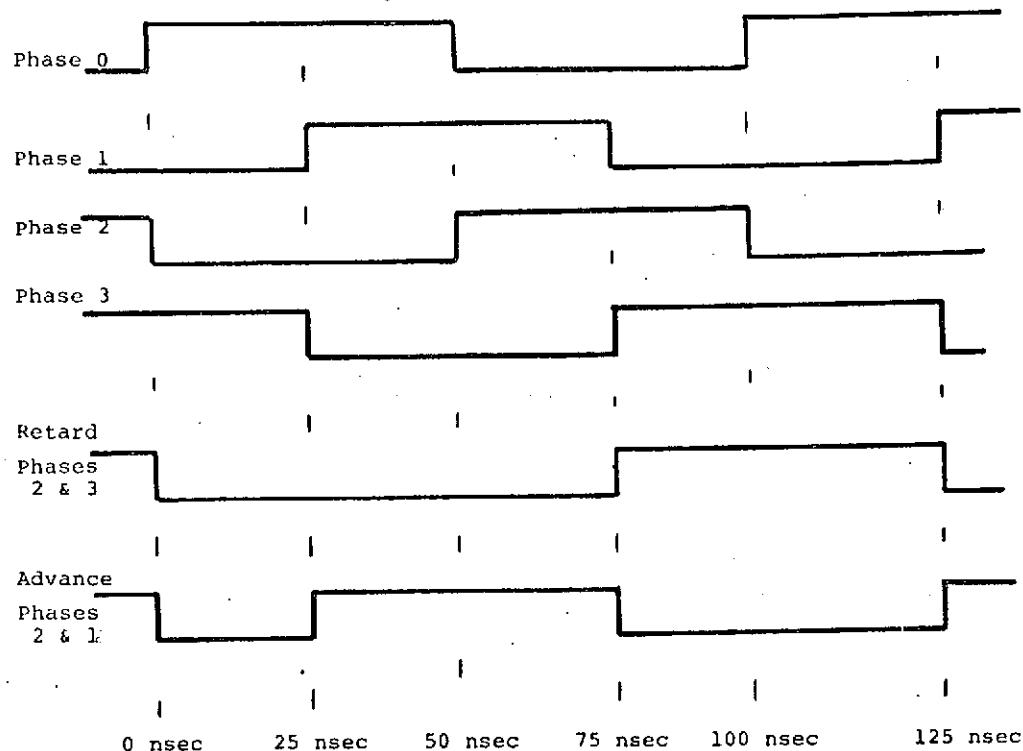
Figure 5-4. Clock Phase Timing Diagram

If the internal code and the received code are within one bit (+100 nsec) of phase lock, an indication is given whenever the received signal strength is above a preset threshold. This receiver threshold should occur each time the satellite antenna illuminates the receiving sites, or approximately 50 milliseconds out of every 783 milliseconds. If the threshold signal is not received for two seconds, the control logic activates the search generator, changing the tracking code generator phase until a threshold (i.e., correlation) is achieved.

When the receiver is in the acquisition or search mode, the code tracking generator is sequenced through the entire 2,047 phase positions relative to the reference generator. When the correlator threshold detectors provide a positive indication, the acquisition mode is stopped and correlation is within ±1 bit.

The range computing circuitry reverts to the tracking mode after the initial acquisition of the received code. In the tracking mode the 10-MHz clock is phase shifted (as previously discussed) in 90° increments to achieve the effective granularity of a 40-MHz clock system. The clock phase shifting is initiated when the correlator phase detector output exceeds the preset threshold criteria.

5.3.3 Search Routine

The rotating ATS-5 satellite imposes a unique search-sequence
requirement on the range acquisition and tracking circuitry.
The usable satellite illumination time at the Wallops Station
is slightly more than 50 milliseconds of every 783 milliseconds
and the correlation system integration time is approximately 1
millisecond. These constraints established the search sequence
shown in Figure 5-5, which achieves system range code phase lock-
on with the ATS-5 satellite within 135 seconds (worst case) for a
2,047-bit code length. If the signal is lost for more than 2
seconds, as measured by the correlator threshold detector circuit,
a search mode is initiated. During normal tracking mode, the
inherent digital memory of the range tracking code generator will
enable re-acquisition of phase lock within the first satellite
illumination burst.

The search pattern times in the receiver are shown in Figure 5-5.
Beginning at an arbitrary zero reference point for the tracking
code generator phase, 12.5-bit positions (fifty 25-nsec steps)
are searched during a 51.2-msec period. These same positions
are searched repeatedly for 821 msec, which is sufficient time
(in excess of 780 msec) to assure that at least one signal burst
has been received from the satellite. The search pattern then
moves to the next 12.5-bit position for the same length of time,
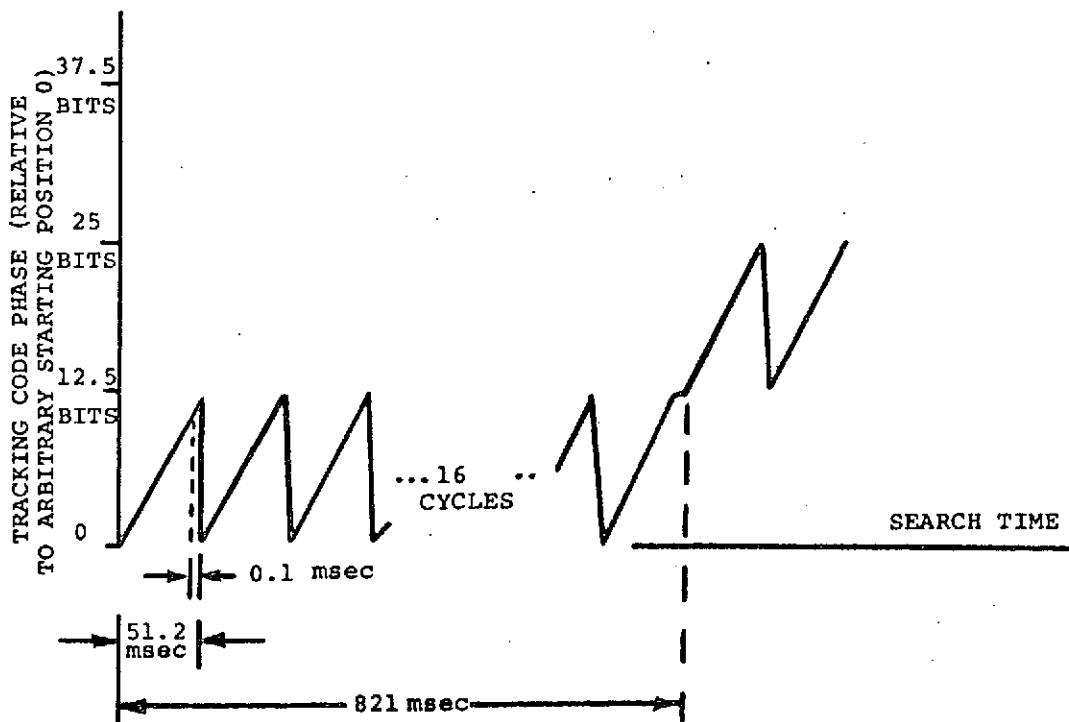
Figure 5-5. Code Search Pattern

5-11

progressing through all the positions in approximately 135 seconds. When correlation is achieved, a receiver threshold signal switches the control logic from the search mode to a tracking mode. The worst-case search time is determined by calculating the number of 12.5-bit searches, that is 2,047/12.5 = 163.7, and multiplying by 0.821 second. The maximum search time, then, is 135 seconds. The presence of a continuous signal (i.e., a non-spinning satellite) would reduce the acquisition time by a factor of approximately 16:1 by allowing a simplified non-repeating search pattern to be implemented.

5.3.4 Tracking Mode Routine

In the tracking mode, the system operates along the Z curve, remaining within $\pm$1/8-bit of the center point (see Figure 5-6). The fine range circuits accomplish this by performing analog-to-digital (A/D) conversions of the correlator DC error voltage and comparing these to preset bounds. If the positive bound (A/D = 25) is exceeded, a signal is sent to the phase selectors to retard the code phase one quarter bit (25 nsec). Similarly, exceeding the negative threshold (0) initiates a 25 nsec phase advance in the code streams.

A/D values measured between these two bounds are valid range readings between 0 and 25 nsec. The clock phase used to drive the tracking code generator provides an indication of the 25-nsec increments. Addition of 0, 25, 50 or 75 nanoseconds to the A/D value is accomplished in the fine range logic and produces the two least significant digits of the range reading.
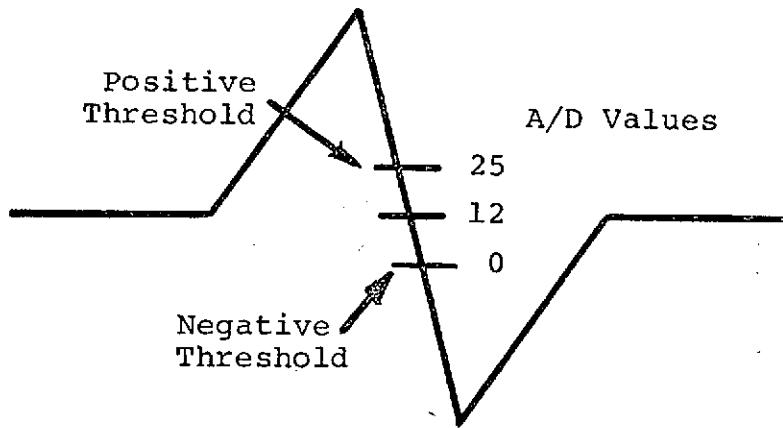
Figure 5-6. "Z" Curve

The range counter determines the remaining range digits by measuring the phase difference between the reference code generator and the tracking code generator. The counter starts incrementing one count every 100 nsec when it receives the sync pulse from the reference generator and stops upon receipt of the sync from the tracking generator.

5.3.5 Data Output and Display

As shown in Figure 5-11 the ALPHA II code correlator displays the range reading to the operator via a 7-segment LED numeric display. Storage elements are provided so that the most recent valid reading is displayed. The data output also is available as a serial bit stream containing the range reading and selected status indicators. The data format consists of four USASCII words using odd parity which allows the information to be transmitted via commonly available data sets and received by the recording device. The signals comply to EIA Standard RS232C levels for ease of interface. The four data words are transmitted when the receiver threshold signal drops if a valid reading had been made while the threshold was present.

5.4 RECEIVER FRONT END

A functional diagram of the receiver front end and IF section is presented in Figure 5-7. The RF preamplifier is a broadband transistorized unit with a measured noise figure of 4.4 dB and a bandwidth greater than 50-MHz. The gain at 1550 MHz is specified as 25 dB minimum. The down-converter is a Schottky-barrier junction - diode mixer with a conversion loss of 8 dB and an optimum noise figure of 8 dB when driven with a local oscillator injection power level of 1 to 10 milliwatts. The total RF-to-IF conversion gain is approximately 110 dB.

The injection chain which supplies the 10-milliwatt, 1480-MHz signal to the down-converter contains several transistor multi- plier stages, a step-recovery diode multiplier and a double balanced mixer. The injection chains require 5-MHz and 1-MHz input signals from the master frequency source. The block diagram also shows generation of the two injection signals required by the code correlator and the ranging computer subsystems.

The 70-MHz IF input impedance is 50 ohms with a nominal sensitivity of approximately -84 dBm. The physical implementation of the 70- MHz IF output is such that other equipments may be interfaced. The IF section was designed with a controlled bandwidth of 25-MHz and a total gain of approximately 90 dB. A broadband AGC detector and amplifier were incorporated to provide gain control of the IF based upon a total detected noise level at the IF output. The
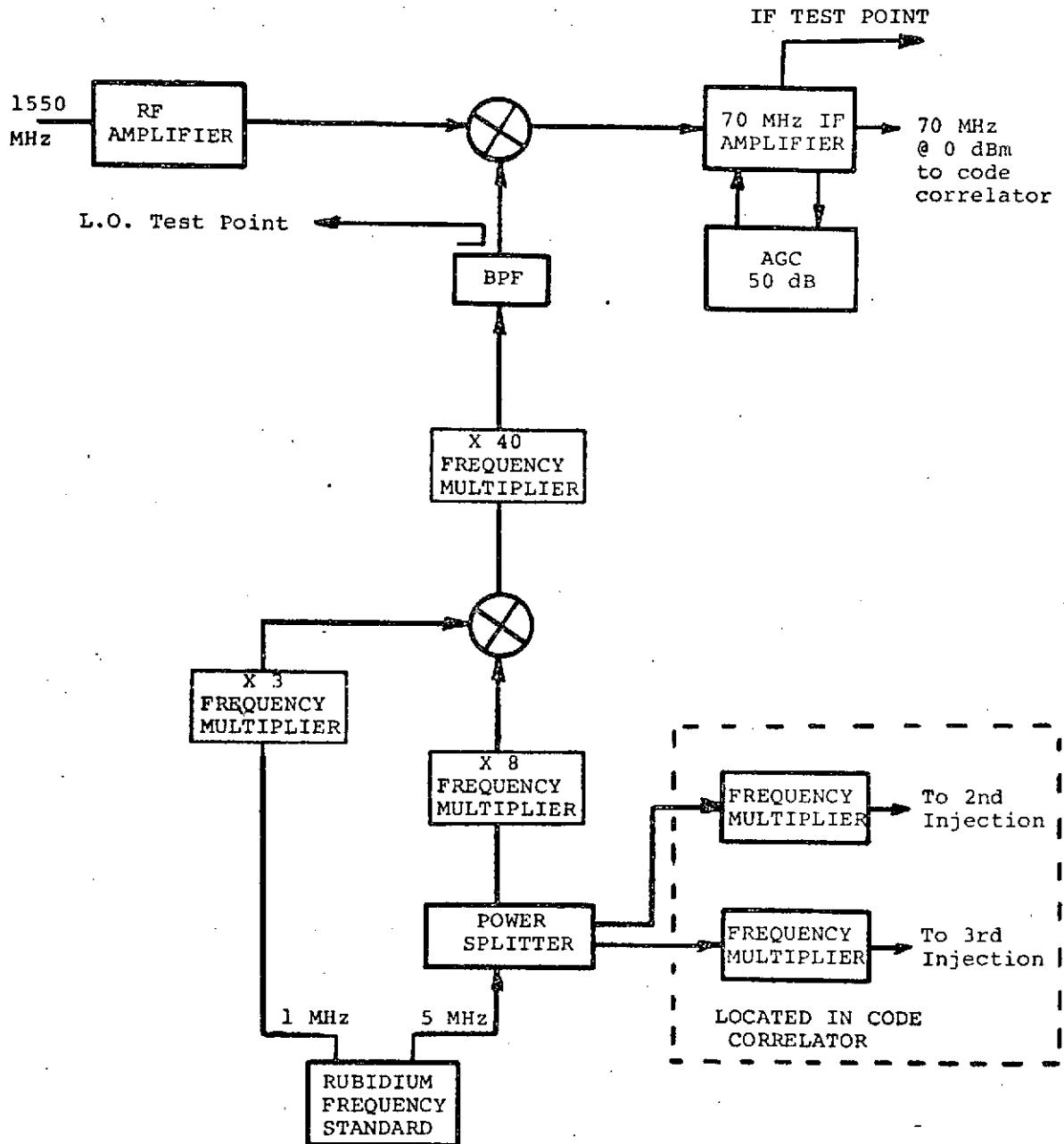
Figure 5-7. Functional Block Diagram of RF Subsystem

wide-bandwidth and stable-phase characteristics of the RF and IF
sections are necessary in order to minimize the influence of
environmental variations upon the signal delays through these
stages. The design techniques associated with the RF and IF
stages and injection chains are conventional but use the latest
state-of-the-art devices. The multiplier stages are well filtered
to remove all spurious products naturally generated in such a
configuration.

5.5 MODULATOR

The ALPHA II modulator installed at the NASA Rosman STADAN Station
is an all-solid-state signal generator used to phase-modulate the
70-MHz IF carrier furnished to the NSAS Rosman transmitter system.
The 70-MHz IF carrier is bi-phase modulated in a PSK manner by the
PN range code, and is compatible with the STADAN interface stand-
ards. The modulator is self-contained and requires only a 5-MHz
master clock signal for operation. The stability of the clock
source governs the stability of the 10-megabit pseudo-random code.
A built-in frequency multiplier chain converts the 5-MHz signal to
a stable 70-MHz carrier by means of a X 7 and a X 2 multiplication.
The resultant carrier is then multiplied by the 10-megabit PRN code
in a phase modulator. The phase modulator shifts the carrier wave
by 180 degrees at each transition of the PN code, thus producing
the bi-phase PSK modulation of the carrier. The modulator is
capable of generating either the 2,047 or 16,383 bit code. The
normal experimental configuration of the modulator at the NASA
Rosman Station consisted of feeding the output of a frequency
synthesizer into the phase modulator at an IF signal frequency
of 70.1-MHz. This was necessitated by the biased bandpass char-
acteristics of the ATS-5 C-band to L-band cross-strapped trans-
ponder. A similar modulator was also employed at the Wallops
Station test configuration for pre- and post-calibration test
purposes.

5.6 RUBIDIUM FREQUENCY STANDARDS

In general, four types of frequency standards are commonly used:

    (1) Atomic hydrogen maser

    (2) Cesium atomic-beam-controlled oscillator

    (3) Rubidium gas-cell-controlled oscillator

    (4) Quartz crystal oscillator

The first two are referred to as primary frequency standards and
the last two as secondary frequency standards. The advantages and
limitations of each standard type are summarized in Table 5-2.
The requirements of the positioning experiment were basically
portability and good short-term stability. Therefore, the rubidium
gas-cell-controlled oscillator was recommended for the test.

TABLE 5-2.   CHARACTERISTICS OF FREQUENCY STANDARDS

Standard	Construction	Advantages	Limitation
Atomic Hydrogen Maser	Active Maser	Primary Standard Long and Short Term Stability	Size and weight
Cesium Atomic Beam Resonator Controlled Oscillator	Atomic beam interaction with fields	Primary Standard Long-term Stability	Short-term stability
Rubidium Gas Cell Resonator Controlled Oscillator	Gas buffered resonance cell with optically pumped state selection	Compact and lightweight Good short-term stability	Secondary Standard Requires calibration
Quartz Crystal Oscillator	Quartz crystal	Very compact, light, rugged and inexpensive	Long-term stability

Two identical Varian Associates Model R-20 Rubidium Frequency Standards were employed during the experiment as the frequency sources. The frequency standard consists primarily of a servo system in which a crystal oscillator is locked to an electron hyperfine transition frequency found in the rubidium atom. This provides the long-term stability reference, and the crystal oscillator provides the short-term stability and spectral purity.

The Model R-20 Rubidium Frequency Standard has the published specifications summarized in Table 5-3, The instrument is designed for highly portable applications, employing a 24 to 30 volt d-c battery-pack input for standby or field-use. During the experiment, the standards were operated from 24-volt, 200-AH batteries which were recharged following each test period. The battery for the remote system also supplied power for the fans and code tracking logic in the code correlator via a solid-state DC/AC inverter. Continuous power was required to preserve the code reference after calibration.

5.7   DATA RECORDING SUBSYSTEM

The serial data stream generated by each code correlator contains the range reading which was permanently recorded on magnetic tape

TABLE 5-3. SPECIFICATIONS FOR VARIAN MODEL R-2
RUBIDIUM FREQUENCY STANDARD

Parameter	Value
Output Frequencies	5 MHz, 1 MHz and 100 kHz, simultaneously at front and rear panel
Output Level	1 V rms, into 50 ohms
Frequency Stability (Standard Deviation)	1×10^{-11} for a one-second averaging time 5×10^{-11} over any one-year period
Environmental Stability	Above long- and short-term stability specifications will be maintained over the following conditions: ● Temperature: 0° to 50°C ● Humidity: 0 to 95% ● Input Voltage: $\pm15\%$ of nominal ● Load: Changed $\overline{\text{from}}$ open to short-circuit at any other terminal ● Magnetic Field: Less than 5×10^{-12} frequency change for any orientation in the Earth's field
Radio Frequency Interference	RFI shielded
Warm-Up Time	Instrument accuracy is $\pm1 \times 10^{-10}$ after less than a one-hour period
Alarm Indicator	Front panel continuity alarm light visually indicates that the output frequency is locked
Input Requirements	24 - 30 V dc nominal; less than 1 amp operating; 2.5 amps warm-up
Packaging	Dimensions are 4-7/8 inches by 7-5/8 inches by 19-9/16 inches. Weight is 20 pounds.

by the data recording subsystem. The tape recording subsystem consisted of a Kennedy Model 1510 incremental tape recorder driven by an AII tape control unit, Model TC-701. The AII tape control unit (TCU), shown in the functional block diagram of Figure 5-8, is specifically designed to record the serial data from each code correlator. It accepts four consecutive ASCII-odd bytes (RS 232C or TTL compatible) at 110 baud, on each of two channels, checks the parity, formats the 28 bits of data, and writes the data on magnetic tape via the 7-track (6 data, 1 parity) Kennedy incremental tape recorder. Successive blocks of four bytes on each TCU channel must be separated by a minimum of 50 milliseconds. The delay between the arrival of data blocks on the two channels must be less than 50 milliseconds. The parity bits must arrive correctly on each channel for any information to be recorded. Inter-record gaps are inserted between information sets.

As shown in Figure 5-8, the TCU receives four ASCII-odd bytes from the code correlator, strips the four control bits from each 11-bit byte, stores the stripped data in a shift register, checks parity, verifies that all four bytes have arrived, and (for two-channel operation) verifies that the block of data on each channel has arrived within 50 milliseconds of the other channel. If these criteria are satisfied, the multiplexer formats the stored data and provides the proper write-clock and gap pulses for the magnetic tape transport. The data format generated by each code correlator is shown in Figure 5-9.

The data format appearing on the magnetic tape can include a "time" representation. When the mode switch is placed in the RECORD position, an elapsed time counter is initiated. The maximum time indication before repeating is 59 minutes 59.9 seconds and the resolution is 100 milliseconds. The time indication is automatically recorded with each data file as three bytes. The data file written on 7-track magnetic tape is shown in Table 5-4. The "C" or parity bit is automatically generated by the tape recorder and is therefore not shown in the table.

During the experiment, the data link to the TCU from the fixed site receiver was simply a direct cable since the code correlator output and the TCU input are RS232C compatible. The data link for data transmission from the remote receiver site was via a pair of RS232C compatible acoustic couplers and a commercial telephone line. This is shown in simplified form in Figure 5-10.

5.8 EQUIPMENT PHYSICAL DESCRIPTION

The three main assemblies which comprise each receiver system are shown in the photographs of Figure 5-11. Each unit is contained in a standard 19-inch wide rack-mounted enclosure.
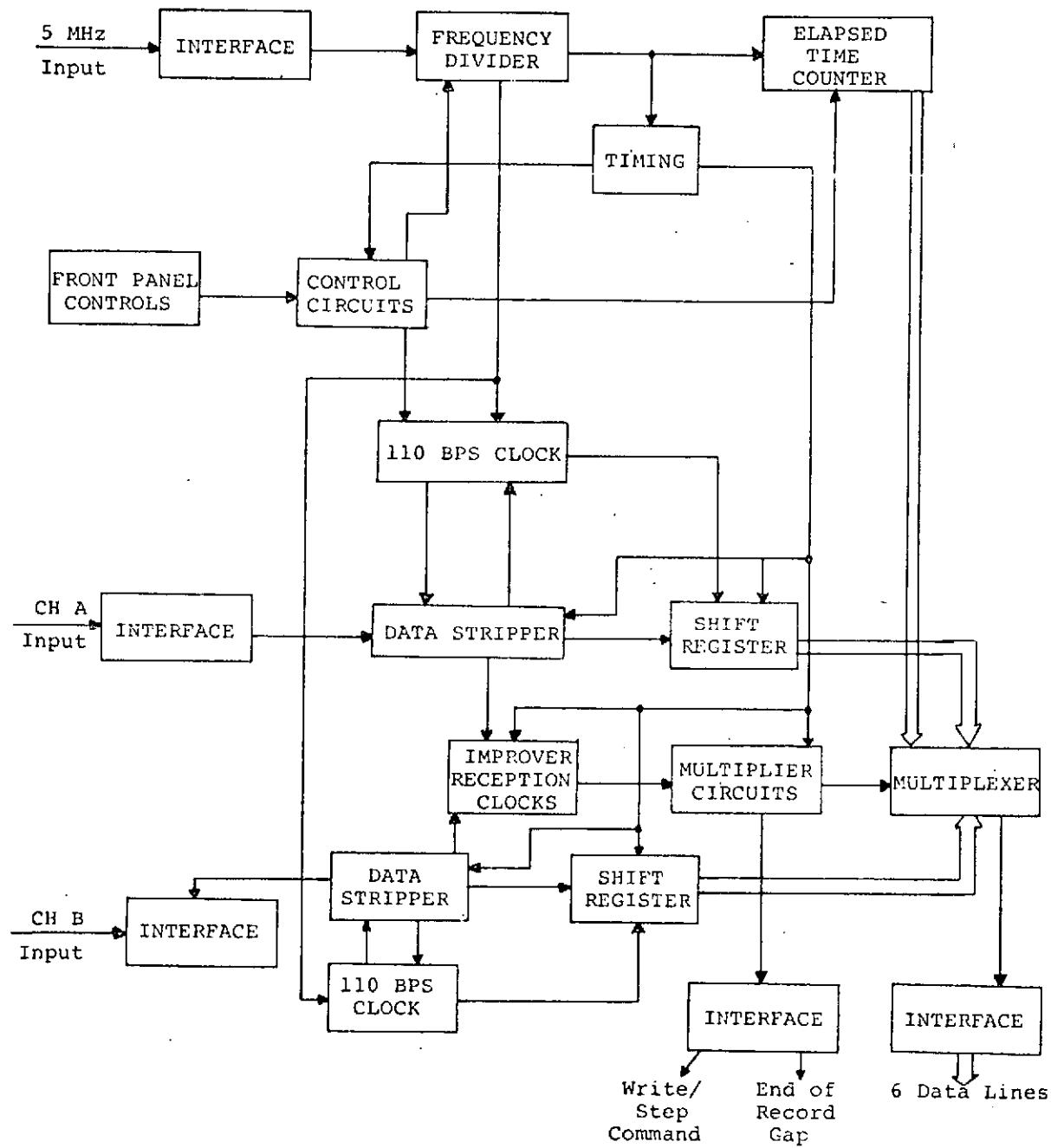
Figure 5-8.   Functional Block Diagram of Tape Control Unit

```
        1 ─┐  START ┌──┬──┬──┬──┬──┬──┬──┬──┬─────────┐
BYTE 1     │    1   │A1│A2│A3│A4│A5│A6│A7│P1│ STOP 1  │     └──
        0 ─┘        └──┴──┴──┴──┴──┴──┴──┴──┘         └───

        1 ─┐  START ┌──┬──┬──┬──┬──┬──┬──┬──┬─────────┐
BYTE 2     │    2   │B1│B2│B3│B4│B5│B6│B7│P2│ STOP 2  │     └──
        0 ─┘        └──┴──┴──┴──┴──┴──┴──┴──┘         └───

        1 ─┐  START ┌──┬──┬──┬──┬──┬──┬──┬──┬─────────┐
BYTE 3     │    3   │C1│C2│C3│C4│C5│C6│C7│P3│ STOP 3  │     └──
        0 ─┘        └──┴──┴──┴──┴──┴──┴──┴──┘         └───

        1 ─┐  START ┌──┬──┬──┬──┬──┬──┬──┬──┬─────────┐
BYTE 4     │    4   │D1│D2│D3│D4│D5│D6│D7│P4│ STOP 4  │     └──
        0 ─┘        └──┴──┴──┴──┴──┴──┴──┴──┘         └───
```
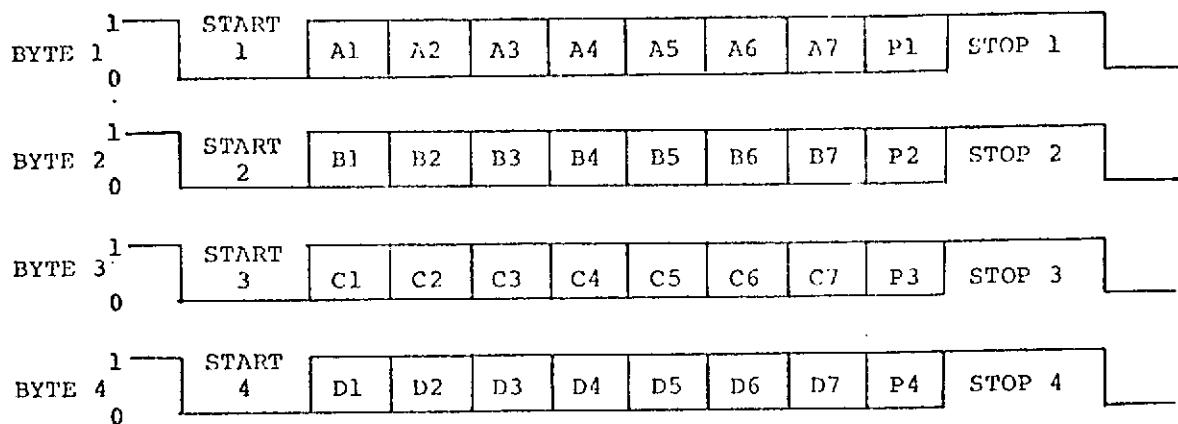
Figure 5-9. Correlator Output Data Format

TABLE 5-4. MAGNETIC TAPE DATA FORMAT

			Data Lines					
			B	A	8	4	2	1
Channel A Data	Bit No.	1	A2	A1	B3	B2	B4	"1"
		2	B1	A7	A6	A5	A4	A3
		3	C2	C1	B7	B6	B5	E
		4	D1	C7	C6	C5	C4	C3
		5	D7	D6	D5	D4	D3	D2
Channel B Data	Bit No.	6	A2	A1	B3	B2	B4	"0"
		7	B1	A7	A6	A5	A4	A3
		8	C2	C1	B7	B6	B5	E
		9	D1	C7	C6	C5	C4	C3
		10	D7	D6	D5	D4	D3	D2
TIME		11	M2	M4	M8	M10	M20	M40
		12	S4	S8	S10	S20	S40	M1
		13	S0.1	S0.2	S0.4	S0.8	S1	S2

E = "1" for CAL, "0" for NORMAL

Commercial Telephone Lines

```
                    ┌───────────┐          ┌───────────┐
                    │ TELEPHONE │          │ TELEPHONE │
                    └───────────┘          └───────────┘
                          │                      ▲
                          ▼                      │
                    ┌───────────┐          ┌───────────┐
                    │ ACOUSTIC  │          │ ACOUSTIC  │
                    │ COUPLER 2 │          │ COUPLER 1 │
                    └───────────┘          └───────────┘
                          │                      ▲
  ┌───────────┐           ▼                      │
  │  FIXED    │     ┌───────────┐          ┌───────────┐
  │ RECEIVER  │────▶│TAPE CONTROL│         │  REMOTE   │
  └───────────┘     │   UNIT    │          │ RECEIVER  │
                    └───────────┘          └───────────┘
                          │
                          ▼
                    ┌───────────┐
                    │INCREMENTAL│
                    │   TAPE    │
                    │ RECORDER  │
                    └───────────┘
```
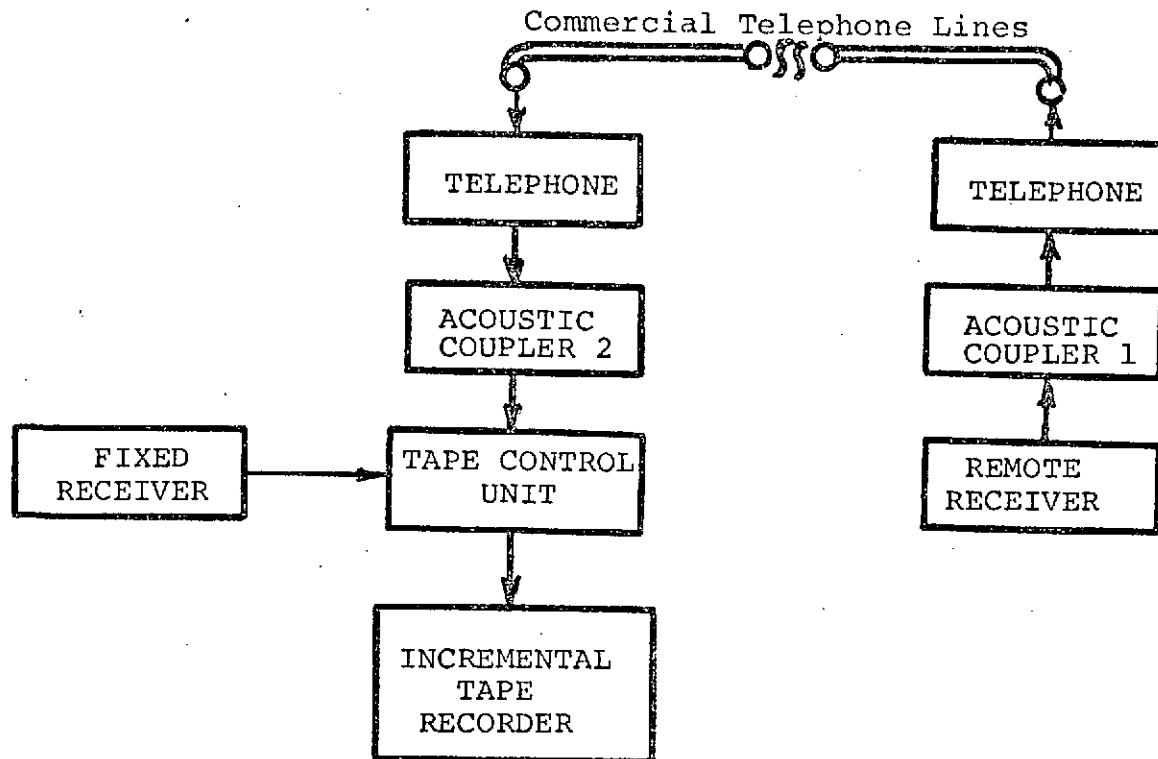
Figure 5-10.   Experiment Data Transmission Link

The RF front end is a 5-1/4 inch high drawer having a depth of
17 inches. The packaging consists principally of shielded RF
subassemblies mounted internally on an aluminum shelf. RF signal
input and output connectors are located in the rear, together
with A-C power connection. This unit contains its own internal
power supply. The receiver down-converter weighs about 25 pounds
and occupies 1.3 cubic feet.

The code correlator unit is 7 inches high by 21 inches deep.
All input and output connnections are on the rear panel. The
front panel includes test points, control switches and an LED
readout display of the range reading in nanoseconds. The readout
display was included to provide a "real-time" check of operation
and reasonableness of data during testing. A "track" light
on the panel is illuminated on each pass of the satellite beam
to indicate signal presence in the receiver channel. Figure 5-12
shows several of the RF subassemblies alongside the printed
circuit cards which comprise the digital ranging circuits.

The power supply furnished the various voltages required by the
code correlator. Meters are included to monitor current and
voltage. This unit is 7 inches high and 15 inches deep, occupying
a total of 1.2 cubic feet. The weight is 35 pounds.

Figure 5-13 shows the AII modulator which was installed at the
NASA Rosman Station, and is also a 19-inch-wide, rack-mounted unit.
The 3-1/2 inch by 19 inch Tape Control Unit is also shown in
Figure 5-13.
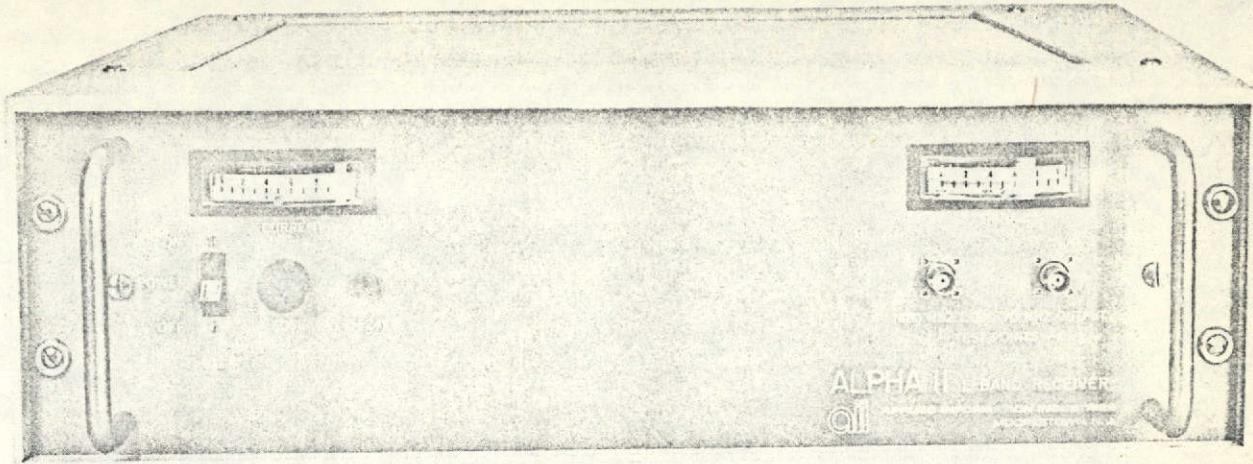
RF Front End
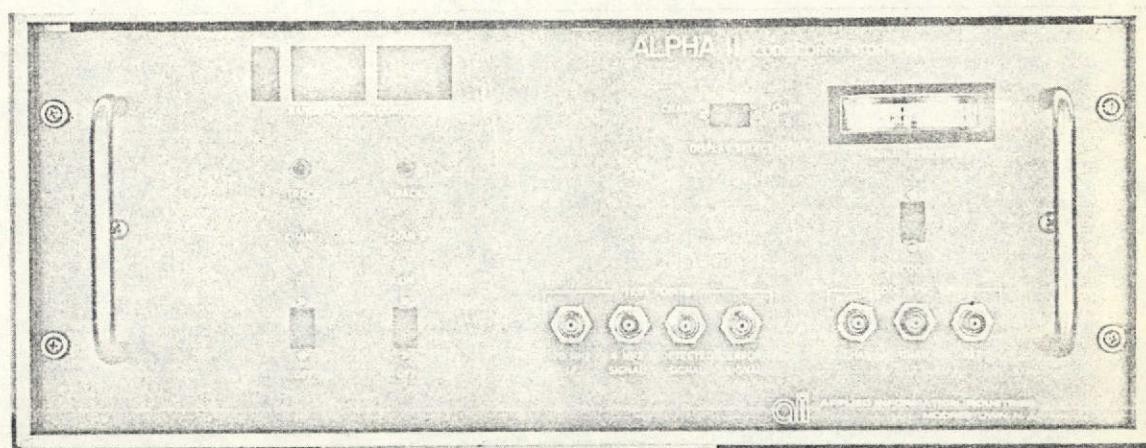
Code Correlator
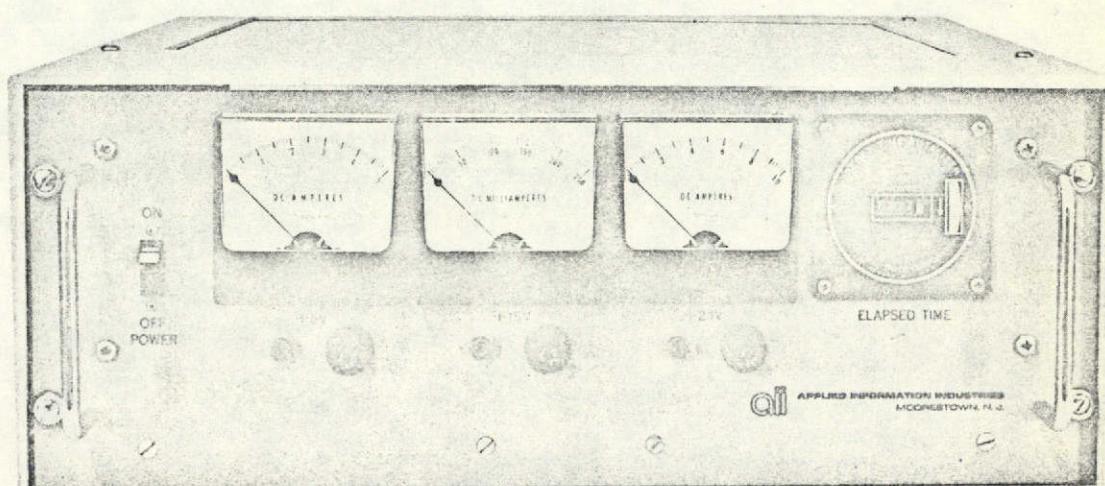
Power Supply

Figure 5-11.   L-Band Correlation Receiver Assemblies
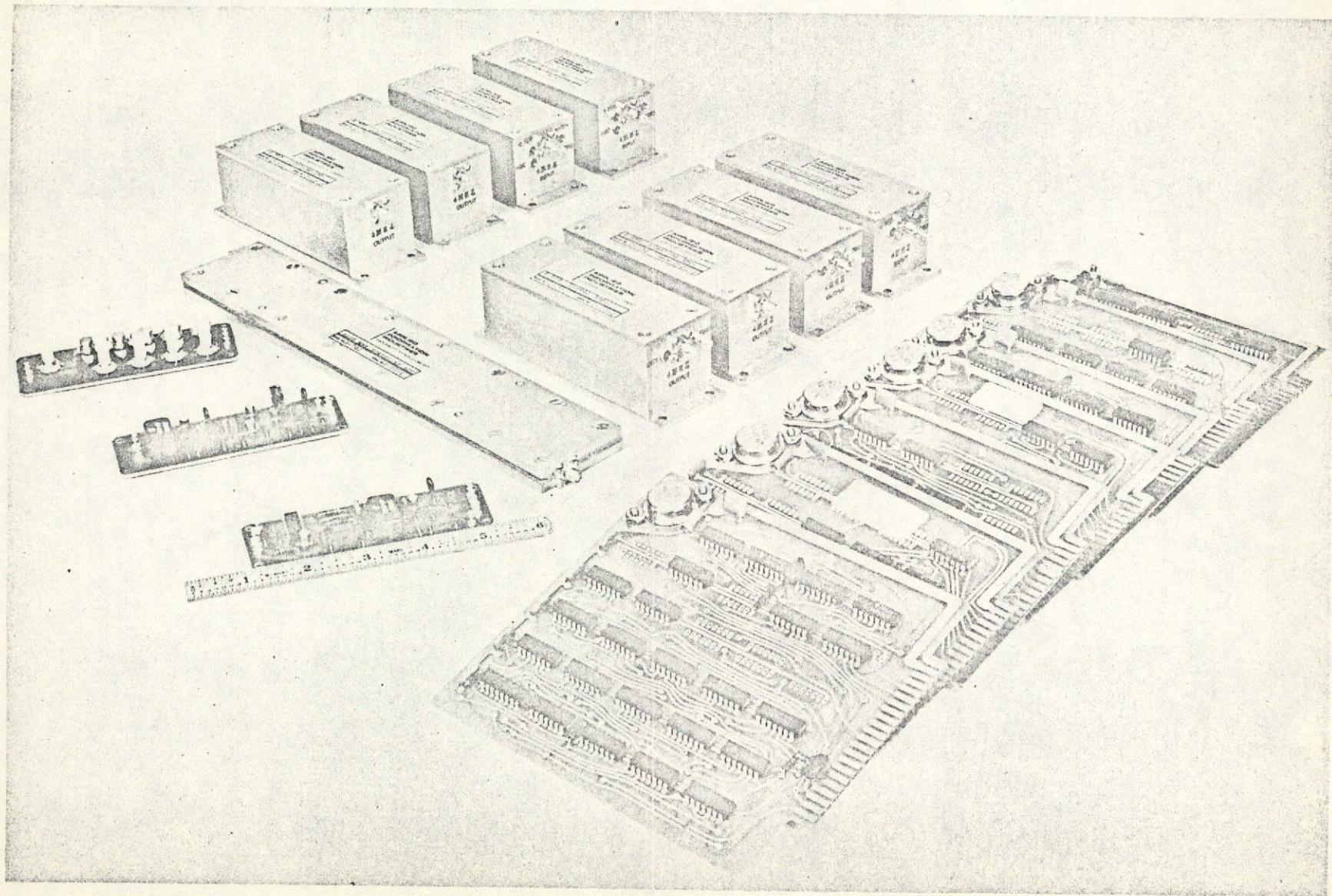
Figure 5-12. Receiver Subassemblies
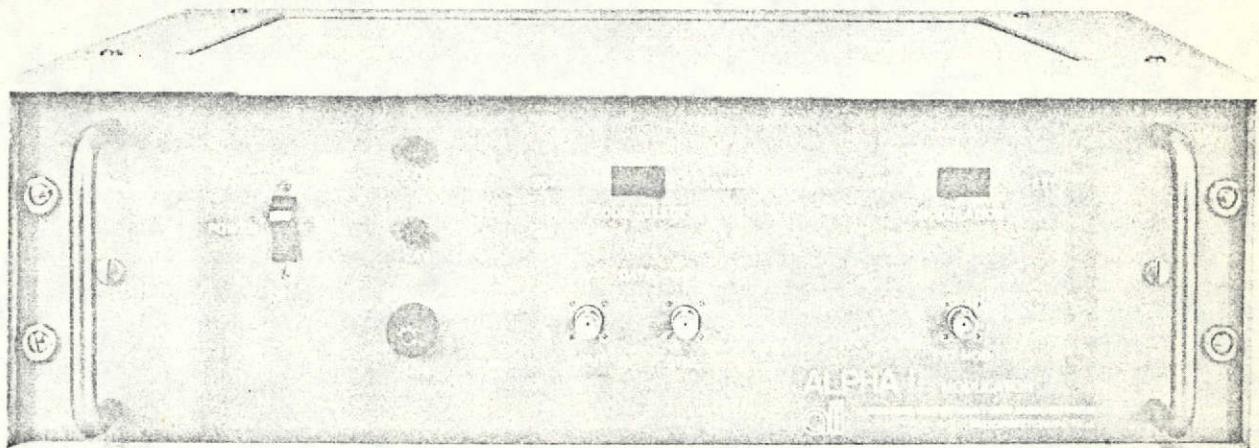
ALPHA II MODULATOR
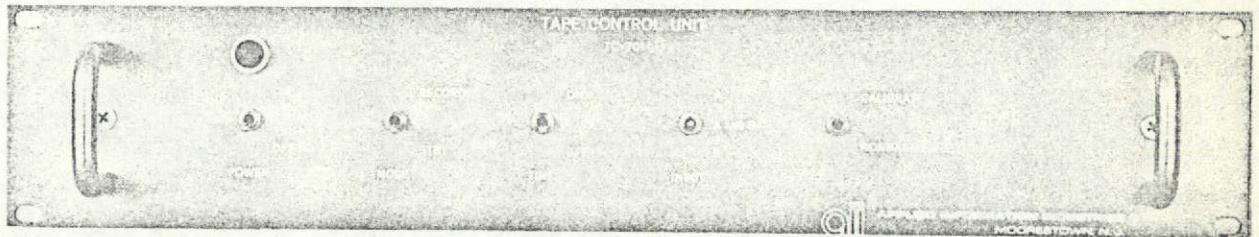
TAPE CONTROL UNIT

Figure 5-13. Modulator and TCU Assemblies

APPENDIX A

DATA SUMMARY

In order to place the data reduction and summary method in proper perspective, the flow of information is traced from the time the two correlators make their measurements until the lines of position (LOP's) are determined.

Assuming that at a given time the code correlators make valid measurements on the respective ranges to the satellite, the range values are sent to the tape recorder subsystem and recorded. The decimal format of these binary numbers is shown in the last 24 columns of Table A-1 (a segment of data from Test 12, July 27), divided in two groups of 12 columns each. This is the rawest form in which data is available. The computer, under control of the Raw Tape Decoder Program, decodes the raw data bits into time, status indicators and coarse and fine range values for both receivers. At this time record numbers are assigned, range values are converted to feet, and the range difference is determined.

A magnetic tape of the converted data is then generated and submitted to the Lines of Position Computer Program. The first operation of this program is to align the recorded time with Greenwich Mean Time. Since the time counter of the incremental tape recorder overflows at 59 minutes 59.9 seconds, all succeeding recorded times must be increased by one hour until the next counter overflow occurs, after which two hours are added, etc. In addition, this program aligns the zero time, corresponding to tape recorder turn-on, with the actual time of the start of test. Thus, the true Greenwich Mean Times for the data presented in Table A-1 are achieved by adding a correction factor of one hour, 20 minutes to the record times indicated.

The next step is the determination of the parabolic fits to the sets of satellite latitude, longitude and geocentric range. These parabolas for test 12 are:

- Latitude $= -.723 + .109t + .019t^2$ deg.

- Longitude $= 105.216 - .048t + .001t^2$ deg.

- Range $= 22717.705 - 2.600t + 1.220t^2$ nmi.

The calibration data is fit to a straight line:

$$L_{12} = -79619.478 - 605.738t$$

The time t is in hours and decimal hours since 0000 GMT.

TABLE A-1.   SAMPLE CODED AND DECODED DATA FROM TEST 12 (JULY 27, 1971)

TIME HH MM SS.SS	RECORD NUMBER	STA CAL S/T THR CHN 1 2 1 2 1 2 1 2 1 2	COARSE1 FINE1 (NSEC)	COARSE2 FINE2 (NSEC)	RANGE1 (FEET)	RANGE2 (FEET)	DELTA R (FEET)	RAW FRAMES 1-6	RAW FRAMES 7-12
0-58-49.40	2053	1 0 0 0 1 1 1 1 1 1	561 22	1172 40	55200.0	115313.9	60113.9	172100524156	004050231522
0-58-50.10	2054	1 0 0 0 1 1 1 1 1 1	561 5	1172 26	55183.3	115300.1	60116.9	175000524116	314050231512
0-58-50.90	2055	1 0 0 0 1 1 1 1 1 1	560 91	1172 24	55169.5	115298.1	60128.7	374200520115	114050231512
0-58-51.70	2056	1 0 0 0 1 1 1 1 1 1	560 70	1172 9	55148.8	115283.4	60134.6	570300520116	444050231512
0-58-52.50	2057	1 0 0 0 1 1 1 1 1 1	560 56	1171 91	55135.1	115265.7	60130.6	573200520136	424050431512
0-58-54.10	2058	1 0 0 0 1 1 1 1 1 1	560 21	1171 62	55100.6	115237.2	60136.5	174100520156	214050431552
0-58-54.80	2059	1 0 0 0 1 1 1 1 1 1	560 15	1171 40	55094.7	115215.5	60120.8	172200520156	004050431552
0-58-56.40	2060	1 0 0 0 1 1 1 1 1 1	559 76	1171 4	55056.4	115189.1	60123.7	573300524616	104050431552
0-58-58.00	2061	1 0 0 0 1 1 1 1 1 1	559 34	1170 77	55015.1	115153.6	60138.5	171300524655	734050031532
0-58-58.70	2062	1 0 0 0 1 1 1 1 1 1	559 22	1170 63	55003.3	115139.8	60136.5	172100524655	614050031532
0-58-59.50	2063	1 0 0 0 1 1 1 1 1 1	559 14	1170 57	54995.4	115133.9	60138.5	171200524555	724050031532
0-59-0.30	2064	1 0 0 0 1 1 1 1 1 1	558 92	1170 41	54973.8	115118.2	60144.4	372200520455	404050031501
0-59-1.90	2065	1 0 0 0 1 1 1 1 1 1	558 66	1169 82	54948.2	115069.1	60111.9	573100520636	204050451501
0-59-2.60	2066	1 0 0 0 1 1 1 1 1 1	558 48	1169 77	54930.5	115055.2	60124.7	570400520656	734050451501
0-59-4.20	2067	1 0 0 0 1 1 1 1 1 1	558 14	1169 38	54897.0	115016.8	60119.8	171700520416	074050451541
0-59-5.00	2068	1 0 0 0 1 1 1 1 1 1	558 19	1169 29	54902.0	115008.0	60106.0	174600520616	454050451541
0-59-5.80	2069	1 0 0 0 1 1 1 1 1 1	557 84	1169 10	54867.5	114989.3	60121.8	371000527216	024050451541
0-59-6.50	2070	1 0 0 0 1 1 1 1 1 1	557 69	1169 18	54852.8	114997.2	60144.4	574500527216	064050451541
0-59-7.30	2071	1 0 0 0 1 1 1 1 1 1	557 43	1168 91	54827.3	114970.6	60143.4	576000527235	424050051541
0-59-8.90	2072	1 0 0 0 1 1 1 1 1 1	557 16	1168 54	54800.7	114934.2	60133.6	173200527255	124050051521
0-59-10.40	2073	1 0 0 0 1 1 1 1 1 1	556 84	1168 2	54769.2	114883.1	60113.9	371000520216	204050051511
0-59-11.20	2074	1 0 0 0 1 1 1 1 1 1	556 68	1168 13	54753.4	114893.9	60140.5	570500520216	624050051511
0-59-12.80	2075	1 0 0 0 1 1 1 1 1 1	556 49	1167 85	54734.8	114866.4	60131.6	574400520236	504050711511
0-59-13.60	2076	1 0 0 0 1 1 1 1 1 1	556 17	1167 66	54703.3	114847.7	60144.4	177200520256	314050711511
0-59-14.30	2077	1 0 0 0 1 1 1 1 1 1	556 6	1167 28	54692.5	114810.3	60117.8	173000520216	054050711551
0-59-15.90	2078	1 0 0 0 1 1 1 1 1 1	555 89	1167 16	54675.7	114798.5	60122.8	374400520216	324050711551
0-59-16.70	2079	1 0 0 0 1 1 1 1 1 1	555 53	1167 2	54640.3	114784.7	60144.4	575200520215	204050711551
0-59-17.50	2080	1 0 0 0 1 1 1 1 1 1	555 42	1166 94	54629.5	114776.9	60147.3	572000520235	124050311551
0-59-20.60	2081	1 0 0 0 1 1 1 1 1 1	554 77	1166 19	54565.6	114703.1	60137.5	577300520215	464050311505
0-59-21.40	2082	1 0 0 0 1 1 1 1 1 1	554 67	1166 16	54555.7	114700.1	60144.4	577100520215	324050311505
0-59-22.20	2083	1 0 0 0 1 1 1 1 1 1	554 49	1165 90	54538.0	114674.6	60136.5	574400520236	024050511505
0-59-22.90	2084	1 0 0 0 1 1 1 1 1 1	554 40	1165 76	54529.2	114660.8	60131.6	570000520256	334050511505
0-59-24.50	2085	1 0 0 0 1 1 1 1 1 1	554 14	1165 35	54503.6	114620.5	60116.9	171200520215	534050511545
0-59-25.30	2086	1 0 0 0 1 1 1 1 1 1	553 89	1165 37	54479.0	114622.4	60143.4	374400520215	734050511545
0-59-27.60	2087	1 0 0 0 1 1 1 1 1 1	553 36	1164 79	54426.9	114565.4	60138.5	173300520256	474050111545
0-59-28.40	2088	1 0 0 0 1 1 1 1 1 1	553 12	1164 59	54403.3	114545.7	60142.4	172200520256	464050111525
0-59-29.20	2089	1 0 0 0 1 1 1 1 1 1	553 11	1164 59	54402.3	114545.7	60143.4	174200520256	464050111525
0-59-29.90	2090	1 0 0 0 1 1 1 1 1 1	552 91	1164 44	54382.6	114531.0	60148.3	374200520256	104050111525

It should be noted here that the range difference (ΔR) in Table A-1 equals $M_2 - M_1$, i.e., the measurement by the B or second receiver, reduced by the measurement of the fixed, or second receiver. However, the Lines of Position Program calculated the LOP's using $M_1 - M_2$ thus causing ΔR to change sign.

The ephemeris and calibration line are evaluated at 2 hours, 18 minutes, 49.4 seconds, corresponding to the first entry in Table A-1. The relative position calculations (see Appendix B) are then made and the longitudes corresponding to the reference latitudes of 37.864253 and 37.864300 degrees are recorded. These longitudes are 75.5075923 and 75.5076569, as given in Table A-7 for Test 12, (page 2 of 3). The other individual records of Table A-1 are also all used to determine the LOP's of Table A-7; but, no smoothing on the observed range differences was attempted in this case. The third longitude shown in the table is the running average of the longitudes corresponding to the first reference latitude. A similar segment of unsmoothed range data is given for Test 2 in Table A-3.

In general, twenty consecutive range differences were fitted to parabolas. These parabolas were then evaluated at the center of the timespan. The LOP's were then determined as described above. The resulting LOP's were then plotted in Figures 4-6 through 4-10 for data collected on July 12, 15, 21, 27 and 28.

```
    ATS-5 EPHEMERIS
    TIME     SAT RANGE   LATITUDE    LONGITUDE
    GMT        NMI         DEG         DEG
163000.0    22781.02     0.150      105.231
170000.0    22778.04     0.038      105.250
173000.0    22774.59    -0.075      105.268
180000.0    22770.74    -0.187      105.282
183000.0    22766.55    -0.295      105.294
190000.0    22762.11    -0.399      105.303


PARABOLIC FIT TO EPHEMERIS-LINEAR TO CAL DATA
                 CONSTANT       LINEAR    QUADRATIC      RMS
LATITUDE        5.1302323     -0.3724861   0.0042857   0.00105
LONGITUDE     103.8968293      0.2165345  -0.0052851   0.00028
GEOC RANGE   22676.5297855    18.4297095  -0.7330221   0.03894
CALIB LINE   89660.2196161  -547.5374731              14.02497


    TIME    RANGE DIF.   CAL. VAL.         LONGITUDES(DEG)
    GMT       (FT)         (FT)      POINT1        POINT2  CUMUL. AVG.
185645.8   100259.69    79286.54   75.5075091   75.5075732   75.5075091
185724.0   100262.80    79280.73   75.5075602   75.5076244   75.5075347
185753.6   100262.91    79276.23   75.5075854   75.5076495   75.5075516
185833.4   100199.66    79270.18   75.5072198   75.5072840   75.5074686
185904.5   100244.23    79265.45   75.5075263   75.5075904   75.5074802
185938.8   100239.49    79260.23   75.5075247   75.5075889   75.5074876
190021.7   100224.30    79253.71   75.5074645   75.5075287   75.5074843
190056.0   100209.99    79248.49   75.5074027   75.5074669   75.5074741
190130.3   100230.67    79243.27   75.5075613   75.5076255   75.5074839
190204.6   100219.54    79238.06   75.5075195   75.5075837   75.5074874
190238.8   100164.17    79232.86   75.5071990   75.5072632   75.5074611
190316.6   100166.46    79227.11   75.5072447   75.5073088   75.5074431
190404.6   100186.19    79219.81   75.5074086   75.5074728   75.5074405
190501.8   100214.99    79211.11   75.5076373   75.5077015   75.5074545
190540.4   100204.87    79205.23   75.5076055   75.5076697   75.5074646
190638.5   100191.57    79200.96   75.5075449   75.5076091   75.5074696
190653.9   100159.11    79196.34   75.5073656   75.5074298   75.5074635
190710.8   100167.37    79191.49   75.5074440   75.5075082   75.5074624
190734.2   100176.09    79187.93   75.5075183   75.5075825   75.5074654
190810.0   100168.41    79182.48   75.5074995   75.5075637   75.5074671
190847.8   100143.54    79176.73   75.5073741   75.5074383   75.5074626
190917.8   100153.57    79172.17   75.5074621   75.5075263   75.5074626
190939.7   100116.12    79168.84   75.5072443   75.5073085   75.5074531
191021.3   100110.98    79162.51   75.5072463   75.5073105   75.5074445
191101.5   100124.39    79156.40   75.5073641   75.5074283   75.5074413
191149.8   100117.59    79149.05   75.5073612   75.5074254   75.5074382
191224.9   100131.60    79143.71   75.5074785   75.5075427   75.5074397
191300.7   100135.06    79138.27   75.5075299   75.5075941   75.5074429
191333.4   100125.24    79133.29   75.5074951   75.5075593   75.5074447
191415.5   100081.40    79126.89   75.5072538   75.5073180   75.5074383
```

TIME	RANGE DIF.	CAL. VAL.	LONGITUDES (DEG)		
GMT	(FT)	(FT)	POINT 1	POINT 2	CUMUL. AVG.
191443.2	100114.68	79122.68	75.5074863	75.5075505	75.5074399
191522.5	100085.61	79116.70	75.5073357	75.5073999	75.5074366
191611.6	100106.23	79109.23	75.5075063	75.5075705	75.5074387
191643.6	100106.75	79104.37	75.5075360	75.5076002	75.5074416
191721.0	100101.18	79098.68	75.5075319	75.5075961	75.5074442
191750.6	100100.47	79094.18	75.5075519	75.5076161	75.5074472
191821.0	100075.52	79089.55	75.5074703	75.5075345	75.5074478
191902.3	100082.12	79083.27	75.5074957	75.5075599	75.5074491
191929.6	100079.95	79079.12	75.5075046	75.5075689	75.5074505
192006.2	100081.19	79073.55	75.5075427	75.5076070	75.5074528
192044.4	100095.34	79067.74	75.5076635	75.5077277	75.5074579
192118.7	100081.70	79062.53	75.5076068	75.5076702	75.5074615
192147.5	100067.57	79058.15	75.5075408	75.5076051	75.5074633
192217.1	100074.13	79053.64	75.5076066	75.5076709	75.5074666
192247.5	100058.42	79049.02	75.5075329	75.5075971	75.5074680
192322.6	100059.50	79043.68	75.5075687	75.5076330	75.5074702
192349.1	100051.69	79039.65	75.5075415	75.5076058	75.5074717
192422.6	100051.07	79034.56	75.5075710	75.5076353	75.5074738
192451.4	100067.21	79030.18	75.5076909	75.5077551	75.5074782
192521.8	100061.92	79025.55	75.5076827	75.5077470	75.5074823
192550.2	100052.08	79021.23	75.5076443	75.5077085	75.5074855
192612.5	100045.68	79017.84	75.5076224	75.5076867	75.5074881
192635.1	100040.26	79014.40	75.5076070	75.5076713	75.5074904
192700.8	100037.90	79010.49	75.5076134	75.5076777	75.5074927
192728.8	100014.74	79006.24	75.5074907	75.5075550	75.5074926
192805.4	100026.09	79000.67	75.5075926	75.5076569	75.5074944
192842.1	100027.26	78995.09	75.5076303	75.5076946	75.5074969
192906.2	100022.10	78991.42	75.5076178	75.5076821	75.5074989
192931.2	100018.03	78987.62	75.5076129	75.5076772	75.5075008
192958.4	100016.26	78983.48	75.5076243	75.5076886	75.5075029
193021.1	100008.19	78980.03	75.5075923	75.5076566	75.5075043

```
ATS-5 EPHEMERIS
   TIME    SAT RANGE   LATITUDE    LONGITUDE
   GMT       NMI         DEG         DEG
163000.0    22781.02    0.150      105.231
170000.0    22778.84    0.038      105.250
173000.0    22774.59   -0.075      105.268
180000.0    22770.74   -0.187      105.282
183000.0    22766.55   -0.295      105.294
190000.0    22762.11   -0.399      105.303


PARABOLIC FIT TO EPHEMERIS-LINEAR TO CAL DATA
             CONSTANT        LINEAR      QUADRATIC      RMS
LATITUDE      5.1302323    -0.3724861    0.0042857    0.00105
LONGITUDE   103.0968293     0.2165345   -0.0052851    0.00028
GEOC RANGE 22676.5297855   18.4297095   -0.7330221    0.03894
CALIB LIFE  89668.2196161 -547.5374731                14.72497


   TIME    RANGE DIF.  CAL. VAL.          LONGITUDES (DEG)
   GMT       (FT)       (FT)      POINT1      POINT2   CUMUL. AVG.
191349.0   100120.51   79130.92  75.5075349  75.5075991  75.5075349
191350.6   100117.71   79130.68  75.5074619  75.5075261  75.5074984
191351.4   100087.22   79130.56  75.5072705  75.5075032  75.5074224
191352.9   100113.77   79130.33  75.5074390  75.5075032  75.5074265
191354.1   100108.86   79130.15  75.5074090  75.5074732  75.5074230
191355.3   100115.74   79129.96  75.5074534  75.5075176  75.5074281
191401.5   100115.74   79129.02  75.5074585  75.5075227  75.5074324
191403.8   100105.01   79128.67  75.5073985  75.5074627  75.5074262
191406.2   100058.69   79128.31  75.5071030  75.5071672  75.5073921
191407.3   100058.83   79128.14  75.5070544  75.5071186  75.5073503
191408.3   100049.84   79127.83  75.5070408  75.5071140  75.5073303
191410.1   100109.84   79127.71  75.5074284  75.5074927  75.5073384
191410.9   100039.02   79127.59  75.5069830  75.5070472  75.5073111
191411.6   100037.06   79127.48  75.5069712  75.5070354  75.5072868
191413.2   100102.96   79127.24  75.5073877  75.5074519  75.5072935
191414.0   100092.14   79127.12  75.5073202  75.5073844  75.5072952
191414.7   100116.73   79127.01  75.5074756  75.5075399  75.5073058
191415.5   100128.53   79126.89  75.5075506  75.5076149  75.5073194
191416.7   100111.81   79126.71  75.5074463  75.5075105  75.5073261
191417.9   100088.27   79126.53  75.5072986  75.5073628  75.5073247
191418.6   100118.82   79126.42  75.5074416  75.5075059  75.5073323
191419.4   100082.30   79126.30  75.5072627  75.5073269  75.5073272
191421.0   100095.09   79126.05  75.5073445  75.5074088  75.5073290
191422.5   100124.50   79125.83  75.5075316  75.5075958  75.5073365
191423.3   100117.71   79125.71  75.5074889  75.5075532  75.5073426
191424.1   100120.66   79125.58  75.5075082  75.5075724  75.5073490
191426.0   100107.87   79125.29  75.5074292  75.5074934  75.5073510
191427.2   100120.66   79125.11  75.5075107  75.5075750  75.5073576
191428.4   100119.68   79124.93  75.5075056  75.5075698  75.5073627
191428.8   100116.73   79124.87  75.5074873  75.5075515  75.5073668
```

TABLE A-3.   EPHEMERIS AND LOP SUMMARY FOR TEST 2 (NO SMOOTHING)   (PAGE 2 OF 4)

TIME GMT	RANGE DIF. (FT)	CAL. VAL. (FT)	LONGITUDES (DEG) POINT1	POINT2	CUMUL. AVG.
191429.9	100136.48	79124.78	75.5076121	75.5076764	75.5073747
191431.1	100111.81	79124.52	75.5074582	75.5075224	75.5073773
191431.9	100131.40	79124.40	75.5075828	75.5076470	75.5073936
191432.7	100119.68	79124.28	75.5075091	75.5075733	75.5073873
191435.8	100045.91	79123.88	75.5070470	75.5071112	75.5073775
191436.6	100125.58	79123.68	75.5075495	75.5076137	75.5073823
191439.7	100094.10	79123.21	75.5073538	75.5074180	75.5073815
191440.5	100109.54	79123.09	75.5074536	75.5075179	75.5073834
191441.3	100112.79	79122.98	75.5074728	75.5075370	75.5073857
191442.0	100127.54	79122.86	75.5075663	75.5076306	75.5073902
191443.2	100128.53	79122.68	75.5075736	75.5076378	75.5073947
191445.1	100086.23	79122.39	75.5073087	75.5073729	75.5073927
191445.9	100095.25	79122.27	75.5073832	75.5073674	75.5073986
191446.7	100119.68	79122.15	75.5075207	75.5075849	75.5073935
191447.5	100134.43	79122.02	75.5076143	75.5076785	75.5073994
191449.0	100127.54	79121.80	75.5075721	75.5076364	75.5074022
191449.8	100119.69	79121.67	75.5075170	75.5075813	75.5074047
191450.6	100128.53	79121.55	75.5075797	75.5076439	75.5074083
191451.4	100111.81	79121.43	75.5074750	75.5075392	75.5074097
191452.5	100117.71	79121.06	75.5075131	75.5075773	75.5074117
191455.1	100120.99	79120.87	75.5074099	75.5074742	75.5074117
191456.0	100143.28	79120.73	75.5076771	75.5077413	75.5074168
191456.8	100125.58	79120.61	75.5075662	75.5076305	75.5074196
191457.6	100144.27	79120.49	75.5076846	75.5077489	75.5074245
191501.9	100053.78	79119.83	75.5071182	75.5071824	75.5074199
191503.8	100108.96	79119.55	75.5074295	75.5074938	75.5074192
191504.6	100081.30	79119.42	75.5072939	75.5073581	75.5074170
191505.9	100085.25	79119.24	75.5073196	75.5073838	75.5074153
191506.2	100107.87	79119.18	75.5074624	75.5075267	75.5074161
191507.0	100099.02	79119.06	75.5074074	75.5074716	75.5074159
191507.7	100073.45	79119.05	75.5072460	75.5073111	75.5074132
191509.2	100131.48	79118.72	75.5076137	75.5076779	75.5074164
191511.6	100070.52	79118.36	75.5072315	75.5072957	75.5074135
191512.4	100082.30	79118.24	75.5073065	75.5073707	75.5074118
191513.2	100111.81	79118.12	75.5074931	75.5075573	75.5074130
191514.0	100121.64	79117.99	75.5075556	75.5076199	75.5074152
191517.1	100111.81	79117.52	75.5074963	75.5075605	75.5074164
191518.6	100109.84	79117.29	75.5074851	75.5075493	75.5074174
191519.4	100096.07	79117.17	75.5073990	75.5074633	75.5074172
191520.6	100121.64	79116.99	75.5075611	75.5076253	75.5074192
191522.5	100110.82	79116.70	75.5074945	75.5075587	75.5074203
191527.2	100109.84	79115.99	75.5074922	75.5075565	75.5074213
191528.0	100089.18	79115.86	75.5069849	75.5070491	75.5074153
191529.6	100112.79	79115.62	75.5075128	75.5075770	75.5074166
191530.3	100031.15	79115.51	75.5069991	75.5070634	75.5074110
191531.1	100119.68	79115.39	75.5075575	75.5076217	75.5074130
191531.9	100065.58	79115.27	75.5072173	75.5072816	75.5074104

TABLE A-3. EPHEMERIS AND LOP SUMMARY FOR TEST 2 (NO SMOOTHING) (PAGE 3 OF 4)

TIME GMT	RANGE DIF. (FT)	CAL. VAL. (FT)	LONGITUDES (DEG) POINT1	POINT2	CUMUL. AVG.
191532.7	100120.66	79115.15	75.5075649	75.5076292	75.5074124
191535.4	100118.69	79114.74	75.5075548	75.5076198	75.5074142
191536.6	100111.81	79114.56	75.5075124	75.5075767	75.5074154
191537.7	100118.69	79114.39	75.5075567	75.5076209	75.5074172
191538.5	100103.94	79114.27	75.5074644	75.5075287	75.5074179
191539.3	100097.05	79114.15	75.5074217	75.5074859	75.5074179
191539.7	100076.40	79114.09	75.5072919	75.5073562	75.5074163
191541.2	100098.04	79113.96	75.5074295	75.5074937	75.5074165
191543.6	100118.69	79113.49	75.5075616	75.5076258	75.5074181
191545.1	100108.96	79113.26	75.5075009	75.5075651	75.5074181
191546.7	100124.92	79113.02	75.5074774	75.5075416	75.5074189
191548.7	100102.96	79112.72	75.5074667	75.5075309	75.5074003
191552.5	100028.20	79112.14	75.5069989	75.5070631	75.5074156
191554.9	100054.76	79111.77	75.5071652	75.5072304	75.5074109
191555.3	100099.04	79111.71	75.5074412	75.5075054	75.5074130
191558.0	100105.91	79111.30	75.5074930	75.5075572	75.5074141
191559.2	100118.69	79111.12	75.5075745	75.5076387	75.5074159
191559.9	100047.88	79111.01	75.5071290	75.5071932	75.5074127
191600.7	100066.56	79110.89	75.5072473	75.5073116	75.5074119
191603.8	100075.42	79110.42	75.5073057	75.5073699	75.5074009
191604.6	100132.46	79110.30	75.5076657	75.5077299	75.5074125
191605.8	100123.61	79110.12	75.5076109	75.5076752	75.5074145
191606.2	100089.19	79110.05	75.5073944	75.5074587	75.5074143
191607.4	100067.55	79109.87	75.5072591	75.5073233	75.5074129
191609.7	100130.50	79109.52	75.5076576	75.5077218	75.5074152
191611.6	100108.86	79109.23	75.5075228	75.5075870	75.5074152
191613.6	100129.84	79108.93	75.5075306	75.5075949	75.5074173
191614.8	100122.63	79108.87	75.5076115	75.5076759	75.5074192
191615.1	100130.50	79108.70	75.5076620	75.5077263	75.5074215
191616.3	100108.99	79108.52	75.5074771	75.5075414	75.5074220
191617.1	100103.94	79108.40	75.5074964	75.5075606	75.5074227
191617.9	100131.49	79108.28	75.5076705	75.5077347	75.5074250
191619.0	100109.84	79108.11	75.5075351	75.5075993	75.5074260
191621.0	100132.46	79107.86	75.5076705	75.5077435	75.5074263
191621.8	100117.71	79107.68	75.5075870	75.5076512	75.5074297
191622.6	100045.91	79107.56	75.5071354	75.5071996	75.5074271
191624.9	100108.86	79107.21	75.5075338	75.5075981	75.5074289
191628.2	100116.73	79106.71	75.5075861	75.5076504	75.5074304
191629.6	100123.61	79106.50	75.5076306	75.5076949	75.5074311
191630.3	100103.94	79106.39	75.5075073	75.5075715	75.5074319
191631.1	100111.81	79106.27	75.5075575	75.5076218	75.5074329
191632.7	100126.56	79106.02	75.5076518	75.5077160	75.5074347
191633.5	100104.92	79105.90	75.5075161	75.5075804	75.5074353
191634.2	100125.58	79105.80	75.5076468	75.5077111	75.5074371
191635.7	100122.66	79105.55	75.5076172	75.5076814	75.5074386
191636.6	100102.96	79105.43	75.5075063	75.5075706	75.5074391
191637.4	100110.82	79105.31	75.5075565	75.5076207	75.5074401

TIME GMT	RANGE DIF. (FT)	CAL. VAL. (FT)	LONGITUDES (DEG) POINT1	POINT2	CUMUL. AVG.
191638.1	100127.54	79105.20	75.5076624	75.5077266	75.5073418
191639.7	100135.41	79104.96	75.5077153	75.5077773	75.5074440
191640.5	100125.91	79104.84	75.5075291	75.5075924	75.5074447
191641.3	100111.81	79104.72	75.5075662	75.5076322	75.5074456
191642.0	100100.28	79104.61	75.5074922	75.5075564	75.5074468
191643.6	100140.33	79104.37	75.5077475	75.5078118	75.5074473
191644.4	100115.74	79104.24	75.5075933	75.5076575	75.5074494
191645.0	100113.77	79104.02	75.5075821	75.5076464	75.5074504
191651.4	100124.59	79103.19	75.5076542	75.5077191	75.5074519
191653.7	100100.99	79102.83	75.5075219	75.5075961	75.5074523

```
     ATS-5 EPHEMERIS
     TIME     SAT RANGE    LATITUDE    LONGITUDE
     GMT        NMI          DEG          DEG
  173000.0    22773.87     -0.118      105.284
  180000.0    22770.00     -0.228      105.298
  183000.0    22765.81     -0.334      105.309
  190000.0    22761.36     -0.435      105.318
  193000.0    22756.74     -0.528      105.323
```

```
PARABOLIC FIT TO EPHEMERIS-LINEAR TO CAL DATA
                    CONSTANT        LINEAR     QUADRATIC      RMS
LATITUDE          7.2793723     -0.6176858   -0.0111429   0.00059
LONGITUDE       102.9904324      0.2310838   -0.0057158   0.00021
GEOC RANGE    22752.3074475     10.0394174   -0.5032261        0
CALIB LINE   -38074.8373629   -618.8420590              18.43029
```

TIME	RANGE DIF.	CAL. VAL.	LONGITUDES (DEG)		
GMT	(FT)	(FT)	POINT1	POINT2	CUMUL. AVG.
170214.9	-27762.06	-48618.34	75.5076328	75.5076964	75.5076328
170239.5	-27828.90	-48622.57	75.5072346	75.5072982	75.5074337
170306.0	-27822.57	-48627.13	75.5072992	75.5073628	75.5073889
170334.4	-27791.00	-48632.01	75.5075247	75.5075883	75.5074228
170346.1	-27792.65	-48634.02	75.5075252	75.5075888	75.5074433
170353.9	-27802.27	-48635.36	75.5074718	75.5075354	75.5074481
170426.3	-27842.61	-48640.93	75.5072479	75.5073115	75.5074195
170500.6	-27814.96	-48646.83	75.5074542	75.5075178	75.5074239
170527.5	-27826.65	-48651.45	75.5074056	75.5074692	75.5074218
170552.0	-27838.94	-48655.66	75.5073511	75.5074147	75.5074147
170613.1	-27863.97	-48659.29	75.5072131	75.5072767	75.5073964
170630.6	-27841.00	-48662.30	75.5073741	75.5074378	75.5073945
170719.0	-27859.21	-48670.62	75.5073046	75.5073682	75.5073876
170754.8	-27851.35	-48676.77	75.5073876	75.5074512	75.5073876
170824.9	-27887.76	-48681.94	75.5071863	75.5072500	75.5073742
170843.9	-27821.46	-48685.21	75.5076218	75.5076854	75.5073897
170901.5	-27892.82	-48688.24	75.5071887	75.5072523	75.5073779
170926.4	-27864.75	-48692.52	75.5073888	75.5074524	75.5073794
170948.6	-27905.50	-48696.33	75.5071528	75.5072164	75.5073666
171025.3	-27906.90	-48702.64	75.5071783	75.5072419	75.5073572
171054.1	-27888.97	-48707.59	75.5073182	75.5073818	75.5073553
171128.4	-27890.24	-48713.49	75.5073423	75.5074059	75.5073547
171212.1	-27917.56	-48721.00	75.5072110	75.5072746	75.5073485
171238.5	-27892.69	-48725.56	75.5073925	75.5074561	75.5073503
171315.6	-27913.16	-48731.92	75.5072981	75.5073618	75.5073492
171350.3	-27853.54	-48737.88	75.5077062	75.5077699	75.5073620
171432.0	-27889.97	-48745.05	75.5075157	75.5075794	75.5073677
171449.2	-27915.41	-48748.01	75.5073715	75.5074352	75.5073678
171521.5	-27894.30	-48753.56	75.5075348	75.5075984	75.5073736
171542.2	-27903.47	-48757.12	75.5074964	75.5075601	75.5073777
171554.3	-27926.75	-48759.20	75.5073610	75.5074247	75.5073771

A-10

TIME GMT	RANGE DIF. (FT)	CAL. VAL. (FT)	LONGITUDES(DEG) POINT1	POINT2	CUMUL. AVG.
171624.3	-27943.03	-48764.35	75.5072866	75.5073502	75.5073743
171647.3	-27927.21	-48768.31	75.5074078	75.5074714	75.5073753
171714.6	-27943.13	-48773.00	75.5073330	75.5073967	75.5073741
171757.9	-27936.01	-48780.44	75.5074185	75.5074821	75.5073753
171828.6	-27939.11	-48785.72	75.5074277	75.5074914	75.5073768
171843.8	-27980.30	-48788.33	75.5071824	75.5072461	75.5073715
171908.8	-27928.45	-48792.63	75.5075325	75.5075962	75.5073758
171931.4	-27973.34	-48796.52	75.5072709	75.5073346	75.5073731
171945.0	-27969.15	-48798.85	75.5073100	75.5073736	75.5073715
172003.7	-27951.78	-48802.07	75.5074370	75.5075007	75.5073731
172030.7	-28009.71	-48806.71	75.5070973	75.5071610	75.5073665
172057.5	-27955.28	-48811.32	75.5074654	75.5075291	75.5073688
172122.1	-27953.09	-48815.55	75.5075022	75.5075659	75.5073719
172159.1	-27965.75	-48821.91	75.5074572	75.5075209	75.5073738
172225.3	-27976.54	-48826.41	75.5074137	75.5074774	75.5073746
172259.9	-27945.25	-48832.36	75.5076433	75.5077070	75.5073803
172319.0	-27977.24	-48835.64	75.5074597	75.5075234	75.5073820
172334.2	-27971.21	-48838.25	75.5075119	75.5075756	75.5073846
172424.1	-27954.23	-48846.83	75.5076657	75.5077294	75.5073903
172431.9	-28013.73	-48848.17	75.5072982	75.5073619	75.5073885
172458.4	-28010.47	-48852.73	75.5073436	75.5074073	75.5073876
172532.4	-27987.95	-48858.57	75.5075174	75.5075811	75.5073901
172607.0	-28024.77	-48864.52	75.5073179	75.5073816	75.5073887
172622.6	-28006.07	-48867.20	75.5074504	75.5075141	75.5073898
172638.2	-28004.37	-48869.88	75.5074757	75.5075394	75.5073914
172700.9	-27971.11	-48873.63	75.5077057	75.5077694	75.5073969
172713.7	-28041.90	-48875.99	75.5072726	75.5073363	75.5073947
172725.0	-28050.05	-48877.93	75.5072319	75.5072956	75.5073920
172744.5	-28018.38	-48881.28	75.5074465	75.5075103	75.5073929
172801.6	-27985.67	-48884.22	75.5076718	75.5077355	75.5073975
172822.7	-28059.27	-48887.85	75.5072280	75.5072917	75.5073947
172835.9	-28061.06	-48890.12	75.5072291	75.5072928	75.5073921
172851.5	-28000.16	-48892.80	75.5076274	75.5076911	75.5073958
172912.2	-28034.84	-48896.36	75.5074284	75.5074921	75.5073963
172927.0	-28012.09	-48898.90	75.5075856	75.5076493	75.5073991
172953.9	-28057.32	-48903.52	75.5073259	75.5073897	75.5073980
173014.2	-28007.87	-48907.01	75.5076565	75.5077202	75.5074019
173032.9	-28008.65	-48910.23	75.5076692	75.5077329	75.5074057
173101.7	-28042.49	-48915.18	75.5074831	75.5075468	75.5074068
173123.9	-28046.14	-48919.00	75.5074809	75.5075447	75.5074079
173141.5	-28047.89	-48922.02	75.5074865	75.5075502	75.5074090
173204.1	-27997.51	-48925.91	75.5078251	75.5078888	75.5074147
173223.6	-28045.87	-48929.26	75.5075387	75.5076025	75.5074163
173238.4	-28082.16	-48931.80	75.5073241	75.5073878	75.5074151
173259.4	-28023.75	-48935.41	75.5077117	75.5077755	75.5074190
173321.3	-28056.09	-48939.18	75.5075286	75.5075924	75.5074204
173348.9	-28053.87	-48943.92	75.5075686	75.5076323	75.5074223

TIME	RANGE DIF.	CAL. VAL.	LONGITUDES(DEG)		
GMT	(FT)	(FT)	POINT1	POINT2	CUMUL. AVG.
173408.8	-28070.41	-48947.34	75.5074831	75.5075468	75.5074231
173421.7	-28107.09	-48949.56	75.5072642	75.5073279	75.5074211
173437.7	-28019.12	-48952.31	75.5078333	75.5078971	75.5074262

TABLE A-5. EPHEMERIS AND LOP SUMMARY FOR TEST 8 (JULY 21, 1971)

```
     ATS-5 EPHEMERIS
     TIME    SAT RANGE   LATITUDE   LONGITUDE
     GMT       NMI         DEG         DEG
   70000.0   22745.43     0.493     104.960
   73000.0   22750.19     0.577     104.966
   80000.0   22754.99     0.651     104.967
   83000.0   22759.75     0.714     104.970
   90000.0   22764.39     0.764     104.976
```

PARABOLIC FIT TO EPHEMERIS-LINEAR TO CAL DATA

	CONSTANT	LINEAR	QUADRATIC	RMS
LATITUDE	-1.8798856	0.4969428	-0.0225714	0.0043
LONGITUDE	105.3036654	-0.0878307	0.0057144	0.00021
GEOC RANGE	22673.0014500	10.7761361	-0.0800084	0.02263
CALIB LINE	68018.8277122	-678.2849545		75.13257

| TIME | RANGE DIF. | CAL. VAL. | LONGITUDES (DEG) | | |
GMT	(FT)	(FT)	POINT1	POINT2	CUMUL. AVG.
75941.0	83184.83	62596.13	75.5074114	75.5074747	75.5074114
80048.5	83200.83	62583.41	75.5075008	75.5076631	75.5075056
80142.0	83169.91	62573.33	75.5074151	75.5074783	75.5074754
80333.2	83175.21	62552.38	75.5076687	75.5077119	75.5075187
80423.9	83167.72	62542.83	75.5076662	75.5077295	75.5075492
80513.8	83134.22	62533.42	75.5075175	75.5075808	75.5075431
80616.6	83125.36	62521.59	75.5075418	75.5076051	75.5075429
80804.7	83091.33	62501.22	75.5074644	75.5075276	75.5075331
80918.6	83097.70	62488.81	75.5075893	75.5076525	75.5075393
81050.1	83074.78	62470.06	75.5075712	75.5076344	75.5075425
81326.2	83021.32	62440.65	75.5074315	75.5074948	75.5075324
81451.2	83022.15	62424.63	75.5075455	75.5076087	75.5075335
82029.0	82929.78	62360.82	75.5073916	75.5074548	75.5075226
82150.6	82922.73	62345.61	75.5074498	75.5075130	75.5075174
82249.9	82909.63	62334.44	75.5074422	75.5075054	75.5075124
82436.4	82873.28	62314.38	75.5073471	75.5074103	75.5075021
82533.8	82885.60	62303.56	75.5074984	75.5075616	75.5075018
82628.0	82884.14	62293.35	75.5075581	75.5076213	75.5075050
82713.3	82837.63	62284.81	75.5073206	75.5073837	75.5074953
82843.0	82850.88	62267.91	75.5075183	75.5075814	75.5074964
82941.5	82817.81	62256.89	75.5073832	75.5074464	75.5074910
83122.2	82814.54	62237.92	75.5074904	75.5075536	75.5074910
83226.9	82766.56	62225.73	75.5072680	75.5073312	75.5074813
83459.9	82748.73	62196.90	75.5073490	75.5074122	75.5074758
83637.4	82738.31	62178.53	75.5074065	75.5074697	75.5074738
83743.2	82743.61	62166.17	75.5075233	75.5075865	75.5074750
83854.0	82709.74	62152.79	75.5073983	75.5074614	75.5074721
84041.6	82698.21	62132.52	75.5074613	75.5075245	75.5074717
84146.4	82691.22	62120.31	75.5074990	75.5075621	75.5074727
84258.6	82663.20	62106.71	75.5074125	75.5074756	75.5074707
84442.0	82650.81	62087.23	75.5074645	75.5075276	75.5074705
84558.4	82648.84	62072.83	75.5075486	75.5076117	75.5074720

```
        ATS-5 EPHEMERIS
         TIME    SAT RANGE    LATITUDE    LONGITUDE
         GMT       NMI          DEG          DEG
         0.0     22717.71     -0.722       105.216
       3000.0    22716.68     -0.664       105.193
      10000.0    22716.27     -0.595       105.169
      13000.0    22716.48     -0.515       105.146
      20000.0    22717.29     -0.426       105.123
      23000.0    22718.70     -0.330       105.101
```

PARABOLIC FIT TO EPHEMERIS-LINEAR TO CAL DATA

	CONSTANT	LINEAR	QUADRATIC	RMS
LATITUDE	-0.7226429	0.1091571	0.0192857	0.00081
LONGITUDE	105.2162500	-0.0477786	0.0006429	0.00026
GEOC RANGE	22717.7054555	-2.6502561	1.2198813	0.00495
CALIB LINE	-79619.4784223	-605.7383393		10.44717

TIME	RANGE DIF.	CAL. VAL.	LONGITUDES (DEG)		
GMT	(FT)	(FT)	POINT1	POINT2	CUMUL. AVG.
13116.0	-59642.20	-80611.54	75.5072061	75.5072708	75.5072061
13212.2	-59650.60	-80621.00	75.5072187	75.5072835	75.5072124
13306.1	-59666.42	-80630.07	75.5071818	75.5072465	75.5072022
13404.6	-59675.39	-80639.91	75.5071936	75.5072583	75.5072000
13505.6	-59681.24	-80650.18	75.5072281	75.5072929	75.5072057
13603.4	-59683.27	-80659.90	75.5072831	75.5073478	75.5072186
13717.5	-59700.56	-80672.37	75.5072607	75.5073254	75.5072246
13833.3	-59714.00	-80685.12	75.5072646	75.5073293	75.5072296
14111.8	-59742.44	-80711.79	75.5072709	75.5073356	75.5072342
14259.5	-59766.38	-80729.91	75.5072460	75N5073107	75.5072354
14513.8	-59792.66	-80752.51	75.5072378	75.5073025	75.5072356
15243.6	-59863.00	-80828.20	75.5073229	75.5073876	75.5072429
15409.4	-59859.64	-80842.63	75.5074456	75.5075102	75.5072584
15547.8	-59862.47	-80859.19	75.5075440	75.5076086	75.5072788
15716.1	-59876.87	-80874.05	75.5075572	75.5076219	75.5072974
15849.0	-59893.44	-80889.68	75.5075622	75.5076269	75.5073140
20031.3	-59918.06	-80906.89	75.5075275	75.5075921	75.5073265
20157.1	-59931.67	-80921.33	75.5075429	75.5076076	75.5073385
20339.4	-59949.95	-80938.54	75.5075485	75.5076131	75.5073496
20519.4	-59981.96	-80955.37	75.5074644	75.5075290	75.5073553
20657.8	-60009.51	-80971.92	75.5074067	75.5074713	75.5073578
20822.9	-60023.82	-80986.24	75.5074171	75.5074818	75.5073605
20955.0	-60021.60	-81001.74	75.5075406	75.5076053	75.5073683
21116.2	-60011.55	-81015.40	75.5077008	75.5077654	75.5073822
21236.6	-60029.94	-81028.93	75.5076800	75.5077446	75.5073941
21402.5	-60064.56	-81043.38	75.5075630	75.5076276	75.5074006
21509.7	-60077.07	-81054.69	75.5075638	75.5076283	75.5074066
21616.8	-60120.76	-81065.98	75.5074936	75.5075582	75.5074097
21721.6	-60104.06	-81076.88	75.5075500	75.5076145	75.5074146
21841.2	-60124.15	-81090.28	75.5075176	75.5075822	75.5074180

TABLE A-6. EPHEMERIS AND LOP SUMMARY FOR TEST 12 (JULY 27, 1971) (PAGE 2 OF 3)

TIME GMT	RANGE DIF. (FT)	CAL. VAL. (FT)	LONGITUDES(DEG) POINT1	POINT2	CUMUL. AVG.
21937.5	-60134.45	-81099.75	75.5075195	75.5075841	75.5074213
22041.5	-60147.31	-81113.52	75.5075144	75.5075790	75.5074242
22143.2	-60154.78	-81120.90	75.5075408	75.5076053	75.5074277
22250.3	-60170.23	-81132.19	75.5075230	75.5075876	75.5074305
22356.7	-60184.12	-81143.36	75.5075143	75.5075789	75.5074329
22510.9	-60201.22	-81155.85	75.5074947	75.5075592	75.5074346
22618.8	-60217.97	-81167.27	75.5074698	75.5075343	75.5074356
22725.2	-60236.79	-81178.45	75.5074300	75.5074945	75.5074354
22830.0	-60265.85	-81189.35	75.5073234	75.5073879	75.5074326
22927.7	-60280.79	-81199.06	75.5072978	75.5073624	75.5074292
23031.8	-60296.84	-81209.84	75.5072729	75.5073574	75.5074254
23138.1	-60308.71	-81221.20	75.5072771	75.5073417	75.5074218
23252.3	-60320.03	-81233.49	75.5072943	75.5073588	75.5074189
23401.8	-60329.36	-81245.18	75.5073185	75.5073831	75.5074166
23512.9	-60360.65	-81257.14	75.5072056	75.5072701	75.5074119
23608.3	-60366.57	-81266.46	75.5072346	75.5072991	75.5074081
23712.3	-60375.41	-81277.23	75.5072554	75.5073199	75.5074049
23807.0	-60389.99	-81286.44	75.5072287	75.5072932	75.5074011
23902.4	-60394.53	-81295.76	75.5072665	75.5073310	75.5073984
24056.4	-60418.24	-81314.94	75.5072532	75.5073177	75.5073955
24202.8	-60432.61	-81326.11	75.5072420	75.5073065	75.5073925
24306.0	-60442.14	-81336.75	75.5072577	75.5073222	75.5073899
24406.2	-60452.36	-81346.88	75.5072654	75.5073298	75.5073875
24505.5	-60460.41	-81356.85	75.5072857	75.5073502	75.5073856
24608.0	-60474.80	-81367.37	75.5072698	75.5073343	75.5073835
24708.1	-60485.99	-81377.48	75.5072713	75.5073358	75.5073815
24812.9	-60495.07	-81388.39	75.5072919	75.5073564	75.5073800
24920.8	-60510.58	-81399.81	75.5072755	75.5073399	75.5073782
25043.6	-60524.97	-81413.74	75.5072842	75.5073486	75.5073766
25144.5	-60535.48	-81423.89	75.5072911	75.5073555	75.5073751
25246.9	-60529.93	-81434.49	75.5074016	75.5074660	75.5073756
25351.8	-60542.53	-81445.41	75.5074001	75.5074645	75.5073760
25448.0	-60552.39	-81454.87	75.5074055	75.5074699	75.5073764
25538.7	-60559.96	-81463.40	75.5074188	75.5074833	75.5073771
25634.9	-60567.81	-81472.85	75.5074370	75.5075014	75.5073780
25726.5	-60577.96	-81481.53	75.5074351	75.5074995	75.5073790
25816.4	-60584.61	-81489.93	75.5074533	75.5075177	75.5073800
25911.9	-60592.25	-81499.27	75.5074721	75.5075365	75.5073814
30007.3	-60599.15	-81508.59	75.5074954	75.5075598	75.5073830
30059.6	-60609.85	-81517.39	75.5074909	75.5075553	75.5073845
30155.1	-60627.69	-81526.73	75.5074451	75.5075095	75.5073854
30246.6	-60643.96	-81535.40	75.5074044	75.5074688	75.5073857
30338.9	-60648.54	-81544.20	75.5074388	75.5075031	75.5073864
30428.1	-60664.71	-81552.47	75.5073959	75.5074603	75.5073865
30532.1	-60685.13	-81563.24	75.5073441	75.5074085	75.5073860
30630.7	-60693.99	-81573.10	75.5073591	75.5074234	75.5073856
30730.8	-60708.32	-81583.21	75.5073412	75.5074056	75.5073850

TIME GMT	RANGE DIF. (FT)	CAL. VAL. (FT)	LONGITUDES (DEG) POINT1	POINT2	CUMUL. AVG.
30841.9	-60722.66	-81595.18	75.5073366	75.5074010	75.5073844
30938.1	-60735.41	-81604.63	75.5073241	75.5073884	75.5073836
31138.3	-60753.31	-81624.86	75.5073567	75.5074211	75.5073833
31238.4	-60761.64	-81634.97	75.5073770	75.5074414	75.5073832
31337.8	-60773.54	-81644.97	75.5073738	75.5074382	75.5073831
31441.8	-60787.32	-81655.74	75.5073644	75.5074287	75.5073829
31538.8	-60797.80	-81665.33	75.5073673	75.5074317	75.5073827
31635.8	-60809.75	-81674.92	75.5073610	75.5074253	75.5073824
31738.3	-60820.34	-81685.43	75.5073700	75.5074343	75.5073823
31832.9	-60830.95	-81694.62	75.5073693	75.5074336	75.5073821
31925.2	-60841.17	-81703.42	75.5073683	75.5074326	75.5073820
32024.6	-60847.85	-81713.41	75.5073984	75.5074627	75.5073822
32117.7	-60863.06	-81722.35	75.5073667	75.5074310	75.5073820
32210.0	-60867.46	-81731.15	75.5074026	75.5074669	75.5073822
32303.1	-60875.04	-81740.08	75.5074194	75.5074837	75.5073826
32354.6	-60886.64	-81748.75	75.5074088	75.5074731	75.5073829
33919.1	-61025.50	-81904.31	75.5076607	75.5077249	75.5073850
34011.4	-61032.57	-81913.11	75.5076801	75.5077443	75.5073890
34102.1	-61036.05	-81921.64	75.5077203	75.5077846	75.5073924
34155.2	-61056.32	-81930.57	75.5076571	75.5077213	75.5073951
34254.6	-61071.03	-81940.57	75.5076368	75.5077010	75.5073976
34348.5	-61088.35	-81949.64	75.5075933	75.5076575	75.5073996
34436.9	-61092.65	-81957.78	75.5076256	75.5076898	75.5074018
34525.3	-61102.51	-81965.92	75.5076226	75.5076868	75.5074040
34614.5	-61111.40	-81974.29	75.5076268	75.5076910	75.5074062
34709.9	-61122.65	-81983.52	75.5076237	75.5076879	75.5074083
34759.9	-61133.79	-81991.94	75.5076147	75.5076788	75.5074103
34849.8	-61141.69	-82000.33	75.5076261	75.5076902	75.5074124
34939.8	-61151.71	-82008.75	75.5076242	75.5076883	75.5074144
35026.7	-61155.87	-82016.64	75.5076556	75.5077198	75.5074166
35119.8	-61171.50	-82025.57	75.5076220	75.5076861	75.5074185
35212.8	-61184.33	-82034.49	75.5076060	75.5076702	75.5074202
35302.8	-61195.10	-82042.90	75.5075994	75.5076636	75.5074219
35359.8	-61214.25	-82052.49	75.5075483	75.5076125	75.5074230
35451.4	-61219.11	-82061.18	75.5075812	75.5076454	75.5074244
35544.4	-61228.46	-82070.09	75.5075874	75.5076515	75.5074259
35640.7	-61241.26	-82079.57	75.5075758	75.5076399	75.5074272
35737.7	-61241.07	-82089.16	75.5076475	75.5077116	75.5074291
35831.5	-61250.09	-82098.21	75.5076568	75.5077209	75.5074311
35924.6	-61244.97	-82107.14	75.5077550	75.5078191	75.5074338
40038.8	-61265.04	-82119.63	75.5077195	75.5077836	75.5074362
40146.7	-61252.41	-82131.05	75.5078837	75.5079478	75.5074400
40304.0	-61250.87	-82144.06	75.5079892	75.5080533	75.5074446

```
ATS-5 EPHEMERIS
 TIME     SAT RANGE   LATITUDE   LONGITUDE
 GMT        NMI         DEG         DEG
   0.0    22717.71    -2.722      125.216
 3600.0   22716.69    -2.664      105.193
10800.0   22716.27    -2.595      125.169
13800.0   22716.47    -2.513      105.146
20000.0   22717.29    -2.426      105.123
23600.0   22718.70    -2.338      105.101


PARABOLIC FIT TO EPHEMERIS-LINEAR TO CAL DATA
                   CONSTANT        LINEAR       QUADRATIC      RMS
LATITUDE         -2.7226429      0.1891571    0.0192257  0.00021
LONGITUDE       105.2162500     -0.0477796    0.0006429  0.00026
GEOC RANGE    22717.7254555     -2.6502561    1.2198813  0.00495
CALIB LINE   -79619.4724223   -605.7323393              10.44717


 TIME    RANGE DIF.   CAL. VAL.             LONGITUDES (DEG)
 GMT       (FT)         (FT)       POINT1       POINT2    CUMUL. AVG.
13202.0   -59651.60   -80618.95  75.5071981  75.5072622   75.5071981
13202.4   -59650.60   -80619.35  75.5072873  75.5072720   75.5072027
13203.2   -59656.50   -80619.49  75.5071708  75.5072356   75.5071981
13203.9   -59643.80   -80619.60  75.5072521  75.5073160   75.5072071
13206.3   -59653.60   -80620.01  75.5071928  75.5072576   75.5072042
13207.1   -59643.80   -80620.14  75.5072558  75.5073205   75.5072120
13207.9   -59634.90   -80620.28  75.5073131  75.5073770   75.5072271
13209.4   -59617.50   -80620.53  75.5074252  75.5074887   75.5072519
13211.0   -59645.70   -80620.80  75.5072483  75.5073131   75.5072515
13211.8   -59655.50   -80620.93  75.5071683  75.5072330   75.5072432
13212.5   -59661.50   -80621.05  75.5071501  75.5072140   75.5072347
13213.3   -59649.70   -80621.18  75.5072357  75.5072994   75.5072339
13214.1   -59651.60   -80621.30  75.5072146  75.5072784   75.5072325
13214.9   -59662.40   -80621.45  75.5071472  75.5072119   75.5072264
13217.2   -59655.50   -80621.84  75.5071746  75.5072393   75.5072229
13217.9   -59642.70   -80621.98  75.5072376  75.5073023   75.5072239
13218.8   -59647.70   -80622.11  75.5072448  75.5073096   75.5072251
13219.6   -59644.70   -80622.24  75.5072648  75.5073295   75.5072273
13220.4   -59659.50   -80622.38  75.5071720  75.5072367   75.5072244
13221.1   -59647.70   -80622.50  75.5072475  75.5073122   75.5072255
13221.9   -59644.70   -80622.63  75.5072675  75.5073322   75.5072275
13222.7   -59647.70   -80622.77  75.5072494  75.5073141   75.5072285
13223.5   -59657.50   -80622.90  75.5071883  75.5072530   75.5072269
13224.3   -59653.50   -80623.04  75.5071929  75.5072476   75.5072249
13225.0   -59658.60   -80623.15  75.5071831  75.5072476   75.5072253
13225.2   -59653.60   -80623.29  75.5072157  75.5072804   75.5072252
13227.4   -59633.80   -80623.56  75.5073112  75.5073760   75.5072262
13229.7   -59635.80   -80623.94  75.5073323  75.5073970   75.5072302
13230.5   -59644.70   -80624.08  75.5072775  75.5073423   75.5072317
13231.3   -59644.70   -80624.21  75.5072785  75.5073432   75.5072332
```

TABLE A-7.   EPHEMERIS AND LOP SUMMARY FOR TEST 12
(NO SMOOTHING) (PAGE 2 OF 3)

TIME GMT	RANGE DIF. (FT)	CAL. VAL. (FT)	LONGITUDES (DEG) POINT1	POINT2	CUMUL. AVG.
13230.1	-5065°.°°	-5°604.35	75.5071?57	75.5072505	75.5075717
13230.°	-5°647.7°	-°°604.47	75.5072610	75.5074°6°	75.5070700
13235.°	-5°058.6°	-°°604.°7	75.5075705	75.5074370	75.5070°0°
13836.0	-5°659.5°	-°°625.°°	75.5071903	75.5070°50	75.5070°00
13236.7	-5°667.4°	-°°625.1°	75.5071411	75.5071750	75.5070004
13237.5	-5°679.3°	-°°625.2°	75.5070°°5	73.5070°51	75.°070°0°
13238.3	-5°653.°°	-°°605.3°	75.5071°0°	75.5071°56	75.0070°0°
13239.1	-5°672.°°	-°°605.53	75.5071°°°	75.5071°56	75.0070°0°
21849.4	-60113.90	-81091.66	75.5075923	75.5076569	75.5075°03
21950.1	-6°116.9°	-81091.7°	75.5075741	75.5076307	75.5075°30
21850.9	-60120.7°	-81091.91	75.5075°04	75.5075649	75.5075°54
21951.7	-6°134.6°	-°1092.°5	75.5074639	75.5075°°5	75.5075°07
21852.5	-6°132.6°	-81092.1°	75.5074902	75.5075542	75.5075042
21854.1	-6°136.5°	-81092.45	75.5074548	75.5075193	75.5075106
21854.8	-6°120.8°	-81092.57	75.5075551	75.5076196	75.5075107
21856.4	-6°123.7°	-°1092.°4	75.5075396	75.5076030	75.5075010
21858.°	-6°138.5°	-81093.11	75.5074469	75.5075113	75.5075120
21959.7	-6°136.5°	-81093.22	75.5074603	75.5075249	75.5075076
21959.5	-6°138.5°	-81093.36	75.5074485	75.5075131	75.5075023
21900.3	-60144.4°	-81093.49	75.5074121	75.5074767	75.5074949
21901.°	-6°111.9°	-81093.76	75.5076199	75.5076845	75.5075944
21902.6	-6°124.7°	-81093.°°	75.5075396	75.5076040	75.5075069
21904.2	-6°119.°°	-81094.15	75.5075726	75.5076370	75.5075113
21905.°	-6°106.°°	-81094.2°	75.5076610	75.5077255	75.5075276
21905.8	-6°121.8°	-81094.42	75.5075618	75.5076264	75.5075231
21906.5	-6°144.4°	-81094.54	75.5074195	75.5074841	75.5075173
21907.3	-6°143.4°	-81094.67	75.5074268	75.5074914	75.5075125
21908.°	-6°133.6°	-81094.94	75.5074909	75.5075554	75.5075115
21910.4	-6°113.9°	-81095.19	75.5076174	75.5076919	75.5075165
21911.2	-6°140.5°	-81095.33	75.5074499	75.5075144	75.5075135
21912.8	-6°131.6°	-81095.60	75.5075081	75.5075727	75.5075132
21913.6	-6°144.4°	-81095.73	75.5074280	75.5074926	75.5075007
21914.3	-6°117.8°	-81095.85	75.5075973	75.5076619	75.5075132
21915.°	-6°122.8°	-°1096.12	75.5075675	75.5076321	75.5075153
21916.7	-6°144.4°	-°1096.25	75.5074317	75.5074963	75.5075100
21917.5	-6°147.3°	-81096.39	75.5074143	75.5074789	75.5075007
21920.6	-6°137.5°	-81096.91	75.5074800	75.5075446	75.5075077
21921.4	-6°144.4°	-81097.04	75.5074373	75.5075019	75.5075053

TABLE A-7.   EPHEMERIS AND LOP SUMMARY FOR TEST 12
(NO SMOOTHING) (PAGE 3 OF 3)

TIME GMT	RANGE DIF. (FT)	CAL. VAL. (FT)	LONGITUDES (DEG) POINT1	POINT2	CUMUL. AVG.
21922.0	-60136.50	-81097.10	75.5074893	75.5075509	75.5075049
21922.9	-60131.60	-81097.09	75.5075009	75.5075647	75.5075053
21924.5	-60116.90	-81097.55	75.5076159	75.5076799	75.5075996
21925.3	-60143.40	-81097.70	75.5074483	75.5075129	75.5075059
21927.6	-60139.50	-81098.00	75.5074821	75.5075466	75.5075061
21928.4	-60140.40	-81098.22	75.5074583	75.5075229	75.5075049
21929.4	-58143.40	-81099.39	75.5074532	75.5075177	75.5075034
21930.0	-60140.30	-81095.47	75.5074227	75.5074873	75.5075013
21930.5	-60135.60	-81098.60	75.5075169	75.5075815	75.5075017
21931.5	-60154.20	-81098.74	75.5073873	75.5074518	75.5074999
21933.1	-60125.70	-81099.01	75.5075697	75.5076343	75.5075005
21934.6	-60147.30	-81099.26	75.5074347	75.5074992	75.5074998
21935.4	-60126.70	-81099.40	75.5075661	75.5076307	75.5075005
21936.0	-60144.40	-81099.53	75.5074549	75.5075195	75.5074995
21937.0	-60146.40	-81099.67	75.5074430	75.5075078	75.5074992
21937.0	-60133.60	-81099.80	75.5075253	75.5075898	75.5074999
21938.6	-60151.30	-81099.94	75.5074141	75.5074797	75.5074970
21939.3	-60111.90	-81100.05	75.5076645	75.5077291	75.5075005
21940.9	-60145.40	-81100.32	75.5074549	75.5075195	75.5074996
21941.7	-60139.50	-81100.46	75.5074990	75.5075634	75.5074996
21942.5	-60125.70	-81100.59	75.5075809	75.5076455	75.5075012
21943.2	-60141.40	-81100.71	75.5074823	75.5075469	75.5075008
21944.9	-60140.50	-81100.99	75.5074890	75.5075545	75.5074999
21947.9	-60154.20	-81101.50	75.5074069	75.5074714	75.5074999
21948.7	-60124.70	-81101.64	75.5075945	75.5076590	75.5075006
21952.6	-60164.10	-81102.29	75.5073497	75.5074143	75.5074979
21954.2	-60125.70	-81102.56	75.5075949	75.5076594	75.5074996
21956.5	-60135.50	-81102.95	75.5075355	75.5076001	75.5075002
21958.1	-60147.30	-81103.22	75.5074627	75.5075273	75.5074996
21959.6	-60147.30	-81103.47	75.5074645	75.5075291	75.5074998
22000.4	-60129.60	-81103.60	75.5075770	75.5076401	75.5075003
22001.0	-60141.40	-81103.74	75.5075038	75.5075683	75.5075003
22002.0	-60142.40	-81103.87	75.5074994	75.5075630	75.5075003
22002.7	-60148.30	-81103.99	75.5074619	75.5075264	75.5074997
22003.5	-60137.50	-81104.13	75.5075312	75.5075958	75.5075002
22005.1	-60150.30	-81104.40	75.5074529	75.5075166	75.5074995
22006.7	-60143.40	-81104.66	75.5074977	75.5075602	75.5074994
22007.4	-60134.60	-81104.79	75.5075549	75.5076189	75.5075002
22008.2	-60140.50	-81104.92	75.5075179	75.5075824	75.5075005
22009.0	-60139.50	-81105.05	75.5075251	75.5075897	75.5075009
22010.6	-60151.30	-81105.32	75.5074523	75.5075169	75.5075002
22011.3	-60148.30	-81105.44	75.5074721	75.5075367	75.5074999
22013.9	-60153.20	-81105.71	75.5074430	75.5075076	75.5074998
22016.9	-60140.40	-81106.36	75.5075161	75.5075806	75.5074998
22017.6	-60141.40	-81106.50	75.5075233	75.5075879	75.5074995
22019.4	-60158.20	-81106.63	75.5074179	75.5074824	75.5074995

TABLE A-8. EPHEMERIS AND LOP SUMMARY FOR TEST 13 (JULY 28, 1971) (PAGE 1 OF 3)

ATS-5 EPHEMERIS

TIME GMT	SAT RANGE NMI	LATITUDE DEG	LONGITUDE DEG
13000.0	22716.69	-0.502	105.148
20000.0	22717.58	-0.413	105.125
23000.0	22719.06	-0.316	105.103
30000.0	22721.10	-0.214	105.083
33000.0	22723.67	-0.108	105.064

PARABOLIC FIT TO EPHEMERIS-LINEAR TO CAL DATA

	CONSTANT	LINEAR	QUADRATIC	RMS
LATITUDE	-0.7400286	0.1416857	0.0111429	0.00058
LONGITUDE	105.2260285	-0.0562857	0.0028571	0.00011
GEOC RANGE	22717.3260009	-2.1040084	1.1200017	0.00849
CALIB LINE	39765.4700302	-638.7839655		10.25137

TIME GMT	RANGE DIF. (FT)	CAL. VAL. (FT)	LONGITUDES (DEG) POINT1	POINT2	CUMUL. AVG.
20020.7	59425.75	38484.23	75.5072118	75.5072764	75.5072118
20205.4	59409.81	38465.65	75.5072407	75.5073053	75.5072262
20349.2	59382.72	38447.23	75.5071979	75.5072625	75.5072168
20522.1	59363.39	38430.75	75.5071907	75.5072553	75.5072103
20649.6	59354.48	38415.22	75.5072429	75.5073075	75.5072168
20836.5	59348.34	38396.25	75.5073367	75.5074013	75.5072368
21028.2	59344.09	38376.43	75.5074485	75.5075131	75.5072670
21228.5	59301.04	38355.09	75.5073254	75.5073900	75.5072743
21416.2	59283.96	38335.98	75.5073511	75.5074156	75.5072828
21614.1	59270.87	38315.06	75.5074148	75.5074793	75.5072960
21816.7	59231.28	38293.30	75.5073165	75.5073811	75.5072979
22023.2	59212.67	38270.86	75.5073561	75.5074207	75.5073027
22233.6	59192.72	38247.72	75.5073921	75.5074567	75.5073096
22452.5	59166.54	38223.07	75.5073003	75.5074639	75.5073160
22638.0	59150.17	38204.35	75.5074271	75.5074917	75.5073234
22809.3	59119.63	38188.15	75.5073475	75.5074121	75.5073249
22923.5	59102.89	38174.99	75.5073340	75.5073986	75.5073255
23047.0	59089.19	38160.17	75.5073514	75.5074160	75.5073269
23205.1	59074.43	38146.31	75.5073554	75.5074199	75.5073284
23332.6	59057.67	38130.79	75.5073584	75.5074229	75.5073299
23504.7	59045.02	38114.44	75.5073933	75.5074578	75.5073329
23638.4	59020.44	38097.82	75.5073546	75.5074191	75.5073339
23756.5	59009.53	38083.96	75.5073831	75.5074476	75.5073361
23917.7	59011.12	38069.55	75.5074946	75.5075591	75.5073427
24022.5	58978.97	38058.05	75.5073720	75.5074365	75.5073438
24232.1	58956.47	38035.06	75.5073915	75.5074560	75.5073457
24336.1	58940.56	38023.70	75.5073708	75.5074352	75.5073466
24430.8	58932.66	38014.00	75.5073892	75.5074536	75.5073481
24531.7	58919.24	38003.19	75.5073803	75.5074448	75.5073492
24624.8	58914.86	37993.77	75.5074191	75.5074835	75.5073516
24725.7	58901.24	37982.96	75.5074090	75.5074735	75.5073534

TIME GMT	RANGE DIF. (FT)	CAL. VAL. (FT)	LONGITUDES (DEG)		
			POINT1	POINT2	CUMUL. AVG.
24832.8	58877.34	37971.05	75.5074050	75.5074694	75.5073550
24932.2	58874.28	37960.51	75.5073966	75.5074611	75.5073563
25033.1	58866.51	37949.71	75.5074237	75.5074882	75.5073583
25145.7	58851.54	37936.83	75.5074198	75.5074843	75.5073600
25255.9	58836.50	37924.37	75.5074125	75.5274770	75.5073615
25403.9	58819.10	37912.30	75.5073875	75.5074520	75.5073622
25503.2	58810.65	37901.78	75.5074084	75.5074728	75.5073634
25557.1	58810.18	37892.22	75.5074730	75.5075374	75.5073662
25707.4	58793.13	37879.74	75.5074532	75.5075176	75.5073684
25758.1	58775.49	37870.75	75.5074050	75.5074694	75.5073693
25850.4	58770.87	37861.47	75.5074414	75.5075058	75.5073710
25943.5	58755.53	37852.05	75.5074108	75.5074753	75.5073719
30051.5	58742.41	37839.98	75.5074131	75.5074775	75.5073729
30147.7	58737.01	37830.01	75.5074494	75.5075139	75.5073746
30240.0	58725.30	37820.73	75.5074409	75.5075053	75.5073760
30344.8	58722.44	37809.23	75.5075042	75.5075686	75.5073797
30442.6	58717.99	37798.97	75.5075487	75.5076131	75.5073823
30549.7	58703.75	37787.07	75.5075428	75.5076072	75.5073855
30659.2	58691.31	37774.74	75.5075513	75.5076157	75.5073889
30757.0	58681.26	37764.48	75.5075603	75.5076247	75.5073922
30905.7	58667.42	37752.29	75.5075590	75.5076234	75.5073954
31002.7	58662.38	37742.18	75.5075988	75.5076632	75.5073993
33937.5	58327.79	37427.25	75.5077183	75.5077826	75.5074052
34027.4	58310.34	37418.40	75.5076709	75.5077351	75.5074100
34129.9	58293.99	37407.31	75.5076464	75.5077106	75.5074142
34223.8	58284.83	37397.75	75.5076566	75.5077209	75.5074185
34325.5	58271.77	37386.80	75.5076520	75.5077162	75.5074225
34422.5	58259.84	37376.68	75.5076486	75.5077128	75.5074263
34516.3	58249.98	37367.14	75.5076543	75.5077135	75.5074301
34603.2	58243.25	37358.82	75.5076711	75.5077353	75.5074341
34657.8	58233.54	37349.13	75.5076788	75.5077430	75.5074380
34751.7	58224.57	37339.56	75.5076903	75.5077545	75.5074420
34844.0	58211.54	37330.28	75.5076740	75.5077382	75.5074457
34937.1	58201.77	37320.86	75.5076795	75.5077437	75.5074493
35027.9	58188.67	37311.25	75.5076609	75.5077251	75.5074525
35121.1	58178.43	37302.41	75.5076635	75.5077276	75.5074556
35214.8	58169.75	37292.88	75.5076766	75.5077408	75.5074589
35302.5	58157.73	37284.42	75.5076610	75.5077252	75.5074619
35355.6	58150.28	37274.99	75.5076812	75.5077454	75.5074649
35446.3	58139.90	37266.00	75.5076798	75.5077440	75.5074680
35538.6	58127.37	37256.72	75.5076668	75.5077309	75.5074707
35631.7	58120.69	37247.29	75.5076919	75.5077561	75.5074737
35721.7	58106.89	37238.42	75.5076679	75.5077321	75.5074764
35808.6	58101.55	37230.10	75.5076937	75.5077579	75.5074793
35854.6	58090.96	37221.94	75.5076850	75.5077492	75.5074820
35942.2	58088.24	37213.49	75.5077283	75.5077925	75.5074852
40029.1	58074.94	37205.17	75.5077036	75.5077678	75.5074880

TABLE A-8.   EPHEMERIS AND LOP SUMMARY FOR TEST 13
(JULY 28, 1971)   (PAGE 3 OF 3)

TIME GMT	RANGE DIF. (FT)	CAL. VAL. (FT)	LONGITUDES (DEG)		
			POINT1	POINT2	CUMUL. AVG.
40124.5	58068.34	37195.34	75.5077323	75.5077964	75.5074911
40214.5	58054.51	37186.47	75.5077082	75.5077723	75.5074938

APPENDIX B

RELATIVE POSITION DETERMINATION

The equations derived in this appendix permit the determination of Lines of Position (LOP's) which locate the movable remote receiver with respect to the fixed receiver at a known position.

The receivers are located in areas for which Type 1 surveys are available. This permits determination of the distance from the fixed receiver to the satellite with minimal error (governed only by the uncertainty in satellite position).

LINE OF POSITION

A Line of Position is defined to be a straight line containing the receiver's position. It is obtained by assuming a reference latitude near the true latitude. On the latitude circle, a point of longitudinal intersection is located. The same procedure may be repeated in order to establish a second point, following which the two points are connected by a straight line. Alternately, a line perpendicular to the line of sight to the satellite may be drawn through one of these points. In either case, a line is obtained which contains the remote receiver. A range reading from the fixed receiver and a range reading from the remote receiver are required for the determination of an LOP.

THE GEOMETRY OF THE LOP

The position of the remote receiver is defined by three quantities, R, ψ and λ, where R is the radius of the Earth, and ψ and λ represent the latitude and longitude, respectively. With one satellite available, only one of these unknowns can be determined. It is mathematically convenient to select latitude and Earth radius as the known quantities and then calculate longitude. Latitude and radius are determined from the international geoid model.

Since position on the Earth's surface is normally given in geodetic coordinates, the position of the fixed receiver as well as the geodetic latitude and Earth radius of the remote receiver are translated to the geocentric coordinates shown in Figure B-1.

If D is the distance between either receiver and the satellite, it follows from spherical trigonometry that

$$D^2 = R^2 + R_S{}^2 - 2RR_S \cos \gamma \tag{B-1}$$

where

$$\cos \gamma = \cos \psi \cos \psi_S \cos (\lambda_S - \lambda) + \sin \psi \sin \psi_S \tag{B-2}$$
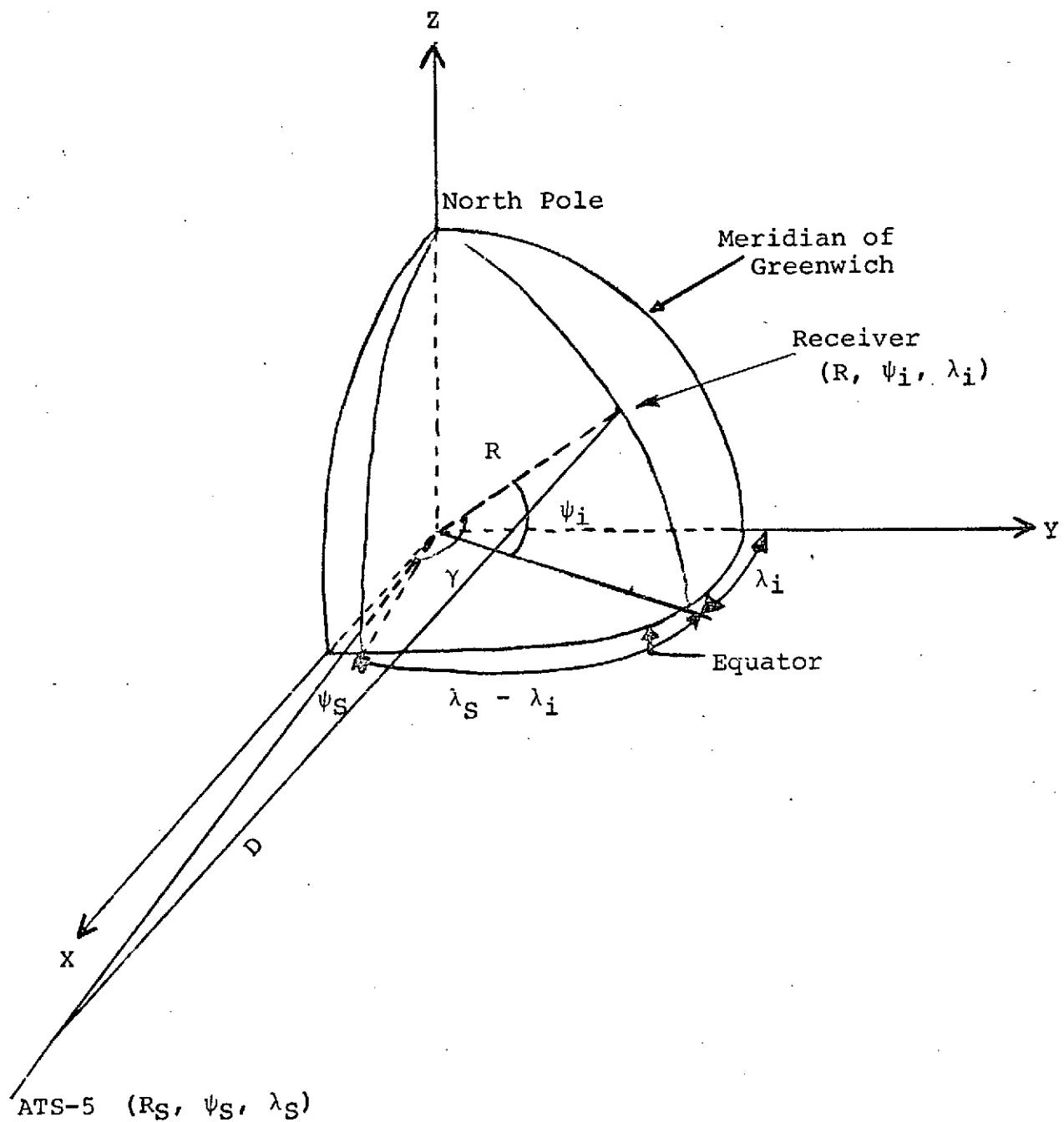
Figure B-1. Geocentric Coordinate System

In the sequel the subscript S refers to the satellite while sub-scripts A and B pertain to the fixed and movable receivers, respectively.

The angle γ defined in equation (B-2) is located at the center of the Earth and between the rays to the satellite and receiver under consideration.

In this framework, the distances D_A and D_B are measured ambiguously as M_A and M_B. The range readings M_A and M_B are contaminated by receiver noise, atmospheric noise, delays in the equipment and atmosphere as well as the relative drift in phase and frequency between the two rubidium frequency standards used. In the absence of these error sources, the range differences $D_B - D_A$ and $M_B - M_A$ both measure the distance between the two receivers. In the presence of these error sources we still write

$$D_B - D_A = M_B - M_A \qquad\qquad\qquad (B-3)$$

where the equivalence is understood to be not mathematically exact. Since the errors induced by the rubidium standards are correctable, equation (B-3) may be rewritten as

$$D_B = D_A + M_B - M_A + At + B \qquad\qquad\qquad (B-4)$$

where the linear function describes the correction factor to the relative phase drift. The relative frequency drift, which would introduce a correction term of the form Ct^2 , is negligible.

The determination of the longitude of the remote site proceeds as follows. Since the latitude, longitude and geocentric range of the fixed site are well known and the position of the satellite is available from NASA ephemeris predictions, $\cos \gamma$ can be calculated. Hence, D_A can be calculated from equation (B-1) and the distance D_B from the remote site to the satellite follows from equation (B-4). Since the geocentric range of the remote site is assumed known,

$$\cos \gamma_B = \frac{R_B^{\,2} + R_S^{\,2} - D_B^{\,2}}{2\,R_B\,R_S} \; ; \qquad\qquad\qquad (B-5)$$

equation (B-2) is used to determine $\cos (\lambda_S - \lambda_B)$

$$\cos (\lambda_S - \lambda_B) = \frac{\cos \gamma_B - \sin \psi_B \sin \psi_S}{\cos \psi_B \cos \psi_S} \tag{B-6}$$

Then,

$$\sin (\lambda_S - \lambda_B) = \pm[1 - \cos^2 (\lambda_S - \lambda_B)]^{\frac{1}{2}} \tag{B-7}$$

and

$$\lambda_B = \lambda_S \pm \tan^{-1} \frac{\sin (\lambda_S - \lambda_B)}{\cos (\lambda_S - \lambda_B)} \tag{B-8}$$

If west longitude is defined positive and increasing westward, the upper (+) signs are used in equations (B-7) and (B-8).

Equation (B-8) shows that λ_B is completely determined in terms of ψ_B and R_B. By changing ψ_B and R_B correspondingly, a new longitude can be calculated. The resulting point when connected to the first point completely defines the LOP.

The LOP can also be specified by one of the points and the azimuth heading, which is given by

$$Az = \beta + \pi \tag{B-9}$$

where

$$\beta = \sin^{-1} \left[\frac{\sin (\lambda_S - \lambda_B) \cos \phi_S}{\sin \gamma_B} \right] \tag{B-10}$$

West longitude is taken to be positive in equation (B-10). In either case, the line of position is completely determined.

The accuracy with which λ_B is determined is a function of the accuracy with which the satellite position is known. It is implicit in the structure of the solution given here that any error in satellite position appears as an error in λ_B. Estimates of the effect of inaccuracies in satellite ephemeris are treated elsewhere.

The listing of the Lines of Position Program is given in Table B-1.

```
DIMENSION ST(10),STT(10),STLAT(10),STLNG(10),STGRA(10),R(2),AL(2),
CSLT(2),SNLT(2),SLT(4),SLG(4),SRA(4),CALPAR(4),CALTM(1000),CALDR(1000),
FA(3),FAN(4),FAM(4),ALOP1(100),ALOP2(100),AVG(100),DR(100),TMFS(100),
CLVL(100)
* CONVERSION CONSTANTS
* FIXED SITE DENOTED BY TERMINAL F IN VARIABLE NAMES
* REFERENCE LATITUDES DENOTED BY TERMINAL 1 OR 2
DRAD =.0174532925
FTNM =6076.115486
ALATF=DRAD*37.936409
ALNGF=DRAD*75.473952
CALL CONV(ALATF,ALTF,RF)
RF=RF+63.61/FTNM
ALAT1=DRAD*37.864253
ALAT2=DRAD*37.864300
CALL CONV(ALAT1,ALT1,R(1))
CALL CONV(ALAT2,ALT2,R(2))
CSLTF=COS(ALTF)
CSLT(1)=COS(ALT1)
CSLT(2)=COS(ALT2)
SNLTF=SIN(ALTF)
SNLT(1)=SIN(ALT1)
SNLT(2)=SIN(ALT2)
* ACCESS EPHEMERIS AND CALIBRATION DATA
* TITLE STORED AS FAN
* CALIBRATION DATA STORED AS FA
100 WRITE (1,($ TEST NUMBER AND DATE:$,Z))
READ (1,(4A6)) FAN
WRITE (1,($ OPEN FILE:$,Z))
READ (1,(3A6)) FA
OPEN (3,INPUT,FA)
1 READ (3,(I5)) NSAT
2 DO 3 I=1,NSAT
READ (3,(4F20.0)) ST(I),STLAT(I),STLNG(I),STR
STGRA(I)=STR/FTNM
3 CALL TCONV(ST(I),STT(I))
* FIT EPHEMERIS DATA TO PARABOLAS
CALL LSTSQ(NSAT,2,STT,STLAT,SLT)
CALL LSTSQ(NSAT,2,STT,STLNG,SLG)
CALL LSTSQ(NSAT,2,STT,STGRA,SRA)
* DETERMINATION OF THE RMS OF THE EPHEMERIS POINTS ABOUT THE INDIVIDUAL
* PARABOLAS
K=3
CALL PPEAC(NSAT,STT,STLAT,SLT,ALAT,K)
CALL PPEAC(NSAT,STT,STLNG,SLG,ALNG,K)
CALL PPEAC(NSAT,STT,STGRA,SRA,AGRA,K)
4 READ (3,(I5)) NCAL
DO 5 I=1,NCAL
READ (3,(2F20.0)) CALT,CALDR(I)
5 CALL TCONV(CALT,CALTM(I))
* FIT CALIBRATION DATA TO A STRAIGHT LINE
CALL LSTSQ(NCAL,1,CALTM,CALDR,CALPAR)
CLOSE (3)
* DETERMINATION OF THE RMS OF THE CAL POINTS ABOUT THE LINE
K=2
```

```
CALL PREAC(NCAL,CALTM,CALDR,CALPAR,ACAL,K)
6 JJ=0
CNTR=0.
* ACCESS SATELLITE MEASUREMENT DATA, FILE NAME FAM
WRITE (1,($ OPEN DATA FILE:$,Z))
READ  (1,(4A6)) FAM
OPEN  (3,INPUT,FAM)
7 JJ=JJ+1
READ (3,(2F20.0)) TMES(JJ),DR(JJ)
IF (TMES(JJ).EQ.0.) GO TO 80
CALL TCONV(TMES(JJ),TMEAS)
* INTERPOLATE ATS-5 EPHEMERIS AT TIME=TMEAS
SLATD=SLT(1)+(SLT(2)+SLT(3)*TMEAS)*TMEAS
SLNGD=SLG(1)+(SLG(2)+SLG(3)*TMEAS)*TMEAS
SRANG=SRA(1)+(SRA(2)+SRA(3)*TMEAS)*TMEAS
SLATR=SLATD*DRAD
SLNGR=SLNGD*DRAD
CSSAT=COS(SLATR)
SNSAT=SIN(SLATR)
CSFS=CSLTF*CSSAT*COS(SLNGR-ALNGF)+SNLTF*SNSAT
* EVALUATE CALIBRATION LINE AT TIME=TMEAS
CLVL(JJ)=CALPAR(1)+CALPAR(2)*TMEAS
RRS=RF/SRANG
DFS=SRANG*SQRT(RRS**2+1.-2.*RRS*CSFS)
DRS=DFS-(DR(JJ)-CLVL(JJ))/FTNM+45/FTNM
* DETERMINE LONGITUDES FOR THE GIVEN LATITUDES
DO 8 I=1,2
RQ=R(I)/SRANG
DQ=DRS/SRANG
COS1 =(RQ**2+1.-DQ**2)/(2.*RQ)
COSDL=(COS1-SNLT(I)*SNSAT)/(CSLT(I)*CSSAT)
SINDL=SQRT(1.-COSDL**2)
8 AL(I)=(SLNGR-ATAN(SINDL/COSDL))/DRAD
ALOP1(JJ)=AL(1)
ALOP2(JJ)=AL(2)
CNTR=CNTR+AL(1)
AVG(JJ)=CNTR/JJ
GO TO 7
* GO TO 7 FOR MORE MEASUREMENT DATA
80 CLOSE (3)
* OUTPUT
IPG=1
WRITE (1,81) FAN,IPG
81 FORMAT(^/20X,4A6,20X,$PAGES,I2/)
WRITE (1,82)
82 FORMAT(10X,$ATS-5 EPHEMERIS$/1PX,$TIME$,3X,$SAT RANGE    LATI
TUDE   LONGITUDE$/10X,$ GMT$,6X,$NMI$,8X,$DEG$,9X,$DEG$)
WRITE (1,91) (ST(I),STGRA(I),STLAT(I),STLNG(I),I=1,NSAT)
91 FORMAT(6X,F8.1,4X,F8.2,F11.3,F12.3)
WRITE (1,92) (SLT(I),I=1,3),ALAT,(SLG(I),I=1,3),ALNG,(SRA(I),I=1,3),AGRA
,CALPAR(1),CALPAR(2),ACAL
92 FORMAT(//5X,$ PARABOLIC FIT TO EPHEMERIS-LINEAR TO CAL DATA$/
23X,$CONSTANT$,7X,$LINEAR$,4X,$QUADRATIC$,5X,$RMS$/
6X,$LATITUDE$,4X,3F13.7,F8.5/6X,$LONGITUDE$,3X,3F13.7,F8.5/
6X,$GEOC RANGE$2X,3F13.7,F8.5/6X,$CALIB LINE$,1X,F14.7,F13.7,13X,F8.5)
WRITE (1,93)
```

```
93 FORMAT(//10X,$TIME  RANGE DIF.  CAL. VAL.$,9X,$LONGITUDES(DEG)$/10X,
$ GMT$,5X,$(FT)$,7X,$(FT)$,8X,$POINT1$,5X,$POINT2$,1X,$CUMUL. AVG.$)
LIN=NSAT+15
DO 97 K=1,JJ-1
WRITE (1,95) TMES(K),DR(K),CLVL(K),ALOP1(K),ALOP2(K),AVG(K)
95 FORMAT(5X,F9.1,F12.2,F11.2,2F11.7,F12.7)
LIN=LIN+1
IF (LIN-50) 97,97,96
96 IPG=IPG+1
WRITE (1,81) FAN,IPG
WRITE (1,93)
LIN=4
97 CONTINUE
WRITE (1,(^))
GO TO 100
STOP
END
SUBROUTINE  CONV(AA,BB,R)
* THIS SUBROUTINE CALCULATES GEOCENTRIC LATITUDE AND EART'S RADIUS
FTNM=6076.115486
RA=20925741.00/FTNM
RB=20855591.00/FTNM
E2=1.-(RB/RA)**2
A =E2/(2.-E2)
T1=A*SIN(2.*AA)
T2=A*A*SIN(4.*AA)/2.
T3=A*A*A*SIN(6.*AA)/3.
BB=AA-T1+T2-T3
R =RB/SQRT(1.-E2*COS(BB)**2)
RETURN
END
SUBROUTINE TCONV(TIME,TMD)
* THIS SUBROUTINE CONVERTS INPUT TIME TO DECIMAL TIME
I1 =TIME/10000.
RES=TIME-I1*10000.
I2 =RES/100.
RET=RES-I2*100.
TMD=I1+(I2+RET/60.)/60.
RETURN
END
SUBROUTINE PREAC(NPNTS,TIME,OBSVAL,FIT,OUT,L)
* THE RMS ABOUT THE MOVING MEAN IS CALCULATED IN THIS SUBROUTINE
DIMENSION TIME(400),OBSVAL(400),FIT(5)
DIF=0.
DO 2 I=1,NPNTS
VAL=0.
DO 1 J=1,L
1 VAL=VAL+FIT(J)*(TIME(I)**(J-1))
2 DIF=DIF+(VAL-OBSVAL(I))**2
OUT=SQRT(DIF/NPNTS)
RETURN
END
```

APPENDIX C

SIGNAL DESIGN

The ALPHA II receiver uses correlation between the received signal and a locally generated signal replica in order to reject the noise on the signal and enhance the accuracy of the range determination. The correlator has excellent noise characteristics, as developed in Appendix D. The signal design is therefore dedicated to the rejection of multipath while retaining the inherent characteristics of the correlator-receiver.

For these reasons pseudo-random codes were selected as signal candidates. The most important properties of these codes* are:

(1) The number of positive bits in one length of the periodic sequence exceeds the number of negative bits by exactly one;

(2) A code sequence multiplied by a shifted replica of itself is the same code sequence shifted to a further location;

(3) Pseudo-random (PRN) codes are conveniently generated by a linear shift register. If the shift register is N stages long, codes of length 2^N-1 can be generated.

Since the essential difference between the various pseudo-random codes is the number of bits L (= 2^N-1) before the code repeats, time sidelobe rejection can be obtained by selecting a code of sufficient length.

The autocorrelation function of some function f(t) is defined by

$$R(\tau) = \lim_{T \to \infty} \frac{1}{2T} \int_{-T}^{T} f(t) \; f(t-\tau) \; dt \qquad (C-1)$$

Relation (C-1) can be written as

$$R(\tau) = \frac{1}{L} \int_{0}^{L} f(t) \; f(t-\tau) \; dt \qquad (C-2)$$

---

*For these and the subsequent discussion reference, e.g., Berkowitz, Modern Radar, Analysis, Evaluation and System Design, Wiley, 1965.

for maximum length codes, since these codes are periodic. The value of the autocorrelation function when τ equals zero, and the two sequences are aligned bit by bit is thus

$$R(0) = \frac{1}{L} \int_0^L f^2(t)\, dt$$

$$= \frac{1}{L} \int_0^L dt \qquad\qquad (C\text{-}3)$$

$$= 1$$

The amplitude $f^2(t)$ equals unity for all times t since it is the bit-by-bit products of +1 and +1 or -1 and -1 amplitudes. If τ is not equal to zero

$$R(\tau) = \frac{1}{L} \int_0^L f(t)\, f(t-\tau)\, dt$$

$$= \frac{1}{L} \int_0^L f(t+T)\, dt \qquad\qquad (C\text{-}4)$$

by the second property. Property one states that there is one more positive bit than there are negative bits. Hence, the time sidelobes described by $R(\tau)$ are the residual of this one positive bit over the total number of bits in the code, or

$$R(\tau) = -\frac{1}{2^N-1} \qquad\qquad (C\text{-}5)$$

The autocorrelation function is as follows:
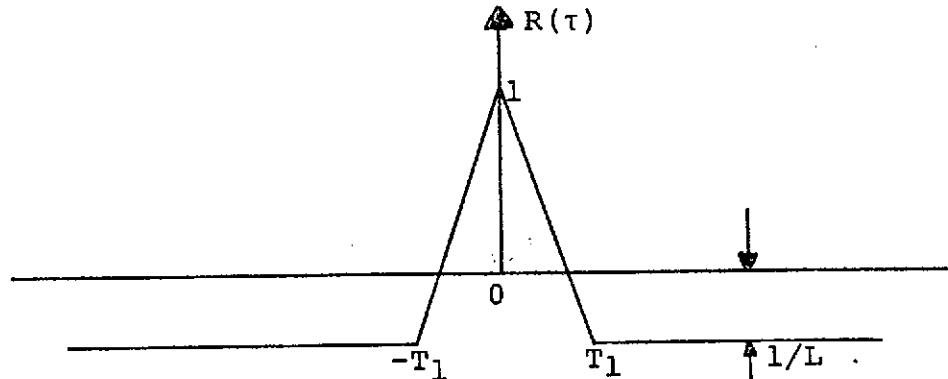
The value 1/L is assumed at T_1, the length of a single bit, and will remain at this level through the (2^N-2)-th bit. If the code is infinitely long, the autocorrelation function will begin to repeat itself assuming the value unity at the (2^N-1)-th bit. If the code is one code length long, $R(\tau)$ is zero beyond the (2^N-2)-th bit.

The power spectrum, $S(\omega)$, has the form $\left(\dfrac{\sin^2 \omega T_1}{\omega T_1}\right)^2$ and is shown schematically in the figure
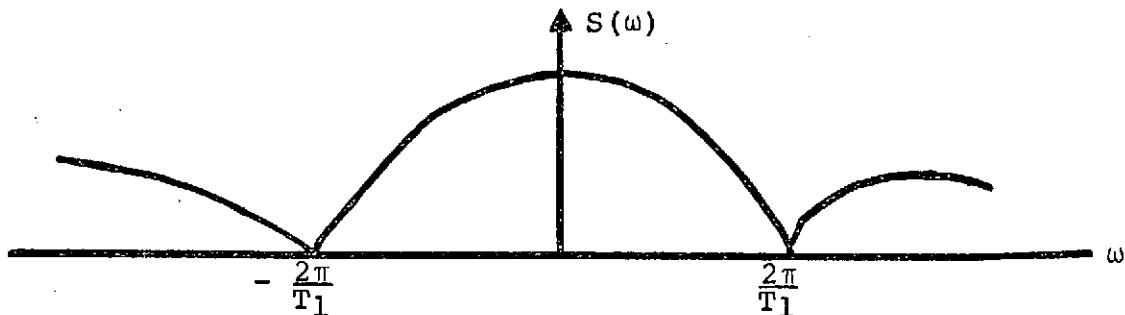
It may be observed that the autocorrelation function and power spectrum are identical to those of a pulse of width T_1.

The codes shown in Table C-1 are maximum length pseudo-random codes generated from a 14-bit shift register. Of course only the first 9 stages are used in feedback connections in order to generate the code of 511 bits in length.

TABLE C-1. CHARACTERISTICS OF MAXIMUM LENGTH
PSEUDO-RANDOM CODES

Code Length	ATS-5 Search Time	*Multipath Rejection	Comments
511	35 secs	-54 dB	
1023	65 secs	-60 dB	
2047**	135 secs	-66 dB	Fundamental ambiguous search code
16,383**	17.4 min	-70 dB	Code for unambiguous motion of satellite

*Multipath rejection obtainable on the basis of the codes structure only and in a 50 Hz bandwidth

**2047 or 16,383 are available in ALPHA II system

APPENDIX D

CORRELATOR ANALYSIS

A matched filter is a device which treats a signal immersed in noise in such a way as to maximize the output signal with respect to a fixed output noise level.

A correlation system acts as a matched filter. If the modulation signal for navigation is matched and the modulations due to path length dynamics and for communications are not matched because they are not known a priori, then these modulations remain at the output of the matched filter and the effective bandwidth should be made to satisfy the relation

$$|H\ (iw)|\ =\ \frac{S(w)}{S(w)\ +\ N(w)} \tag{D-1}$$

where $|H(iw)|$ is the magnitude of the filter characteristic, $S(w)$ is the power spectral density of the signal including modulation due to path dynamics and the communication signal, and $N(w)$ is the noise power spectral density. The expression gives minimum error in reproduction of the residual modulation with noise present.

In the AII ALPHA II receiver, the response approaches the optimization criteria and, hence, has optimum signal-to-noise behavior. The correlator functional block diagram is shown in Figure D-1.
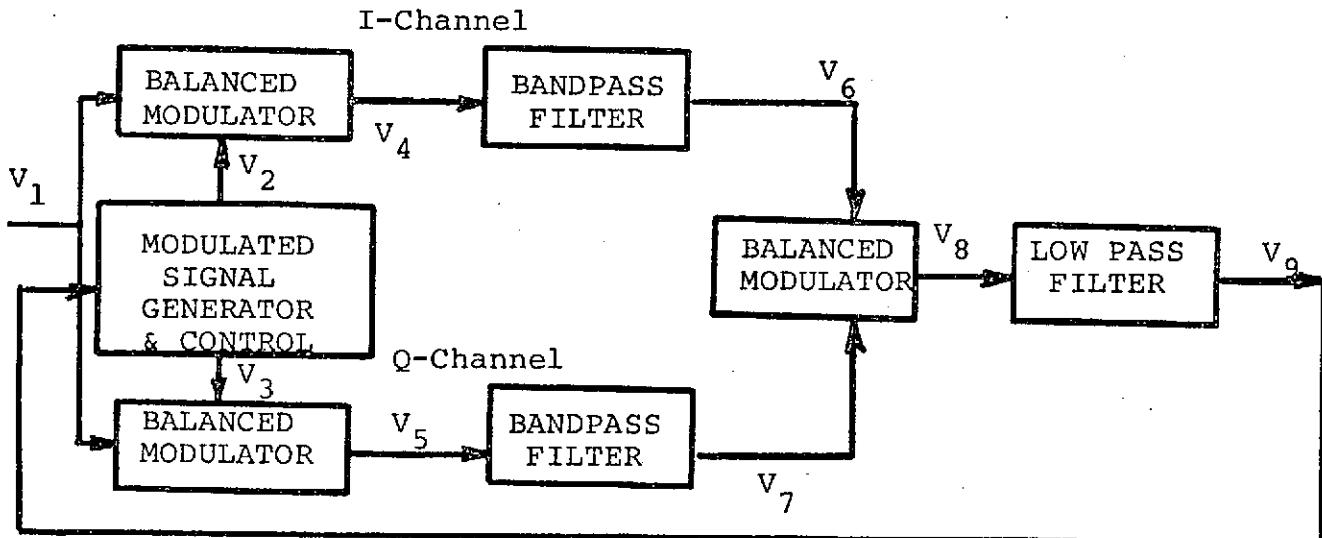

Figure D-1. Correlator Functional Block Diagram

The basic correlation system is a matched filter for the incoming signal. The transmitted bi-phase PSK signal is given by

$$V_O = B \; f(t) \; \cos \omega_O t \qquad (D-2)$$

where B is the signal magnitude at the source, $f(t)$ is the modulation and has values of ± 1 only, and ω_O is the radian carrier frequency.

This signal is delayed by the propagation time, reduced in amplitude during transmission and is translated in the receiver to the intermediate frequency ω_1.

The signal applied to the correlator is

$$V_1 = A \; f(t - \tau) \; \cos (\omega_1 t - \omega_O \tau) \qquad (D-3)$$

This signal is contaminated by noise, $n(t)$, which may be written with in-phase and quadrature components as

$$n(t) = n_c \cos (\omega_1 t - \omega_O \tau) + n_s \sin (\omega_1 t - \omega_O \tau) \qquad (D-4)$$

The n_c and n_s components are independent variables of time and may be assumed to be normally distributed with spectral density

$$G_{n_c} = G_{n_s} = 2 \; N_O$$

Without change in notation, the signal plus noise will also be denoted by V_1.

The delay, $\tau = \tau(t)$, contains the doppler terms. Let

$$\tau(t) = \frac{R(t)}{C} \qquad (D-5)$$

where $R(t)$ is the distance the wave travels between transmitter and receiver and C is the speed of light. Then,

$$\omega_O \; \tau(t) = \frac{\omega_O}{C} R(t) = \frac{2\pi}{\lambda_O} R(t) \qquad (D-6)$$

Expanding,

$$\omega_O \; \tau(t) = \frac{2\pi}{\lambda_O} \; [R(0) + \dot{R}(0) \; t + \frac{\ddot{R}(0) \; t^2}{\underline{2}} + \; . \; . \; .] \qquad (D-7)$$

$$\omega_O \; \tau(t) = \frac{2\pi}{\lambda_O} \; R(0) + \frac{2\pi}{\lambda_O} \dot{R}(0) \; t + \frac{\pi}{\lambda_O} \ddot{R}(0) \; t^2 \qquad (D-8)$$

The term $\frac{2\pi}{\lambda_o} R(0)$ is the initial range, $\frac{2\pi}{\lambda_o} R(0)t$ is the doppler

term whose corresponding frequency is $\frac{R(0)}{\lambda_o}$, and $\frac{\pi}{\lambda_o} \dot{R}(0)t^2$ is the acceleration term.

The signal is multiplied in the correlator I-channel balanced modulated by the locally generated modulation function, $F_2 = f(t-T)$. The balanced modulator performs the function described by:

$$V_4 = V_1 \, f \, (t-T) \tag{D-9}$$

or

$$V_4 = A\, f(t-\tau)f(t-T)\, \cos\,(\omega_1 t - \omega_o \tau) + n_c\, f(t-T)\, x$$
$$\cos\,(\omega_1 t - \omega_o \tau) + n_s\, f(t-T)\, \sin\,(\omega_1 t - \omega_o \tau) \tag{D-10}$$

Similarly, the Q-channel balanced modulator multiplies V_1 with V_3, where

$$V_3 = f \, (t-T + T_o/2) - f(t-T - T_o/2) \tag{D-11}$$

The output becomes

$$V_5 = V_1 \, [f(t-T + T_o/2) - f(t-T - T_o/2)] \tag{D-12}$$

or,

$$V_5 = Af(t-\tau)\,[f(t-T + T_o/2) - f(t-T - T_o/2)]\, x$$
$$\cos\,(\omega_1 t - \omega_o \tau) + [n_c \cos\,(\omega_1 t - \omega_o \tau) +$$
$$n_s \sin\,(\omega_1 t - \omega_o \tau)]\, x\, [f(t-T + T_o/2) -$$
$$f(t-T - T_o/2)] \tag{D-13}$$

The output voltages (V_4, V_5) from the balanced modulators are filtered by the bandpass filters, whose outputs (V_6, V_7) respectively become approximately

$$V_6 = \overline{A\, f(t-\tau)\, f(t-T)}\, \cos\,(\omega_1 t - \omega_o \tau) + n_R \tag{D-14}$$

·Where the noise terms are

$$n_R = q_{1R} \cos\,(\omega_1 t - \omega_o \tau) + q_{2R} \sin\,(\omega_1 t - \omega_o \tau) \tag{D-15}$$

$$q_{1R} = \overline{n_c\, f(t-T)}, \tag{D-16}$$

$$q_{2R} = \overline{n_s\, f(t-T)} \tag{D-17}$$

In the difference channel, the signal plus noise assumes the form

$$V_7 = \overline{A\ f(t-\tau)[f(t-T + T_o/2) - f(t-T - T_o/2)]} \cos$$

$$(\omega_1\ t - \omega_o\ \tau) + n_\Delta \qquad \text{(D-18)}$$

where

$$n_\Delta = q_{1\Delta} \cos (\omega_1\ t - \omega_o\ \tau) + q_{2\Delta} (\omega_1\ t - \omega_o\ \tau) \qquad \text{(D-19)}$$

while

$$q_{1\Delta} = \overline{n_c\ [f(t-T + T_o/2) - f(t-T - T_o/2)]} \qquad \text{(D-20)}$$

$$q_{2\Delta} = \overline{n_s\ [f(t-T + T_o/2) - f(t-T - T_o/2)]} \qquad \text{(D-21)}$$

Averages are indicated by superposed bars. Autocorrelation functions $R\ (\tau-T)$ and $R_\Delta\ (\tau-T)$ are

$$R\ (\tau-T) = \overline{f(t-\tau) f(t-T)} \qquad \text{(D-22)}$$

$$R_\Delta (\tau-T) = \overline{f(t-\tau)[f(t-T + T_o/2) - f(t-T - T_o/2)]} \qquad \text{(D-23)}$$

The noise and code are independent. The spectrum of the code is flat while f^2 equals unity. The following spectral densities result in the single sided IF bandwidth of $B_1/2$

$$G_{q_{1R}} = G_{q_{2R}} = 2N_o \qquad \text{(D-24)}$$

$$G_{q_{1\Delta}} = G_{q_{2\Delta}} = 4N_o \qquad \text{(D-25)}$$

The expressions for V_6 and V_7 may be rewritten as

$$V_6 = A\ R\ (\tau - T) \cos (\omega_1\ t - \omega_o\tau) + n_R \qquad \text{(D-26)}$$

$$V_7 = A\ R_\Delta\ (\tau-T) \cos (\omega_1\ t - \omega_o\ \tau) + n_\Delta \qquad \text{(D-27)}$$

Note that the cosine terms contain the received phase information including doppler.

The output available at point V_6 can be used to measure doppler when lock-on occurs ($\tau = T$). The error signal is V_8 and is given by

$$V_8 = V_6 \cdot V_7 = A^2\ R\ (\tau-T)\ R_\Delta\ (\tau-T) \cos^2 (\omega_1\ t - \omega_o\ \tau) +$$

$$\text{noise terms} \qquad \text{(D-28)}$$

After filtering in the low pass filter the error voltage resulting from the first term of V_8 becomes

$$V_9 = \frac{1}{2} A^2 R (\tau - T) \cdot R_\Delta (\tau - T) \qquad \text{(D-29)}$$

This is used to control the phase of the tracking code generator. Near lock-on, we have $(\tau \approx T)$

$$V_9 = \frac{1}{2} A^2 R_\Delta (\tau - T) \qquad \text{(D-30)}$$

for the error signal output and $AR(0)$ for the doppler signal output.

The lock-on point is chosen such that the autocorrelation function nulls at $\tau = T$ and is linear. With pseudo-random code modulation, two decoders are required in the Q-channel.

The receiver noise results from the noise terms indicated in the expression for V_8. These noise terms are

$$V_{10} = \frac{A}{2} R_\Delta (\tau - T) \, \overline{q}_{1R} + \frac{A}{2} R (\tau - T) \, \overline{q}_{1\Delta} +$$

$$(\overline{q_{1\Delta} \, q_{1R}} + \overline{q_{2\Delta} \, q_{2R}})/2 \qquad \text{(D-31)}$$

The bar now indicates averaging in the low pass filter bandwidth B_2. In order to determine the error induced by the noise, the noise power must be determined. Since the q parameters are normal, zero mean and each is assumed independent of the other three, equivalently to the determination of power, the variances are to be determined.

The quantities $\overline{q}_{1R}$ and $\overline{q}_{1\Delta}$ are both flat over the IF bandwidth B_1, hence over the bandwidth B_2 they contribute $2 N_o B_2$ and $4 N_o B_2$, respectively.

The power associated with $\overline{q_{1\Delta} \, q_{1R}}$ can be determined by convoluting the power spectral densities of $q_{1\Delta}$ and q_{1R}. Since both are flat over the same bandwidth B_1, the result is a triangle with base-width $2B_1$ and magnitude at zero frequency of $8 N_o^2 B_1$. Thus, the variance of $\overline{q_{1\Delta} \, q_{1R}}/2$ (and because of symmetry also $\overline{q_{2\Delta} \, q_{2R}}/2$) is $8N_o^2 B_1 B_2/4$. Those two terms together thus contribute $4N_o^2 B_1 B_2$.

The variance of V_{10} becomes thus

$$\sigma_{10}{}^2 = \left[\frac{A}{2} R_\Delta (\tau-T)\right]^2 \sigma^2(\bar{q}_{1R}) + \left[\frac{A}{2} R(\tau-T)\right]^2 \sigma^2(\bar{q}_{1\Delta})$$

$$+ \sigma^2 \left[\frac{\overline{q_{1\Delta} q_{1R}} + \overline{q_{2\Delta} q_{2R}}}{2}\right]$$

$$= \left[\frac{A}{2} R_\Delta (\tau-T)\right]^2 2N_oB_2 + \left[\frac{A}{2} R(\tau-T)\right]^2 4N_oB_2$$

$$+ 4N_o{}^2B_1B_2 \qquad\qquad (D-32)$$

The noise voltage ΔV_{10} will cause a timing error $\Delta\tau$ as can be seen from the figure (Z-curve) shown below.
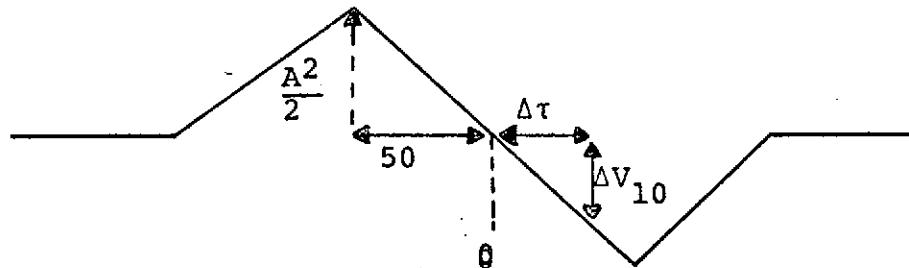
Since near lock-on $(\tau \approx T)$, $R(\tau-T) \approx 1$ while $R_\Delta(\tau-T)$ is equal to unity when the error correcting signal has to correct for a 50 nsec shift

$$\frac{\Delta\tau}{\Delta V_8} = \frac{50}{A^2/2}$$

Hence,

$$\Delta\tau = 100 \frac{\Delta V_8}{A^2}$$

The variance is then

$$\sigma_\tau{}^2 = (100)^2 \frac{\sigma_8{}^2}{A^4} \qquad\qquad (D-33)$$

Substituting the expression of $\sigma_{10}{}^2$ into this result and taking the square root

$$\sigma_{\tau} = 100 \left[\frac{R_{\Delta}{}^2 (\tau - T)}{2A^2} N_o B_2 + \frac{N_o B_2}{A^2} + \frac{4N_o{}^2 B_1 B_2}{A^4} \right]^{1/2} \quad \text{(D-34)}$$

near lock-on. Introducing the bitwidth W, which is 100 nsec, i.e., twice the 50-nsec shift corresponding to maximum signal error voltage, then

$$\sigma_T = \frac{W}{2} \left[\frac{2N_o B_2}{A^2} R_{\Delta}{}^2 (\tau - T) + \frac{4N_o B_2}{A^2} + \frac{16N_o{}^2 B_1 B_2}{A^4} \right]^{1/2} \quad \text{(D-35)}$$

The signal power, S, is $A^2/2$. The noise power N depends upon the way bandwidth is defined. In terms of the audio bandwidth

$$N = N_o B_2$$

Hence,

$$\sigma_T = \frac{W}{2} \left[\frac{N}{S} R_{\Delta}{}^2 (\tau - T) + \frac{2N}{S} + \left(\frac{N}{S} \right)^2 \frac{4B_1}{B_2} \right]^{1/2} \quad \text{(D-36)}$$

Under the assumption of a sufficiently large signal-to-noise ratio in the IF bandwidth B_1 (considered subsequently), the third term under the square root may be neglected.

The magnitude of the first term would be 50% the magnitude of the second term if the maximum error voltage, $A^2/2$, were permitted, corresponding to a displacement of 50 nsec.

$$\frac{N}{S} R_{\Delta}{}^2 (\tau - T) = \frac{N}{S} \text{ at } \tau - T = 50 \text{ nsec} \quad \text{(D-37)}$$

In actual operations, a four phase clock is used. The effect of this clock is that range measurements are only made when the signal plus noise voltage is within $\pm$ 12.5 nsec of the nulling point, O, along the slanted line. Hence,

$$\left| \frac{N}{S} R_{\Delta}{}^2 (\tau - T) \right| \leq \left(\frac{12.5}{50} \right)^2 \frac{N}{S} = \frac{1}{16} \frac{N}{S} \quad \text{(D-38)}$$

The maximum value assumed by this term is 1/32th that of the second term and is thus neglected. Hence,

$$\sigma_T \approx \frac{W}{2} \left[\frac{2N}{S} + \frac{N}{S}^2 \frac{4B_1}{B_2} \right]^{1/2}$$ (D-39)

$$\approx \frac{W}{2\sqrt{\frac{S}{2N}}}$$

if this second term is negligible.

This is so when

$$\frac{16 N_o^2 B_1 B_2}{A^4} \ll \frac{4N_o B_2}{A^2}$$ (D-40)

which results from equation (D-35). Simplifying,

$$\frac{4N_o B_1}{A^2} \ll 1$$

or

$$\frac{S}{N_1} \gg 2$$

This is the signal-to-noise in the IF bandwidth B_1. The measured S/N in the 1600 Hz IF bandwidth at NASA Wallops was 6 to 10 dB or 4 to 10 numerically. The indicated assumption is thus justified.

If instead of the audio bandwidth, a double-sided bandwidth is used in tracing the S/N from IF to the filter in which the measurements are made, equation (D-39) assumes the form

$$\sigma_T \approx \frac{W}{2} \left[\frac{N}{S} \left(1 + \frac{B_1}{B_2} \right) \right]^{1/2}$$ (D-41)

APPENDIX E

EFFECTS OF BAND LIMITING ON CORRELATION RECEIVER PERFORMANCE

A signal of the type

$$T(t) = A\, f(t)\, \cos \omega_o t \qquad (E\text{-}1)$$

is transmitted through the satellite transponder which band limits the signal. The consequence of this limiting is a modified signal defined by

$$T_m(t) = A\, g(t)\, \cos \omega_o t \qquad (E\text{-}2)$$

where $f(t)$ is the original code and $g(t)$ is the modified code due to bandwidth restraints. The received signal, after delay of τ seconds, is

$$R(t) = g(t - \tau)\, \cos \omega_o (t - \tau) \qquad (E\text{-}3)$$

The correlation receiver provides an output amplitude of

$$|S| = \overline{f(t-T)g(t-\tau)} \qquad (E\text{-}4)$$

where the bar over the product of code and bandwidth-modified code implies averaging over some time interval (integration time).

The frequency transform of the product, $f(t-T)g(t-\tau)$, is the convolution of the two signals in the frequency domain. Setting $T = \tau$ and transforming $f(t-T) = F(\omega)$ and transforming $g(t-\tau) = G(\omega)$,

$$P(i\omega) = \int_{-\infty}^{\infty} F(V) * G(\omega-V)\, dV \qquad (E\text{-}5)$$

$$G(\omega) = H(\omega)\, F(\omega) \qquad (E\text{-}6)$$

where $H(\omega)$ is the band characteristic function of the satellite transponder. Hence,

$$P(i\omega) = \int_{-\infty}^{\infty} F(V) * F(\omega-V)\, H(\omega-V)\, dV \qquad (E\text{-}7)$$

The average signal amplitude output, equation E-4, is the D-C ($\omega = 0$) spectrum of equation E-7.

$$|S| = P(0) = \int_{-\infty}^{\infty} F(V) * F(-V) H(-V) \, dV \qquad \text{(E-8)}$$

$F(\omega)$ is symmetrical for a maximum length PN code and

$$|S| = P(0) = \int_{-\infty}^{\infty} |F(V)|^2 H(V) \, dV \qquad \text{(E-9)}$$

The largest value $|S|$ can take is for $H(V) = 1$, then,

$$|S|_{max} = \int_{-\infty}^{\infty} |F(V)|^2 \, dV \qquad \text{(E-10)}$$

If $H(V) = 1$, when $V \geq 0$ and $H(V) = 0$ otherwise, then

$$|S| = \int_{0}^{\infty} |F(V)|^2 \, dV = 1/2 \, |S|_{max} \qquad \text{(E-11)}$$

A loss of half the spectrum results in a signal amplitude reduction to half its value and the signal output power is reduced by 6 dB. This is the case for the ATS-5 C-band to L-band cross-strap mode and the 10 megabit ALPHA II PN code.

E-2

APPENDIX F

AN ALTERNATE METHOD OF LOP COMPUTATION

An alternate method of computing relative position is described here.

The quantity ΔR is the magnitude of the vector $\vec{\Delta R}$ which is directed from the fixed receiver to the satellite. The geometry involved may be understood by referring to Figure F-1. The distances R_A and R_B are radii of concentric spheres S_A and S_E. If the elevation and azimuth of the satellite are known as functions of time, the line of sight (LOS) from the fixed receiver A to the satellite can be established. The distance R is measured along the LOS and the surface through the end point C perpendicular to the LOS is established. To a first order approximation, this surface is the sphere S_B since the radii of curvatures are extremely large, and thus, virtually planar. The line CD may be drawn in the "plane" S_B locating D on the surface of the Earth. The perpendicular to AD on the surface of the Earth is then the LOP containing B. The origin of some x-y coordinate system may be placed at the fixed site and the observed LOP's described in this coordinate system.

One could then introduce the known location of the fixed receiver on the surface of the Earth which implies a transformation of coordinates from the fixed site to the center of the Earth. If the azimuth and elevation of the satellite at the fixed site are known ΔR can be determined in this Earth-centered coordinate system. The terminus of ΔR can then be expressed in longitude and latitude.

Knowledge of the satellite position and the location of the fixed site is equivalent to knowledge of the azimuth, elevation and geocentric coordinates of the fixed site. Using spherical trigonometry, equations can be determined relating these two sets of parameters. In either case the LOP's are determined relative to the fixed site. In both cases satellite position error is present either directly or indirectly.

Since the purpose of the relative ranging tests at Wallops was to determine range and thereby to accurately measure position, the relative separation between the two sites had to be known precisely as a check on the LOP calculations. Therefore, sites were selected for which a first order survey was available. In addition, the orientation of the range difference vector in three dimensional space needed to be known with high precision. This information can only be obtained from measured elevation and azimuth angles or equivalently from satellite ephemeris and fixed site coordinates. This information permitted determination of the LOP's for the remote site.
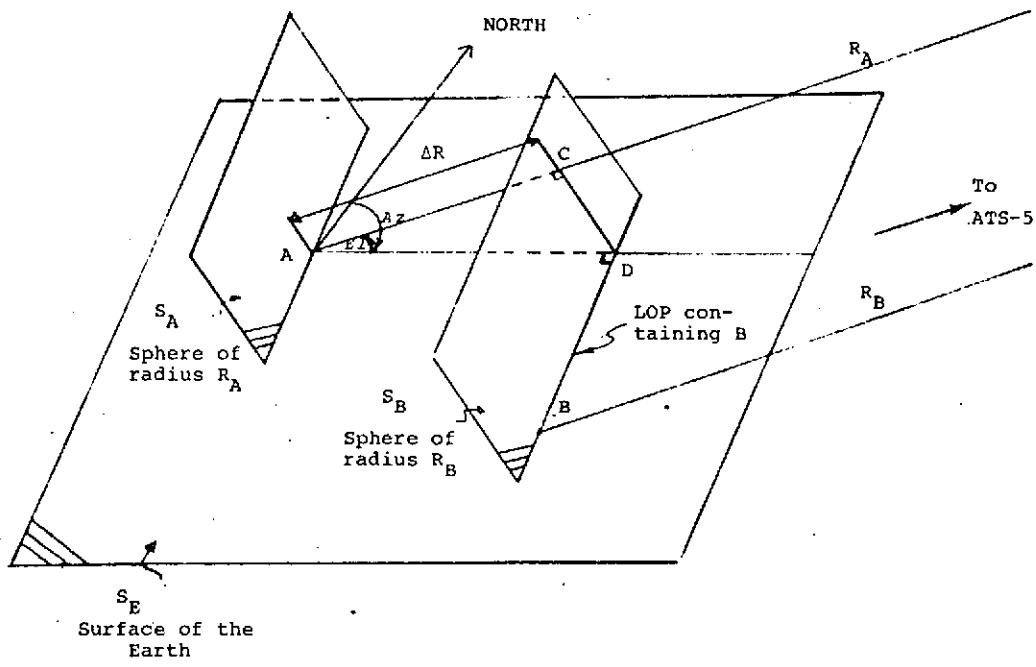
Figure F-1.   Local Line of Position Geometry